ABSTRACT

Title of Thesis:	MODELING OF HVAC CONFIGURATIONS FOR DE-CARBONIZATION IN A MID-SIZE HOSPITAL
	Zachary J. Grant, Master of Science, 2022
Thesis Directed By:	Research Professor Yunho Hwang, Mechanical Engineering

As the threat of climate change becomes more imminent, there has been increasing emphasis on technologies that reduce carbon emissions in the HVAC sector. The clear path forward given existing technologies is electrification since electricity production has future potential to become cleaner. In terms of building type, high ventilation requirements and near continuous occupancy make healthcare facilities some of the highest energy users. HVAC equipment runs all day and night in these facilities with little change. Conventional HVAC equipment such as a boiler is proven to consume more energy than heat pump systems. More specifically, the Variable Refrigerant Flow (VRF) heat pump and the Ground Source Heat Pump (GSHP) are areas of ongoing research. This analysis included creating whole-building energy models using EnergyPlus and OpenStudio to compare the energy consumption for these heat pump configurations and some cheaper electrification alternatives. The results suggested that the GSHP system possessed the greatest potential for energy savings and thus decarbonization given its higher efficiency during times of extreme ambient temperatures compared to other options.

MODELING OF HVAC CONFIGURATIONS FOR DE-CARBONIZATION IN A MID-SIZE HOSPITAL

by

Zachary J. Grant

Thesis submitted to the Faculty of the Graduate School of the
University of Maryland, College Park, in partial fulfillment
of the requirements for the degree of
Master of Science
2022

Advisory Committee:
Research Professor Yunho Hwang, Chair
Professor Michael Ohadi
Professor Bao Yang

Acknowledgments

I would like to thank Dr. Yunho Hwang for his willingness to take me on as one of his students and who helped guide me through this thesis research. I would also like to thank the facilities department at Mid Coast Hospital for their willingness to provide me with all of the necessary information to conduct this research.

Table of Contents

List of Tables

List of Figures

Nomenclature

ACCH	Air-Cooled Chiller
ACH	Air Changes Per Hour
AHU	Air-Handling Unit
ASHP	Air-Source Heat Pump
CAV	Constant Air Volume
Cfh	Cubic Feet Per Hour
Cfm	Cubic Feet Per Minute
CHWR	Chilled Water Return
CHWS	Chilled Water Supply
COP	Coefficient of Performance
CUH	Cabinet Unit Heater
EAT	Entering Air Temperature [°F]
ESP	External Static Pressure [in wg.]
EWT	Entering Water Temperature [°F]
GSHP	Ground-Source Heat Pump
In wg.	Inches of Water Gauge
LAT	Leaving Air Temperature [°F]
LHV	Lower Heating Value [varies: see Table 1]
LPR	Low-Pressure Return
LPS	Low-Pressure Supply
LWT	Leaving Water Temperature [°F]
MBH	1000 British Thermal Units Per Hour

OA	Outdoor Air
Psig	Pounds Per Square Inch Gauge
RPM	Revolutions Per Minute
TSP	Total Static Pressure [in wg.]
VAV	Variable Air Volume
VCC	Vapor Compression Cycle
VCV	Variable/Constant Volume
VRF	Variable Refrigerant Flow

Chapter 1: Introduction

1.1 Background

According to the U.S. Energy Information Administration (EIA) in their report titled Annual Energy Outlook 2022, space heating accounts for 23.5% of energy consumption in commercial buildings nationwide for 2021 [1]. Natural gas has become the primary source of energy for this sector. According to the EIA, natural gas supplied around 84.5% of the total space heating power for the commercial sector in 2021 [1]. This is mostly because natural gas reserves have made the price cheaper compared to alternatives. Furthermore, natural gas produces lower CO_2 emissions compared to other fuel sources such as coal and fuel oil. Looking to the future, the United States Government has expressed its desire to lower carbon emissions and strive for a clean energy future. Given current technologies, widespread electrification is the best way to accomplish this.

1.1.1 Electricity Generation

An often-overlooked point when studying widespread electrification is how said electricity is produced. Figure 1 shows the fuel mix for electricity generation in New England compared to that for the nation as a whole. Renewables (including nuclear and biomass), account for 46.2%. Of the remaining 53.8%, 53.2% is from natural gas.

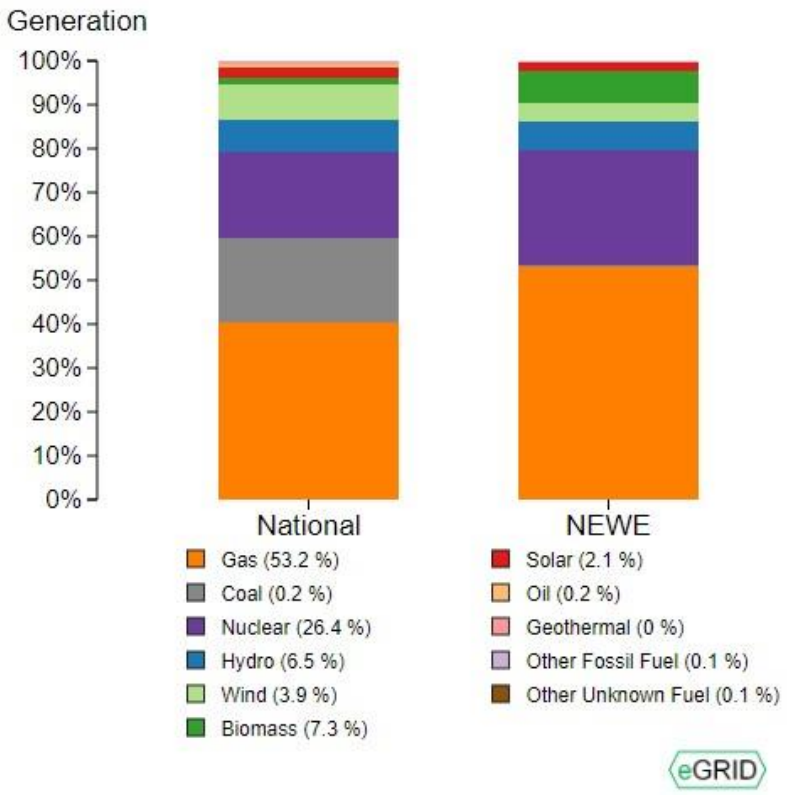

Figure 1 – eGRID Profile of Electricity Generation Source Energy [2]

An energy analysis of the primary energy source provides an estimate of total CO_2 emissions for electricity generation. Heat rate is the total heat input required to produce one kWh of electricity. Lower heating value (LHV) is the heat output on a per unit volume or mass basis of a fuel. The summary is provided in Table 1. Note that biomass is not included in calculating CO_2 emission, though it is acknowledged that burning biomass does have some non-net emissions. The total estimated emissions are 0.514 lbs of CO_2/kWh or, in English units, 0.1507 lbs of CO_2/kBtu of electricity produced. This value is used later to compare emissions, but for now, it illustrates that electrification does not necessarily mean a reduction in CO_2. In the future, the EIA predicts a large increase in solar and wind capacity, from 4% to 22% and 9% to 14% respectively, which would likely lower the total emissions as a result of electricity generation [1].

The potential for increased use of renewable energy for electricity production is the main driving force behind the push for widespread electrification.

Table 1 – CO_2 Emissions Estimated for Electricity Generation in New England

Fuel Source	**Percentage**	**Heat Rate (Btu/kWh) [3]**	**LHV [4]**	**CO_2 Emissions Rate [5]**	**Total CO_2 Emissions (lbs/kWh)**
Natural Gas	53.2	7,732	983 Btu/ft^3	0.12096 lbs/ft^3	0.5062
Fuel Oil	0.2	11,259	128,991 Btu/gal	22.46 lbs/gal	0.003921
Coal	0.2	10,655	12,468 Btu/lb	2.4649 lbs/lb	0.004213
Total					**0.514**

1.2 Variable Refrigerant Flow Heat Pump Basics

Variable refrigerant flow (VRF) systems are more common around the world than they are in the United States, however, they provide a viable option for energy savings. Most VRF systems are comprised of three main components: the outdoor unit, the control unit, and the terminal units. The outdoor unit houses a compressor and one of the heat exchangers (condenser/evaporator depending on operation mode). The control unit houses the expansion valves as well as the electrical controller. The terminal units contain the other heat exchanger. Figure 2 shows a schematic of a VRF system with two terminal units. The four-way valve shown in both the outdoor and indoor units allows the heat pump to redirect refrigerant flow direction for heating and cooling mode.

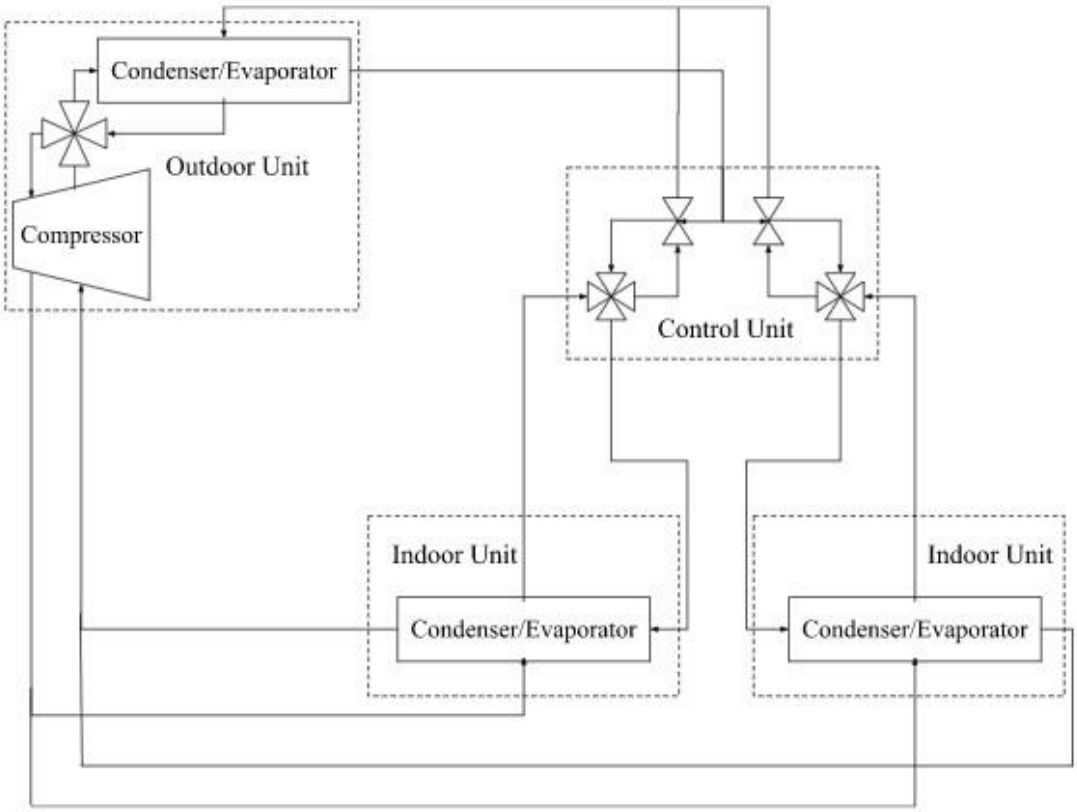

Figure 2 – Basic VRF Diagram

The VRF system runs on a basic vapor compression cycle (VCC) where the refrigerant is compressed, exchanges heat with ambient/indoor air, expands through a valve, and transfers heat to ambient/indoor air. The difficulty in implementing single-unit vapor compression heat pumps in large buildings is that there needs to be extensive ductwork to transfer outdoor air into the unit for heat transfer. This is generally why large buildings have outdoor units that heat or cool air. The problem with a completely outdoor unit is that there is no ability for individual zone temperature control since all supply air is at one temperature. Variable refrigerant flow systems solve this problem as they only require piping for refrigerant flow and allow for zone-level control. In cooling mode, the refrigerant transfers heat to the outdoor air and then passes to the control unit. The control unit opens and closes the valves to the indoor units based on cooling/heating load needs. The refrigerant then passes through the terminal unit and absorbs

heat from the indoor air thus cooling the space. The compressor within the outdoor unit is a variable speed compressor which has much better part load operation and cuts back on inefficiencies during times of low load. The system runs in reverse for heating operation. One of the main drawbacks to VRF systems is that they must be accompanied by a dedicated outdoor air system since there is no ductwork.

Thermodynamically, VRF systems provide high efficiency. An EES study of a vapor-compression cycle in the heating mode provided insight into comparison to a typical boiler system [6]. Since VRF systems feature variable speed compressors, the analysis assumed that the isentropic efficiency of the compressor stays constant. Furthermore, the analysis assumed that there was no pressure drop through piping or across the heat exchangers and that the expansion process was isenthalpic. The analysis further assumes that the refrigerant temperatures in the heat exchangers are 20°F plus or minus the air temperatures and that the fluid properties of air are constant. The refrigerant has the standard 10°F (~5°C) subcooling out of the condenser and 10°F (~5°C) superheating out the evaporator for system reliability. Table 2 contains the cycle parameters including the air inlet and outlet conditions on both sides. Figure 3 shows the Pressure-Enthalpy (P-h) diagram of the cycle as modeled with the specified parameters.

Table 2 – EES Vapor Compression Cycle Parameters

Parameter	**Value**
Refrigerant	R-410A
Isentropic Compressor Efficiency (η_c)	0.8
Outdoor Inlet Air Temperature	45°F
Indoor Inlet Air Temperature	70°F
Indoor Outlet Air Temperature	90°F
Air Flow Rate Through Condenser	35,000 cfm

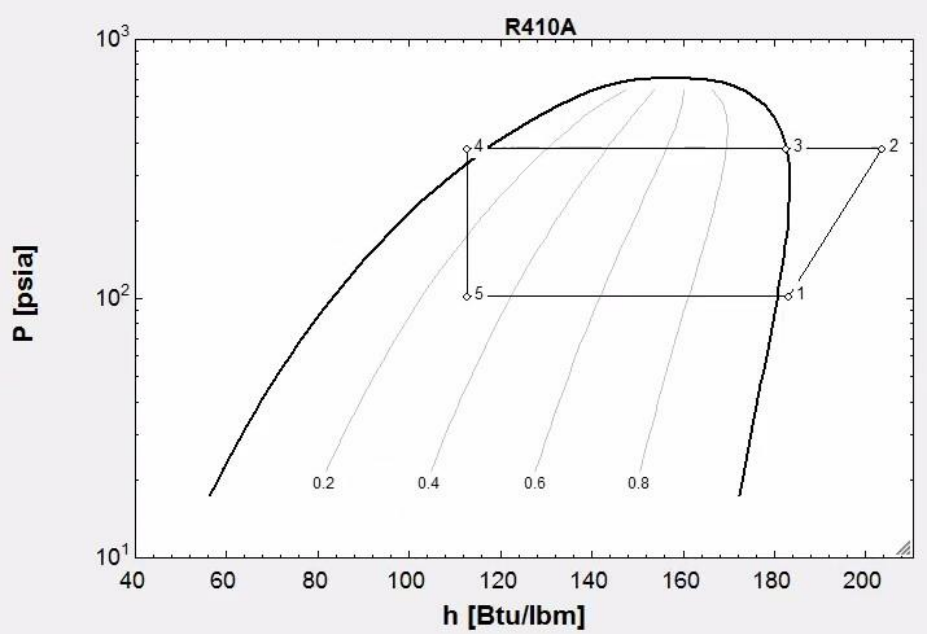

Figure 3 – P-h Diagram of Vapor Compression Cycle

Analysis of this cycle yielded a coefficient of performance (COP) of heating of 4.48. The total heat transfer rate to the air was 741.0 MBH and the power usage of the compressor was 165.6 MBH. A hot water coil, however, must supply the heat via direct heat transfer from hot water heated by a boiler. If the boiler efficiency is 80%, this yields a power input of fuel of 926.3 MBH. This fuel may take the form of natural gas, fuel oil, propane, or other boiler fuel supplies.

The further analysis investigated the effect of outdoor air temperature on. The indoor conditions remained constant but the outdoor inlet temperature varied from -10°F to 50°F. Table 3 contains the outdoor air temperature with its associated COP of heating. COP drastically decreased as outdoor air temperature decreased. This is largely due to the increase in compressor work with no increase in heating capacity. These effects are more drastic when inefficiencies such as heat exchanger piping losses, and further compressor losses are considered. This analysis illustrates a variable refrigerant flow system's energy savings potential and potential drawbacks.

Table 3 – Parametric Analysis of Outdoor Air Temperature on COP

Temperature (°F)	COP
-10	2.61
-4	2.74
2	2.88
8	3.03
14	3.20
20	3.39
26	3.60
32	3.84
38	4.11
44	4.42
50	4.78

*Indoor Air Temperature: 70°F

1.3 Ground-Source Heat Pump Basics

VRF systems are a form of an air-source heat pump since one of their temperature reservoirs is the ambient air. Ground-source heat pumps (GSHP), however, take advantage of the relatively constant temperature to eliminate the variation in performance experienced by air-sourced heat pumps in extreme ambient conditions. This is because the hot and cold reservoirs between which the heat pump operates are closer in temperature. This analysis investigates closed-loop GSHPs which pump a working fluid through a network of ground heat exchangers to either absorb or reject heat. One of the most common types of ground heat exchangers is a vertical bore field. Vertical bore fields are long tubes that extend deep into the ground and loop back up. The system pumps the working fluid through the bore field and to the condenser/evaporator in the heat pump. The working fluid is most commonly an antifreeze solution to prevent freezing in the winter. The heat pump itself, like the VRF system, runs on a basic vapor-compression cycle. Figure 4 shows a diagram of a basic GSHP.

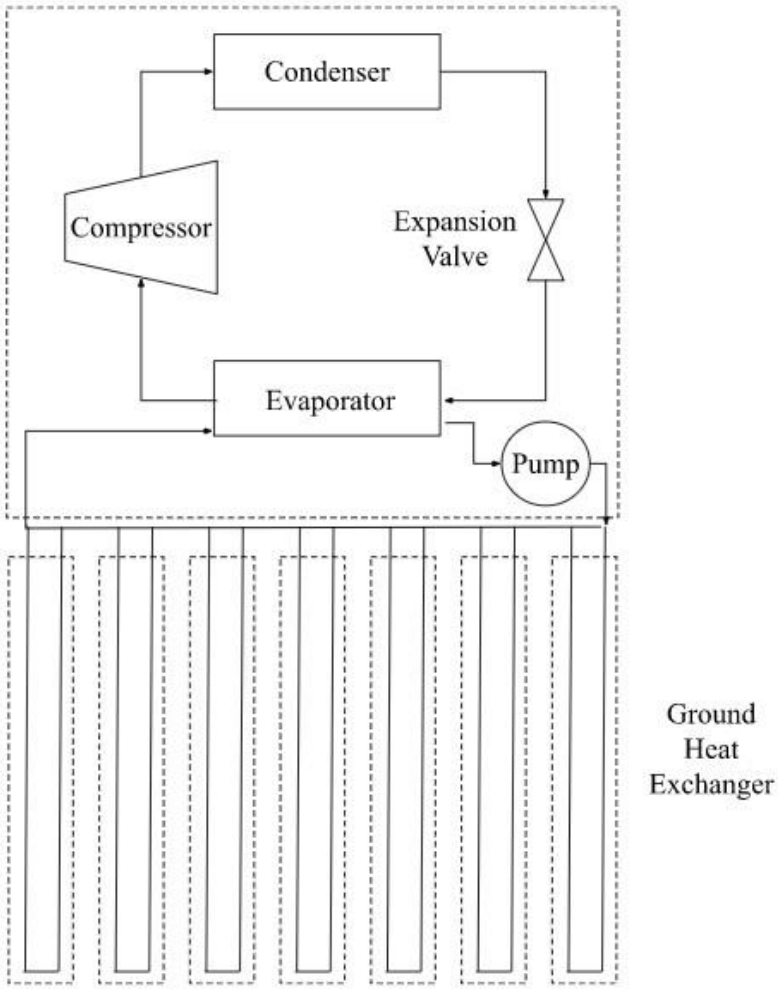

Figure 4 – GSHP Diagram

Theoretically, since the ground is a large thermal mass and the deep ground temperature is not affected by seasonal changes, the cold reservoir during heating operation is assumed constant. In the analysis of a heat pump, this is to say that the "ambient" temperature does not change and is constant at 45°F. In theory, this means that the COP would stay constant at 4.48 no matter the outdoor temperature. This phenomenon is very useful in cold climates.

One potential challenge with GSHPs is load balancing. While in the short term the ground temperature stays relatively constant, over long periods there is the possibility for changes in temperature if the heating and cooling loads are not balanced. For example, in hot climates, the load is cooling-dominated which in turn can increase the ground temperature

significantly lowering the efficiency of the heat pump. Conversely, in colder climates, the load is heating dominated which will decrease ground temperature resulting in lower efficiency. It is important when designing GSHPs to pay particular attention to heating and cooling load to optimize performance.

1.4 Literature Review

The literature contains extensive studies regarding energy savings potential in existing commercial buildings. This literature review is focused on technologies that contribute to the further electrification of the facility.

1.4.1 Electric Reheat

Raftery et al. (2018) attempted to quantify energy losses in hot water reheat systems. The case study included simulations on a five-story, 118,400 ft^2 office building in California. A natural gas boiler supplies the 98 VAV terminal units with hot water reheat coils. Their method included using sensors installed on VAV units to calculate both useful and wasted hot water reheat energy. The study found that only about 21% of gas energy is converted to useful reheat energy with an uncertainty of at most 14% [7]. These losses come from transmission losses (moving hot water from the boiler to the coil in the VAV unit) as well as heat exchanger inefficiencies within the coil itself. Furthermore, they conducted an economic analysis of hot water and electric reheat systems. Electric reheat systems are generally more energy efficient than hot water reheat systems due to their limited transmission losses. They also exhibit cheaper installation costs which the authors estimate to be around $\$2.79/ft^2$ [7]. The drawback is that utility costs result in the operating costs being higher. They found that hot water reheat systems

are slightly more cost-effective than electric reheat systems in the long term due to low natural gas prices in the United States, however, this analysis changes with changing source prices.

1.4.2 Electric Water Heating

Further potential for electrification while maintaining a VAV system is implementing electric water heating in place of a natural gas boiler. A study by A study by Ibrahim et al. (2013) looked at different water heating systems and evaluated them based on energy and environmental aspects. They stated that electric water heaters have low maintenance costs and a longer service life compared to gas water heaters. Furthermore, electric water heaters do not produce any local pollutants and have fewer standby losses. The drawbacks, however, are that electric water heaters generally consume more primary energy than gas water heaters due to inefficiencies in electricity production. This is largely dependent on the location within the country and how electricity is produced. Electric water heaters also have historically higher operating costs due to the low price of natural gas in the United States [8].

1.4.3 Variable Refrigerant Flow Heat Pump

One of the most efficient means of electric heating is via heat pump technology. In large buildings where it is difficult to have individualized heat pumps, a variable refrigerant flow system is a viable alternative. Due to their complexity, it is difficult to fully quantify dynamic performance, however, numerous studies attempt it. Zhou et al. (2017) created an EnergyPlus model of a VRF system and compared the results to experimental data. At this time, EnergyPlus did not have a built-in VRF system, and instead, they constructed a VRF system based on existing air-cooled heat pumps. They implemented modifier curves based on typical characteristics of VRF systems. The model building was the Thermodynamics Lab Building at

Shanghai Jiaotong University in China. Their results showed that the model was able to predict power usage to within 28.3% with the weekly average error in COP limited to within 6.4% [9].

Zhu et al. (2013) attempted to create their model for the analysis of VRF systems. Their approach featured a machine learning algorithm that simultaneously solved individual component models (i.e. Evaporator, Condenser, Expansion Valve) and adjusted parameters until all components were balanced. Their model predicted energy consumption and COP to be within 4.6% and 1.2% respectively [10]. After, Zhu et al. (2013) attempted to apply this model to a VRF system in heating mode combined with an outdoor air processing unit. The model building was again the Thermodynamics Lab Building at Shanghai Jiaotong University in China. Model validation was based on the data from the 2007 Zhou experiments. The model predicted energy consumption and COP to be within 12.5% and 6.2%, respectively [11]. The important conclusion was that VRF systems demonstrate the ability to maintain comfortable zone conditions and setpoints. Zhu et al. (2014, 2015) further investigated optimal control strategies for maximum energy savings in VRF systems [12, 13]. This thesis does not consider different control strategies; however, it recommends it as future work.

Ozahi et al. (2016) conducted a simulation on an existing cultural center building to compare VRF performance to a conventional HVAC system. The model building was 95,282 ft^2 with a total capacity of 1,400 people. The building was made of reinforced concrete with one basement and four above-ground levels. The existing HVAC system consisted of two liquid-fueled boilers that create hot water to pass through fan coil units. The HVAC system also featured air-cooled chillers which created chilled water to pass through the chilled water coil in the air-handling unit. Their model resulted in predicted electricity consumption of 1,447,594 kBtu and fuel consumption of 145,492 lbs/year for the conventional HVAC system [14]. The

system used fuel oil which has a lower heating value of around 17.0 kBtu/lb. This resulted in 3,920,958 kBtu of total energy consumption per year. The model predicted an electricity consumption of 1,717,392 kBtu for the VRF system with no fuel consumption. This resulted in a total energy savings of 56%. They further conducted an economic analysis of the two systems and concluded that the VRF system resulted in a 44% profit as compared to the conventional system. It is important to note that this analysis was based on the installation and operating costs in Turkey and not the United States.

Kim et al. (2017) attempted to model the potential energy savings of VRF systems from variable air volume (VAV) systems across all U.S. climate locations. They utilized EnergyPlus and the new VRF modeling module. The building was a mid-size office building that consisted of three floors totaling 53,281 ft^2. The simulated conventional system was a gas furnace and air-sourced heat pump inside a packaged rooftop unit with VAV terminal boxes with electric reheating coils. Their model resulted in energy savings for all climate zones while still maintaining the ability to achieve proper zone conditions. For climate zone 6A, the VRF system exhibited heating energy and total HVAC energy savings of 44% and 39%, respectively over the VAV system [15].

Zhang et al. (2019) conducted a literature review on recent developments in VRF systems since 2015. Specifically, concerning energy modeling, they concluded that though the complexity of VRF systems presents difficulties, current modeling techniques have proved highly accurate. Modeling software such as EnergyPlus provides tools for the comparison of energy-saving options. In general, the literature has shown that VRF systems are more energy efficient than VAV systems but do not quite reach the level of efficiency of ground-source heat pumps [16].

1.4.4 Ground-Source Heat Pump

GSHPs are becoming more popular as a means of electrification. This literature review focuses on baseline performance characteristics rather than component design. Ozgener and Hepbasli (2017) conducted a modeling experiment in an attempt to evaluate the performance of GSHP systems. Their model predicted a heat pump COP between 3.12 and 3.64 [17]. This model demonstrated the ability of the GSHP to operate at a relatively constant COP as compared to air-source heat pumps which are affected greatly by varying outdoor air temperatures.

Liu and Hong (2009) conducted simulations to compare the energy efficiency between VRF and GSHP systems. Since EnergyPlus had yet to release the VRF modeling module, they used a user-created function in the EnergyPlus predecessor, DOE-2. They ran their simulations in Miami, FL, and Chicago, IL to observe performance in both hot and cold climates. They found that in Miami the GSHP system resulted in a 9.4% energy savings over the VRF system [18]. In Chicago, the energy savings were 24.1% [18]. They concluded that the energy savings potential of GSHPs is greater in climates that have heating-dominated loads.

Wang (2013) conducted simulations to compare the energy efficiency between VRF and GSHP systems using the new EnergyPlus VRF module. The model building was a small, one-story office building with a total floor area of 5,005 m^2. The model assigned schedules for occupancy and plug loads. The model ran in three different U.S. climate zones that included the cities of Chicago, Baltimore, and Atlanta. The model assumed the baseline VRF EnergyPlus template which assigned a cooling COP of 3.29 and a heating COP of 3.55. Furthermore, the VRF template assigned all of the modifier curves based on experimental data of a typical VRF system. The study resulted in a 19.0%, 18.5%, and 17.6% reduction in electricity consumption for the GSHP system over the VRF system in Chicago, Baltimore, and Atlanta, respectively [19].

These results corroborated the conclusion by Liu and Hong that the energy savings potential is greater in heating-dominated climates. Wang further investigated the peak electrical demands of a GSHP and VRF system. For Chicago, Baltimore, and Atlanta, the peak electrical demand reduction was 40%, 35%, and 31%, respectively [19]. This allows the electrical grid to better manage the load. Finally, the GSHP system was much better at maintaining a setpoint than the VRF system. For the GSHP system, the unmet heating hours were 17, one, and zero for Chicago, Baltimore, and Atlanta respectively [19]. For the VRF system, those numbers were 454, 185, and 49 [19].

Zhou et al. (2016) conducted simulations to assess the feasibility of GSHP systems in office buildings in China. More specifically, they investigated the effect of the cooling-to-heating load ratio on performance. They found that in cold regions, a GSHP system should be stable within 20 years when the ratio of cooling load to heating load is between 0.2:1 and 5:1 [20]. They did find, however, that when the loads are not balanced the soil temperature drastically changes over time which can lead to system performance degradation. For example, with a cooling and heating consumption ratio of 0.2:1, the average soil temperature dropped from 15.5℃ (60℉) to 2℃ (35.6℉) [20]. This study further showed that GSHP systems lose substantial energy efficiency in extreme cold or extremely hot climates (i.e. where the cooling-to-heating consumption ratio falls outside the specified stability range).

Liu et al. (2017) attempted to model a hybrid GSHP system for an office building in China to evaluate its feasibility and performance. The hybrid system they proposed featured a GSHP with a gas boiler as an auxiliary heat source. The purpose of the boiler was to solve the loading problem presented by Zhou et al. (2016) in colder climates. The GSHP operated at a set cooling-to-heating consumption ratio and the boiler provided additional heating. The COP during

the heating season of the hybrid system was higher than the COP of just the GSHP system without the auxiliary boiler (2.79 compared to 2.62) [21]. Furthermore, over the course of ten years, the hybrid system so no long-term decrease in average soil temperature whereas the basic GSHP system saw a 5°C decrease [21].

Karytsas and Choropanitis (2017) conducted a principal component analysis for GSHP systems to understand the barriers against and actions toward their implementation in Greece. Their study found that they provide between 33% and 43% energy savings over natural gas and air-source heat pump systems resulting in a large reduction in carbon dioxide emissions, however, their payback period is around a decade [22]. Long payback periods, high initial investment costs, and lack of technical knowledge are some of the largest barriers to implementation. They recommended providing financial incentives and establishing certifications/technical regulatory guidelines as an action to spur diffusion into the market.

Yin et al. (2019) conducted an in-field performance evaluation and economic analysis on residential GSHPs during heating operations in Iowa. Their study consisted of 32 GSHPs with 16 having vertical ground heat exchangers and 16 having horizontal ground heat exchangers. 28 out of 32 of the GSHPs exhibited lower calculated COPs compared to their nominal values. The average COP was 80% of the nominal value over the course of the experiment [23]. GSHPs with vertical borehole heat exchangers had less variation in COP than GSHPs with horizontal heat exchangers. They estimated a median energy cost savings of 70-77% compared to natural gas systems [23]. Furthermore, they estimated a median carbon dioxide emissions reduction of 45% compared to natural gas systems.

In 2022, Kapicioglu and Esen conducted an economic and environmental assessment of GSHP systems in Turkey. Similar to Wang, they found that air-source heat pumps required

supplemental heating in the months with high heating load due to decreased efficiency whereas GSHPs did not. Their model found that GSHPs exhibited a 31.1% and 63.5% lower operating cost than natural gas and air-source heat pump systems [24]. These values were based on Turkish energy prices. Furthermore, over a 20-year design life, they predicted that a GSHP system reduces carbon emissions by 28.9% and 36.7% in comparison with natural gas and air-source heat pump systems respectively [24].

1.5 Objective of Study

HVAC system electrification is a key component of a decarbonized energy future. At the present, many large commercial buildings still utilize gas-fired hot water boilers as a means of providing heating. While natural gas burns much cleaner than alternatives such as diesel, fuel oil, or coal, the logical next step is to continue toward total decarbonization. The purpose of this study is to investigate potential electrification options and compare them in terms of energy consumption, carbon emissions, and operating costs using current energy prices to establish a baseline with which to continue more in-depth research. While operating costs are not the true focus of this analysis, it is an important consideration when discussing the likelihood of widespread adoption. More specifically, this study investigates the following configurations:

- Gas-Fired Boiler with VAV Electric Reheat
- Electric Boiler with VAV Hot Water Reheat
- Variable Refrigerant Flow Heat Pump System
- Ground-Source Heat Pump System

This analysis uses the whole-building energy modeling software EnergyPlus along with the OpenStudio interface to run dynamic, whole-year, simulations for comparison. The model facility is a mid-sized hospital located in Brunswick, Maine, and all conclusions drawn should be

specific to this particular type of facility. Given their high ventilation requirements and 24-hour operation, their energy use is much different from other types of buildings. Evaluation of these technologies for other facilities requires a different analysis.

Chapter 2: Case Study Building

Mid Coast Hospital, located in Brunswick, Maine, is the building used in this analysis and shown in Figure 5. The facility has a total floor area of 171,382 ft^2 spread across two above-ground floors and a basement level. The building has three sections: A, B, and C as shown in Figure 6. Sections A and B were constructed in 2000. Section C was added in 2009 and contains the new emergency department and part of the surgical wing. This analysis only uses section C as the wing is self-contained and connected to the rest of the building by a set of fire doors on the top two floors. Section C contains its air handler, chiller, and VAV system making it a representative model.

Figure 5 – Mid Coast Hospital [25]

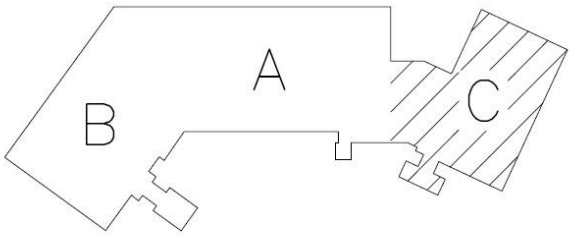

Figure 6 – Building Sections [26]

2.1 HVAC System

2.1.1 Air Handing Unit

The air handling unit (AHU) for this facility is a 2009 Haakon designed for 35,000 cfm. The unit features a supply fan, return fan, four chilled water coils, four steam heating coils, and a humidifier. The unit has a minimum OA flow rate of 12,800 cfm. Tables 4, 5, and 6 contain the specifications for the AHU components.

Table 4 – Supply/Return Fan Specifications [27]

SUPPLY FAN (TYP 2)						RETURN FAN (TYP 2)					
FAN TYPE	DIA.(IN)	E.S.P. (in. w.g)	T.S.P (IN WG)	MOTOR HP	FAN RPM	FAN TYPE	DIA.(IN)	E.S.P. (in. w.g)	T.S.P (IN WG)	MOTOR HP	FAN RPM
SPF CLASS 3	27	3.0	8.6	60	2,015	SPF CLASS 1	30	2.5	3.5	25	1,280

Table 5 – Chilled Water Cooling Coils Specifications [27]

CHILLED WATER COOLING COILS											
NO. OF COILS	FPM	EAT db/wb (°F)	LAT db/wb (°F)	TOTAL MBH	SENS MBH	P.D. (in.wg.)	FLUID	GPM	EWT °F	LWT °F	P.D. (FT)
4	400	80/67	52.1/51.8	1,622	1,059	0.81	30% PROP. GLYCOL	283	44	56	16.4

Table 6 – Steam Heating Coils/Humidifier Specifications [27]

STEAM HEATING COILS									HUMIDIFIER	
NO. OF COILS	FPM	EAT db (°F)	LAT db (°F)	TOTAL MBH	STEAM LBS/HR	P.D. (in.wg.)	FLUID	STEAM PRESS PSIG	PSIG	#/HR.
4	497	0	50.4	1,914	1,992	0.04	LPS	5	5	650

Both outdoor and recirculated air enters the air handler via the supply fan and passes over the steam or cooling coils if necessary to achieve the proper setpoint. This temperature setpoint is further discussed later. The air then passes through the humidifier if necessary to achieve the proper humidity setpoint. Again, this setpoint is further discussed later. The air continues to the VAV boxes in the individual zones and is returned by the return fan. Other components of the air handler not discussed are dampers, sound attenuators, and air filters. Figure 7 contains a simplified diagram of the air handler.

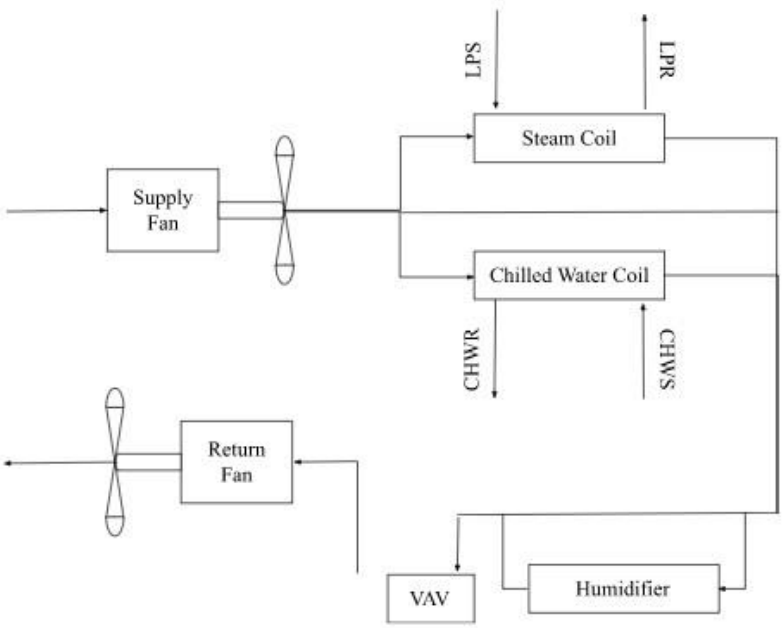

Figure 7 – Air Handler

2.1.2 Air-Cooled Chiller

The air-cooled chiller for this building is a Trane RTAC 140 High-Efficiency model. This chiller works off a vapor-compression cycle to create chilled water to supply cooling coils. There are two main types of vapor-compression chillers in production: air-cooled chillers and water-cooled chillers. Generally speaking, water-cooled chillers allow for greater energy efficiency as the condenser operates at the ambient wet bulb temperature rather than the ambient dry bulb temperature. The ambient wet bulb temperature is always less than or equal to the dry bulb temperature. Lower condensing temperature means that the cycle is more efficient. The drawback, however, is that places with extremely cold temperatures have to implement control measures to keep water from freezing in the cooling tower in the winter months. Energy expended for heating, in some cases, may outweigh the energy savings. Mid Coast Hospital utilizes the second form of a vapor-compression chiller, the air-cooled chiller. The air-cooled chiller uses ambient air to cool the refrigerant in the condenser. A chiller is preferred in a large

building due to its large cooling and dehumidification capacity compared to traditional air conditioning units. Figure 8 contains a simplified diagram of the air-cooled chiller. Table 7 contains the specifications for the chiller components. Notice that the chilled water produced contains 30% propylene glycol. The purpose of this is to act as an anti-freeze. Engineers carefully select propylene glycol concentration to balance anti-freeze needs with heat transfer efficiency.

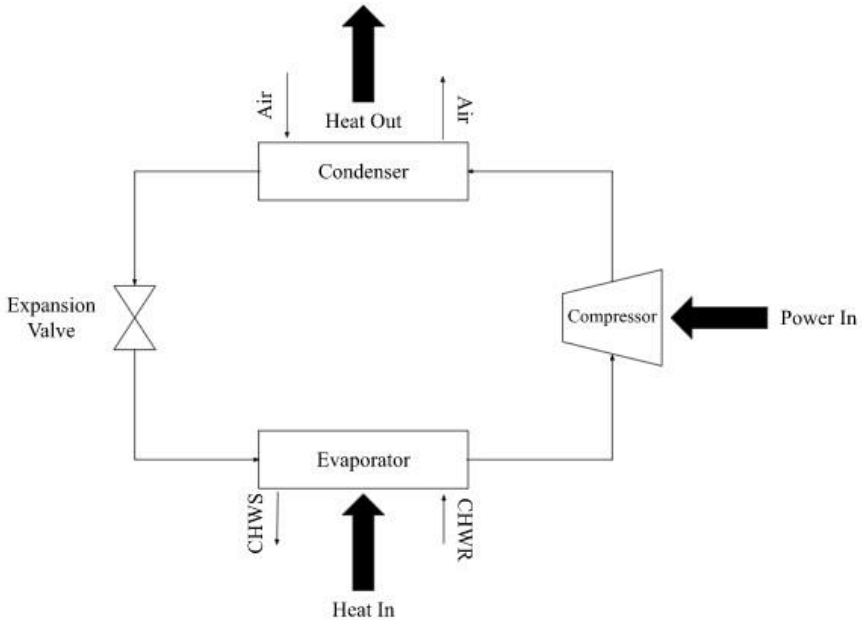

Figure 8 – Air-Cooled Chiller

Table 7 – Air-Cooled Chiller Specifications [27]

TYPE	FLUID	CAPACITY TONS	EVAPORATOR				CONDENSER FANS			COMPRESSORS		EFFICIENCY EER
			EWT (°F)	LWT (°F)	GPM	WATER PD (FT.)	EAT (°F)	NUMBER	KW	NUMBER	RLA	
AIR COOLED	30% PROP GLYCOL	131.1	56	44	275	6	95	10	1.5 EACH	2	113 EACH	9.8

Chilled water produced in the air-cooled chiller supplies the cooling coil within the AHU. The coiling coil provides cold air to the VAV boxes for zone cooling as well as dehumidifies incoming air to meet facility comfort requirements. Pumps pass the water through the air-cooled chiller, to the coiling coils, and back through a pump house containing a buffer tank to manage water volume. Figure 9 contains a basic diagram of the chilled water loop. The chilled water

loop also has various valves to control flow rate and pressures as well as equipment to monitor and replenish glycol levels in the water. Appendix A contains the full chilled water loop diagram.

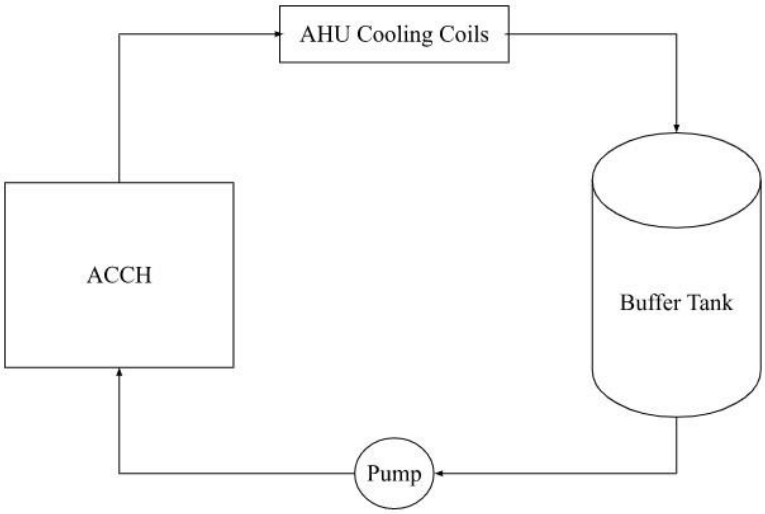

Figure 9 – Chilled Water Loop

2.1.3 Hot Water/Steam Loop

Three firetube boilers provide steam and hot water to the entire facility. All three boilers are Cleaver Brooks CBLE-250 models installed in the year 2000. Each boiler is rated to supply steam at 8,625 lbs/h and burn 10,206 cfh of natural gas. An HVAC schedule supplied by the facility contains all of the boiler characteristics. The boiler supplies two main loops throughout the hospital.

The steam loop supplies steam at 212°F to the preheat coils and the humidifier within the air handler. After the steam leaves the boiler at 100 psig, it passes through several expansion valves creating low-pressure steam at 10 psig before it passes through the preheat coils and humidifier. Figure 10 contains a simplified diagram of the steam loop. Appendix B contains the full steam loop diagram for further reference.

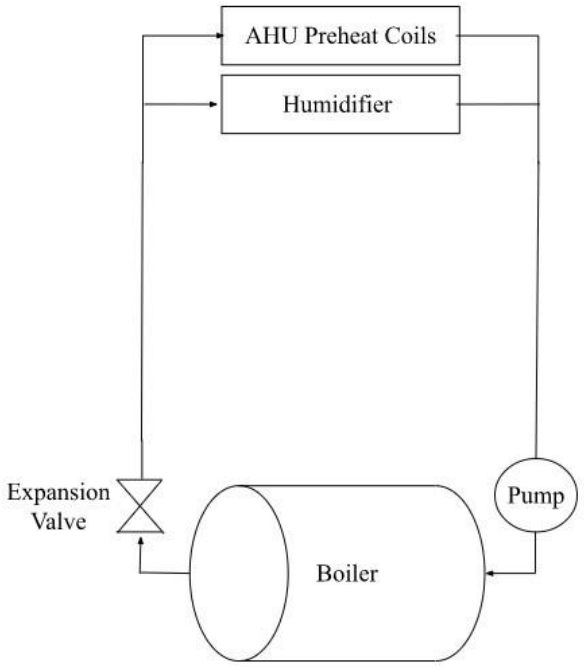

Figure 10 – Steam Loop

The hot water loop supplies hot water at 180°F to the reheat coils in the VAV boxes as well as reheat coils within the unit space heaters. Low-pressure supply steam from the boiler passes through a heat exchanger to reheat the returned water. The water also passes through various valves to control individual unit operating points. Figure 11 contains a simplified diagram of the hot water loop. Appendix C contains a diagram of the full hot water loop.

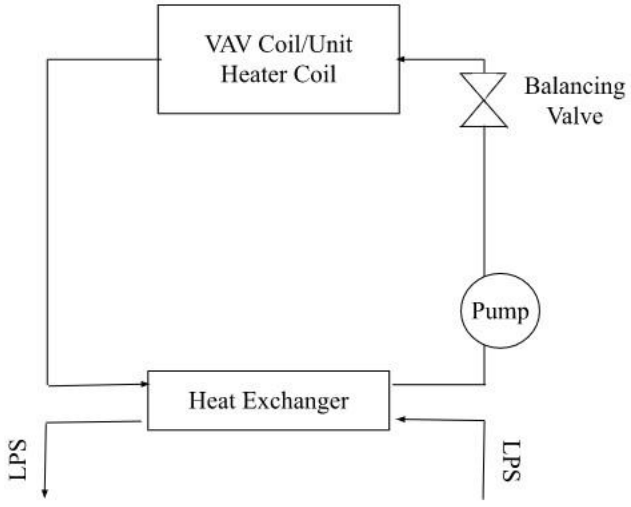

Figure 11 – Hot Water Loop

2.1.4 VAV Boxes

A variable air volume (VAV) box is zone-level HVAC equipment that allows air to be distributed from the air handler to the zone. As opposed to constant air volume (CAV) boxes which have a fixed air flow rate, VAV boxes allow for the air flow rate to be varied to meet ventilation and heating/cooling requirements. VAV boxes have a specified design range for flow rates and are sized based on HVAC requirements. VAV systems are more energy efficient than CAV systems due to their ability to reduce capacity during times of reduced load. A study by Lu and Warsinger (2020) featured model simulations and concluded that a VAV system can achieve 24%-42% energy savings over a CAV system in large residential buildings [28]. Hospitals have large baseline ventilation requirements that increase during times of peak occupancy. A VAV system provides flexibility while also minimizing energy usage.

Within the VAV boxes are hot water reheat coils to provide zone-level temperature control. The steam coils within the AHU only serve to preheat the air. The hot water coils are supplied by the hot water loop via the boiler. The thermostat setting by the zone determines the air and water flow rates. All VAV boxes in the building are Enviro-Tec SDR or SDL models. The HVAC schedule for each VAV reheat box was provided by the facility. Table 8 contains the specifications for VCV-5 as a reference. Appendix D contains the specifications for all VAV boxes.

Table 8 – VCV-5 Specifications [27]

DESIGNATION	LOCATION	SERVICE	TYPE	DESIGN RANGE (CFM)	△ PRESS IN. H_2O (MAX)	HOT WATER COIL								
						MBH	EAT °F	AIR △P IN H_2O	FPI MAX	MIN. NO. OF ROWS	EWT °F	LWT °F	GPM	MAX △P FT. H_2O
VCV-5	SEE PLANS	SEE PLANS	VARIABLE VOLUME	65-250	0.7	SEE PLANS	55	0.5	10	10	180	160	SEE PLANS	8

2.1.5 Unit Heaters

In addition to the VAV system, there are unit heaters in dedicated places throughout the building. Zones without a VAV box, such as entryways and stairwells, are generally where they are located. Some zones that are serviced by the VAV system also have supplemental heaters because of their proximity to doors. All of the unit heaters contain hot water coils that provide the heating capacity. The water is supplied by the hot water loop. Unit heaters provide air at a fixed flow rate. Table 9 contains the specifications for CUH-1. Appendix E contains the specifications for all unit heaters.

Table 9 – CUH-1 Specifications [27]

DESIGNATION	LOCATION	TYPE	FAN							HOT WATER COIL			
			CFM	RPM	# FANS	MOTOR (HP)	V	ø	HZ	MBH	EAT	GPM	EWT
CUH-1	SEE PLANS	FLOOR	345	875	1	1/10	120	1	60	25	60	4.0	180

2.2 Building Materials

The facility provided the construction materials for the roof, exterior walls, interior walls, and interior ceilings/floors.

2.2.1 Roof, Exterior Floor, and Interior Ceiling/Floor

From interior to exterior, a roofing membrane, cover board, tapered rigid insulation, vapor barrier, and a concrete slab compose the roof. The entire roofing assembly has an effective insulation of R-30 which is per ASHRAE recommendations for large hospitals in climate zone 6 [29]. Figure 12 shows the roofing assembly as presented in the architectural drawings for the building.

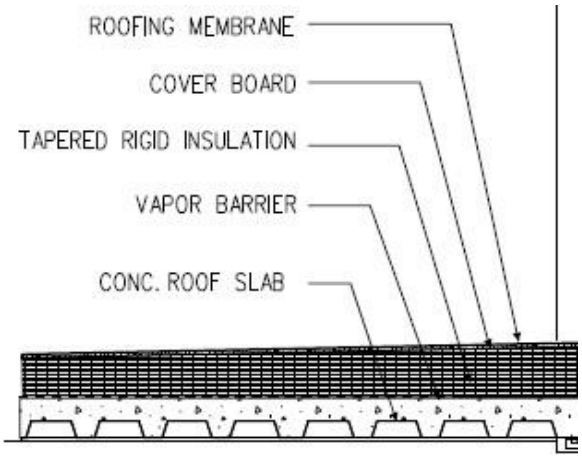

Figure 12 – Roof Construction [30]

From exterior to interior, the exterior floor is comprised of crushed stone, tapered rigid insulation, a vapor barrier, and a concrete slab. The effective insulation is R-17.5 which is per ASHRAE recommendations for large hospitals [28].

The interior ceilings and floors are comprised of a concrete slab with either carpet or tile on the top (floor side) depending on the room and have an effective insulation of R-0.5.

2.2.2 Exterior and Interior Walls

From interior to exterior, five eight-inch gypsum wallboard, six-inch metal studs, exterior sheathing, three-inch spray polyurethane foam insulation, two-inch nominal air gap, and three and five eight-inch face brick compose the exterior wall. The entire exterior wall has an effective insulation of R-20 which complies with ASHRAE standards for large hospitals in climate zone 6 [29]. Figure 13 shows the exterior wall partition presented in the architectural drawings for the building.

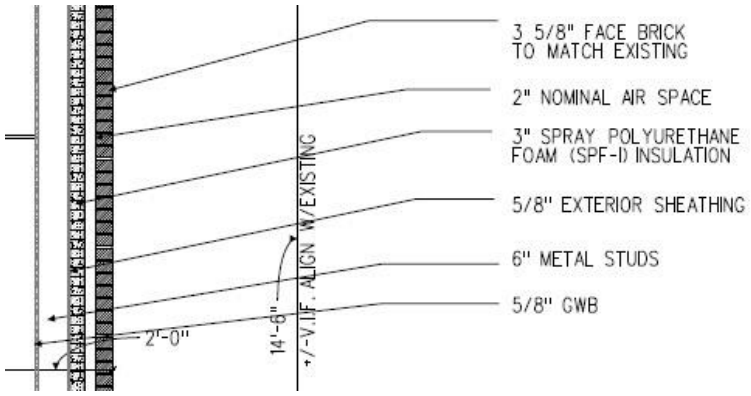

Figure 13 – Exterior Wall Construction [30]

The interior walls are composed of six-inch metal studs with five eight-inch gypsum wallboard on both sides and have an effective insulation of R-1.

Chapter 3: EnergyPlus Modeling of Building

This analysis uses the whole-building energy modeling software EnergyPlus [31]. The U.S. Department of Energy initially launched EnergyPlus in April 2001. Since then, there have been countless versions with increasingly more complex capabilities. This model uses EnergyPlus version 9.6 released in September 2021.

OpenStudio is a software tool used for EnergyPlus modeling developed by the National Renewable Energy Laboratory, Argonne National Laboratory, Lawrence-Berkeley National Laboratory, Oak Ridge National Laboratory, and Pacific Northwest National Laboratory [32]. OpenStudio Application is a graphical user interface that runs on the OpenStudio Application Programming Interface (API) and allows for ease of simulation by providing a user-friendly platform. Within the application, the user can draw floorplans, create construction materials, and drag and drop components to design HVAC systems (among other capabilities). OpenStudio drastically lowers model development time. This model uses OpenStudio version 3.3 released in November 2021 and OpenStudio Application version 1.3 released in December 2021 [33].

The modeling was linear in that EES models helped prove the concept and establish a general reference for relative performance. The baseline EnergyPlus model contained the components specified in the plans provided by the facility. Since the facility did not provide a control method, this analysis required iterations of the model with various control methods until the model was within a reasonable range of the energy bill summary. Subsequent models described in this section provided a comparison to the baseline. Figure 14 shows a flow chart of the modeling approach.

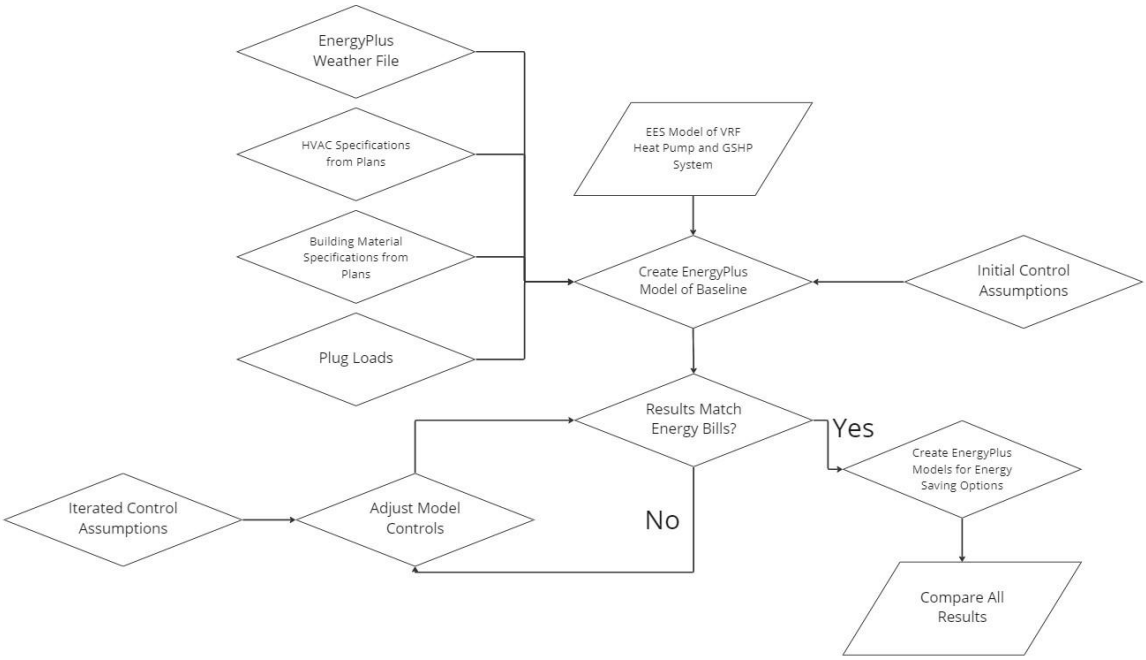

Figure 14 – Modeling Approach

3.1 Building Envelope

The building contains two above-ground floors and a very small section of the basement. This model neglects the basement as it comprises a small portion of the floor area and contains only a mechanical room with its self-contained HVAC equipment.

There are numerous different approaches to applying thermal zones to a building envelope. In most energy simulation models, it is not practical to assign each space a thermal zone. A literature review conducted by Shin and Haberl (2019) concluded nobody has clearly defined a set of rules for HVAC zoning in simulation, however, the conventional approach is the perimeter and core model [34]. Figure 15 contains a diagram of a perimeter and core model in a simple, rectangular one-story building. The perimeter and core model operates on the assumption that the exterior rooms on the same wall as well as interior rooms have similar HVAC requirements because they have similar sun exposure, shading, window glazing, etc. Shin and Haberl [30], discuss studies that prove this is much more accurate than many alternatives. This

model, however, attempts to predict the energy use of a hospital rather than a typical office or residential building. Hospitals have very specific ventilation requirements which make zoning much more difficult. Given this, the zoning for the building follows the actual HVAC zoning contained in the plans. The building is small enough for the program to run successfully.

Figure 15 – Perimeter and Core Zoning Model

3.1.1 Floor Plan

The first floor consists of 50 fully-enclosed spaces, one open area/passageway, two stairwells, and two elevator shafts. Figure 16 contains the floor plan of the first floor.

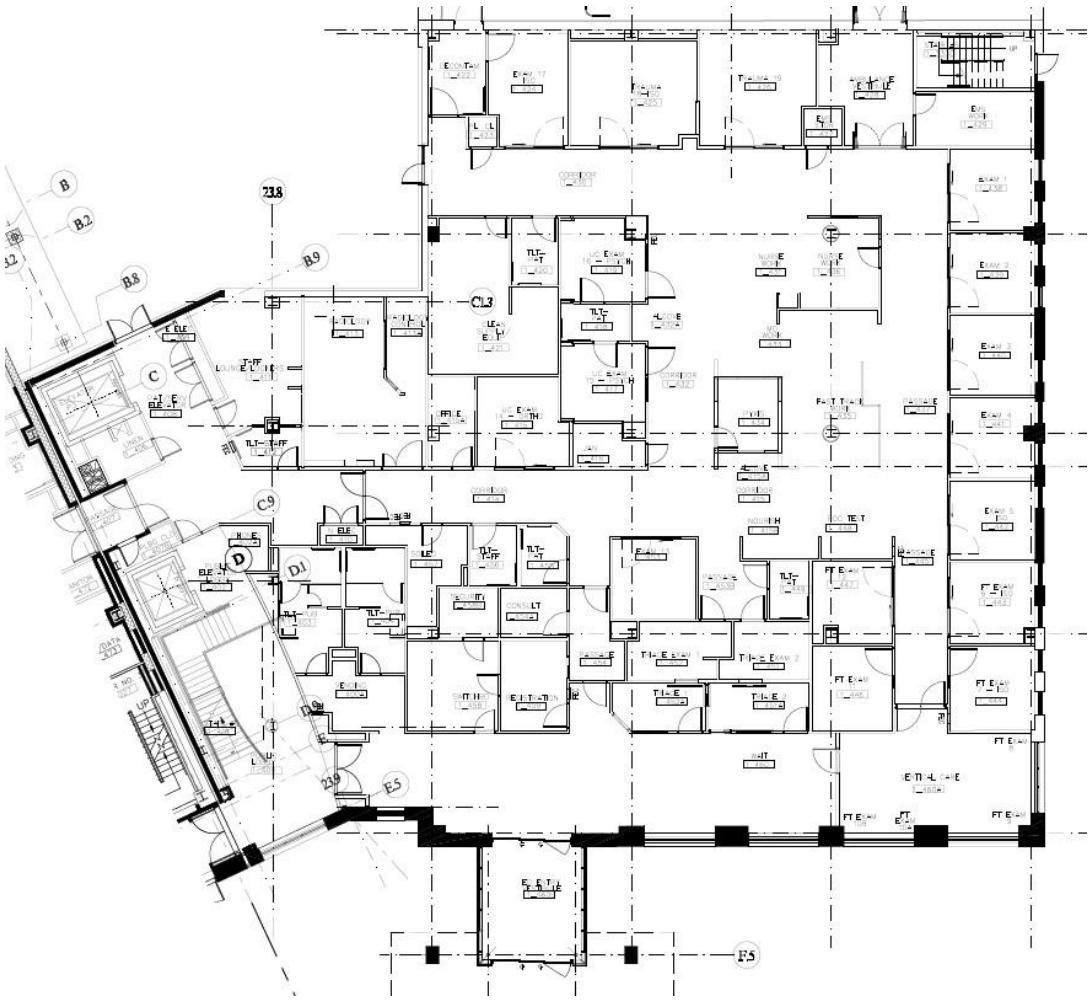

Figure 16 – First Floor Plan [26]

Due to application constraints with building size, individually assigning a separate space to each room resulted in program failure. Instead, spaces are assigned by thermal zones of HVAC equipment with a few exceptions. The model further combines adjacent identical exam rooms with the same HVAC specifications as well as adjacent rooms that are classified as miscellaneous (and thus hard to accurately model) such as office space and storage that also have the same HVAC requirements. This results in each space having its thermal zone with specified HVAC equipment. In terms of modeling, HVAC equipment having control over one zone greatly decreases run time. Furthermore, fewer spaces mean fewer individual faces for the program to

run heat transfer calculations on, thus further decreasing run time. Figure 17 contains the floor plan of the first floor within the model along with associated space numbers.

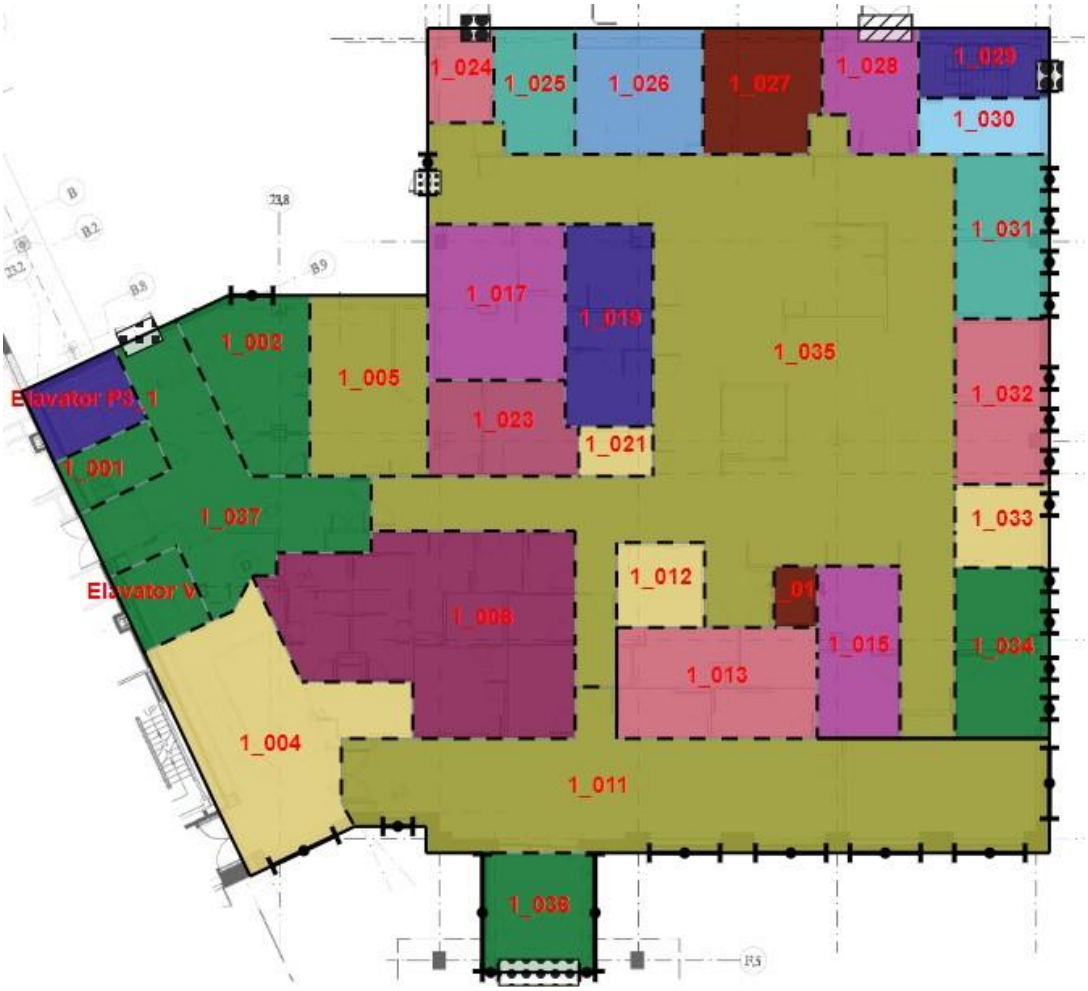

Figure 17 – Modeled First Floor Plan

The second floor consists of 66 fully-enclosed spaces, two open areas/passageways, two stairwells, and two elevator shafts. Figure 18 contains the floor plan for the second floor.

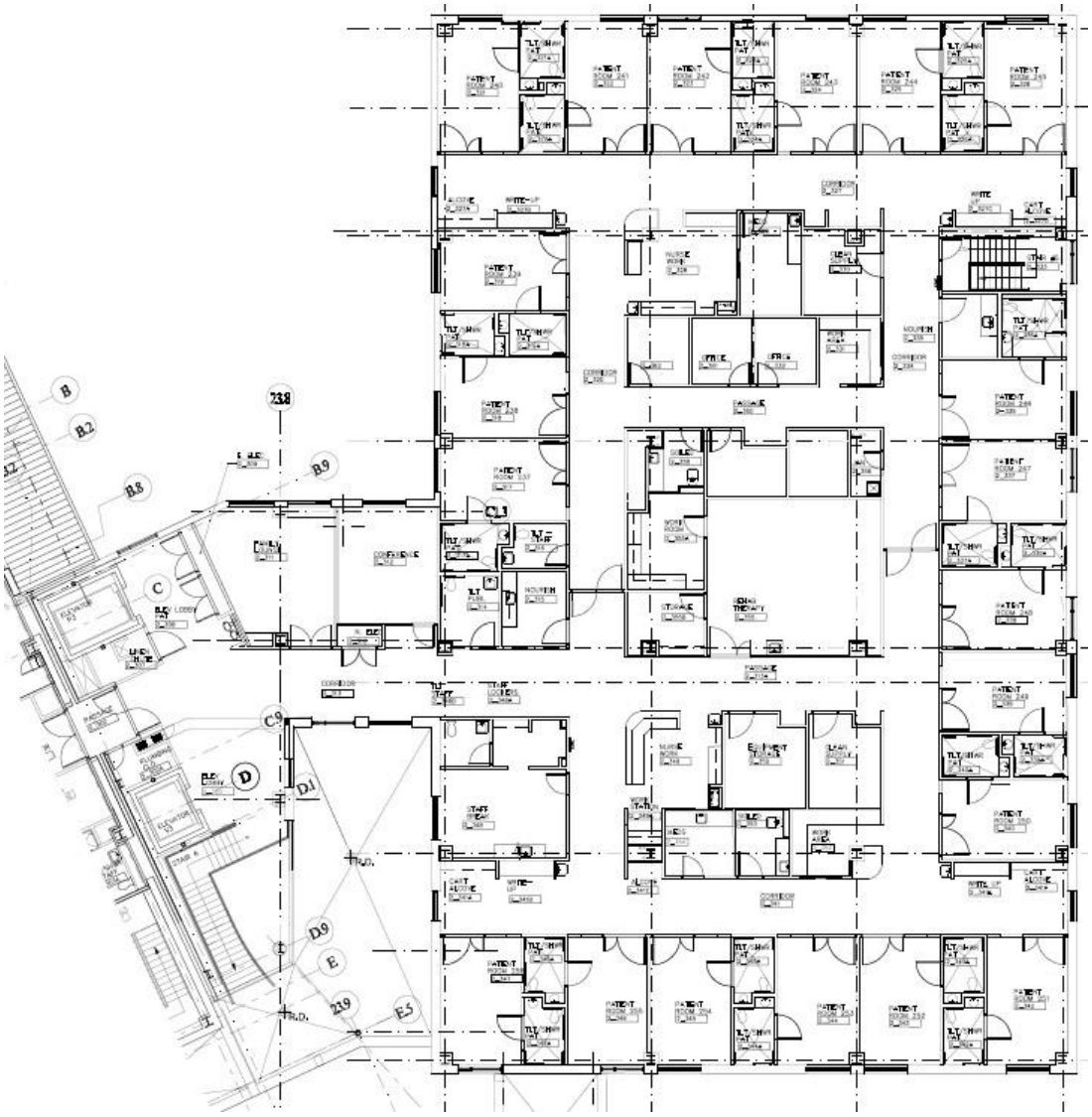

Figure 18 – Second Floor Plan [35]

Similar to the first floor, the second floor contains too many rooms for the program to run efficiently. HVAC thermal zones are the spaces with a few exceptions. The model combines adjacent identical patient rooms with the same HVAC specifications into one space. The model further combines adjacent bathrooms into one space since they have no HVAC equipment. Finally, the model combines miscellaneous adjacent rooms that have similar HVAC requirements located in the center of the building into one space. Each space has its thermal

zone. Figure 19 contains the floor plan for the second within the model along with associated space numbers.

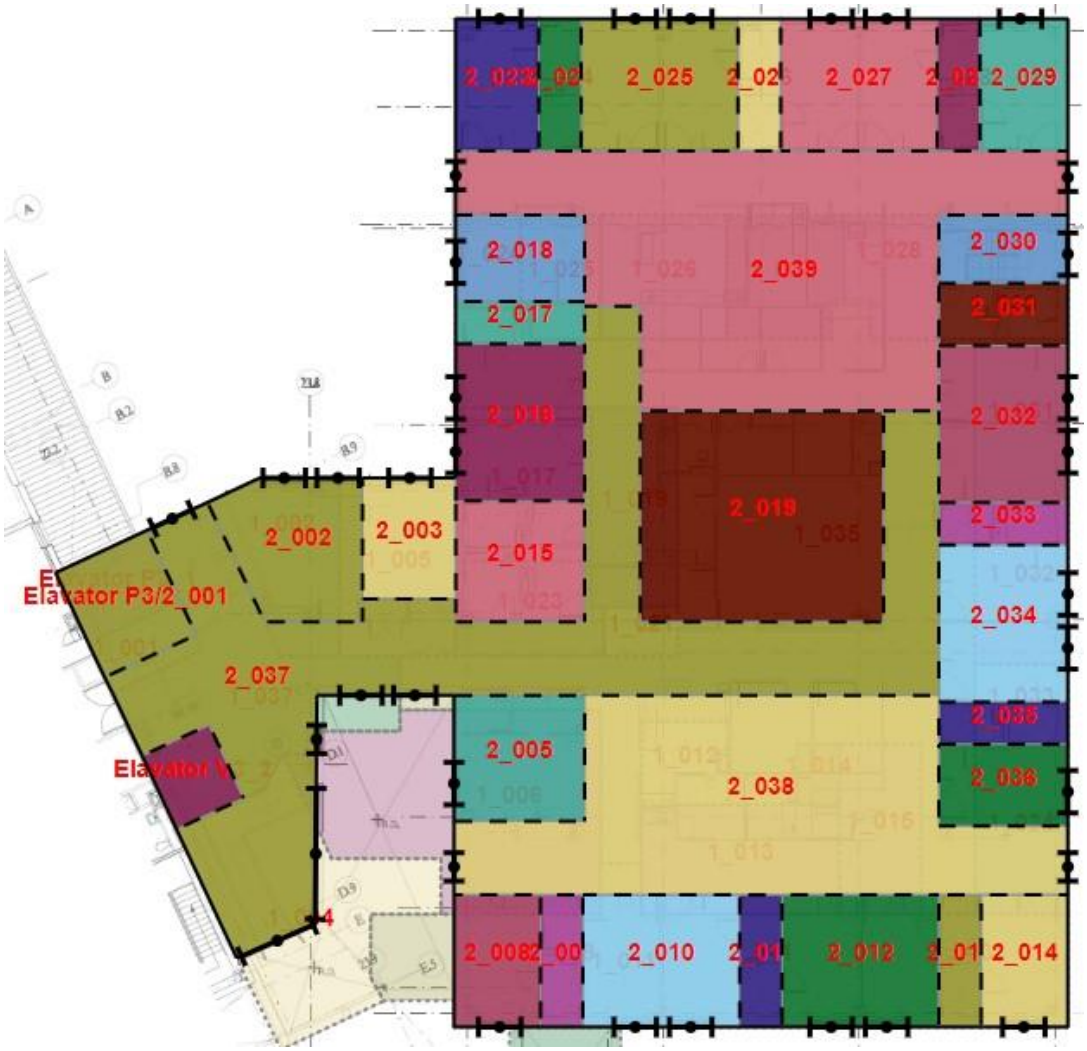

Figure 19 – Modeled Second Floor Plan

3.1.2 Fenestration Elements

The window and door schedules specify the dimensions for all exterior doors and windows. Figures 17 and 19 show the locations of these elements along their perimeter. The facility did not provide the details regarding window and door construction so the model makes assumptions. All exterior windows are double-pane with two 6mm thick glass panes with a 13mm air gap. This construction is a typical exterior window for climate zone 6A contained

within the OpenStudio library. Table 10 contains the spectral data for each glass pane. For the sake of consistency, this model does not assume any use of blinds since doing so would require uninformed assumptions.

Table 10 – Spectral Data for Windows

	Outer	**Inner**
Solar		
Transmittance	0.429	0.775
Front Side Reflectance	0.308	0.071
Back Side Reflectance	0.379	0.071
Visible		
Transmittance	0.334	0.881
Front Side Reflectance	0.453	0.08
Back Side Reflectance	0.505	0.08
Infrared		
Transmittance	0	0
Front Side Emissivity	0.84	0.84
Back Side Emissivity	0.82	0.84
Conductivity (Btu-in/h-ft^2-R)	6.24	6.24

The building contains three different types of exterior doors: glass, metal, and overhead. Similar to the windows, the facility did not provide construction materials so the model makes assumptions. All three constructions are typical exterior doors for climate zone 6A contained within the OpenStudio library. Table 11 contains the spectral data for glass doors. The metal and overhead doors have similar construction. The model assumes both metal and overhead doors have a total thermal resistance of 2.0 ft^2-h-F/Btu which is per ASHRAE recommendations for large hospitals in climate zone 6 [29]. Figure 20 shows the final 3-D model of the building as rendered by the OpenStudio software.

Table 11 – Spectral Data for Glass Doors

	Outer	Inner
Solar		
Transmittance	0.24	0.775
Front Side Reflectance	0.160	0.071
Back Side Reflectance	0.320	0.071
Visible		
Transmittance	0.300	0.881
Front Side Reflectance	0.160	0.08
Back Side Reflectance	0.290	0.08
Infrared		
Transmittance	0	0
Front Side Emissivity	0.84	0.84
Back Side Emissivity	0.60	0.84
Conductivity (Btu-in/h-ft^2-R)	6.24	6.24

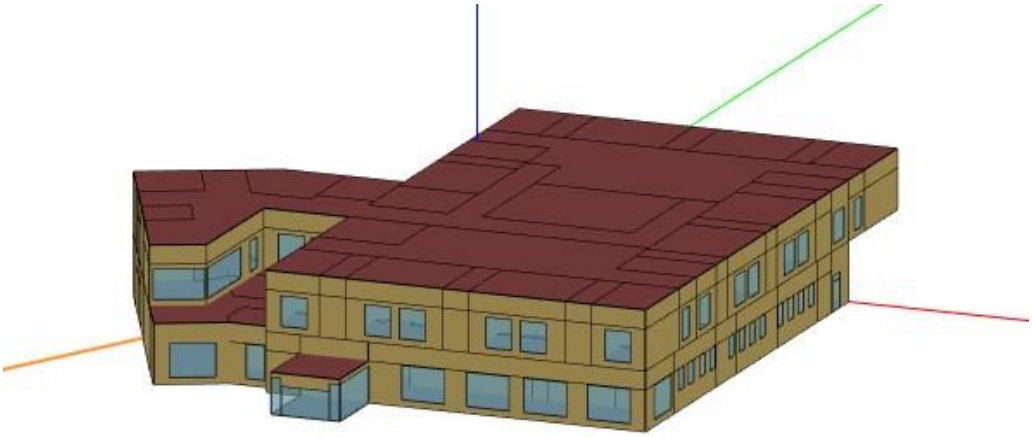

Figure 20 – 3-D Building Model

3.2 Electrical/Plug Loads

The facility did not provide information on the electrical demands of the building. The model assumes interior lighting loads based on ASHRAE recommendations for large hospitals. Table 12 contains the lighting power density by room type. If a room type is not included specifically, the model assumes 0.9 W/ft^2 per ASHRAE recommendations for large hospitals

[29]. The model does not assume the use of light dampers and instead operates in a full-on/off mode according to the schedule.

Table 12 – Lighting Power Density by Space Type [29]

Space Type	Lighting Power Density (W/ft^2)
Patient Room	0.7
Corridor/Nursing	0.7
Triage/Trauma	1.5
Treatment/Exam/Isolation	1.0
Radiology	0.8
Lobby	0.9
Conference/Lounge/Office	0.9
General (Not listed above)	0.9

This model does not attempt to assume all plug loads but instead defines the most common appliances found within a hospital. The model assigns every exam, treatment, isolation, triage, and patient room a computer which the nurses and physicians use throughout the day. The power consumption is based on a typical desktop and monitor combination. The model computer is a Dell – Inspiron Compact Desktop with a rated power consumption of 180W [36]. The monitor is an Acer 27" IPS LED Monitor with a rated power consumption of 17.5W [37]. The total combined power consumption is assumed to be 197.5W when in operation.

This model further assigns a television to each patient's room. The power consumption is based on a typical mid-size television. The television assumed the average power consumption of a 32" television. The total power consumption is assumed to be 28W when in operation [38].

The model does not assume any further plug loads as doing so relies on unsubstantiated assumptions.

3.3 HVAC

The construction of the HVAC systems within the model is as per the specifications provided by the plans and in Chapter 2. The model makes a few assumptions regarding ventilation, infiltration, equipment, and setpoints.

3.3.1 Ventilation

The facility did not provide specifics of outdoor air minimums so the model assumes the minimums defined by ANSI/ASHRAE Standard 170-2013. Table 13 contains the minimum outdoor airflow by space type. Those space types indicated with an asterisk use the minimum outdoor airflow for a typical room of that type specified by the OpenStudio library and not from the standard. The total air changes are specified by the HVAC equipment's capacity.

Table 13 – Outdoor Air Minimums [39]

Space Type	Minimum Outdoor ACH
Patient Room	2
Corridor/Nursing	2
Exam/Treatment	2
ER Decontamination	2
Isolation	2
Radiology	3
Trauma	3
Triage	2
Storage	0
Toilet	0
Office	0
Elevator	0
Entryway/Vestibule	0
Conference/Lounge/Break*	20

Note: Units for spaces with an asterisk is ft^3/min per person occupancy

3.3.2 Infiltration

Infiltration rates are difficult to quantify as they vary greatly based on construction, building age, and weather conditions. There are, however, guidelines for building energy

modeling that provides estimates. This model uses the Pacific Northwest National Laboratory's *Infiltration Modeling Guidelines for Commercial Building Energy Analysis* as a baseline. There are four modeling coefficients in EnergyPlus that help specify the infiltration rate. They are the constant coefficient (A), temperature coefficient (B), wind speed coefficient (linear term) (C), and wind speed coefficient (quadratic term) (D) [40]. The equation for infiltration rate is as follows:

$$Infiltration = (I_{design})(F_{schedule})[A + B|(T_{zone} - T_{odb})| + C(WindSpeed) + D(WindSpeed^2)] \quad (1)$$

The EnergyPlus engineering reference has three different models for infiltration: Constant, DOE-2, and BLAST. Table 14 contains the coefficients for each model.

Table 14 – Infiltration Model Coefficients [40]

Model	A	B	C	D	Reference Wind Speed
Constant	1.0	0	0	0	None
DOE-2	0	0	0.224	0	10 mph
BLAST	0.606	0.03636	0.1177	0	7.5 mph

The guidelines set forth by PNNL recommend using the DOE-2 model based on literature review and sensitivity analysis [41]. The DOE-2 model does not consider temperature differences across the boundary nor does it assume any constant infiltration rate. The reference temperature denotes that at 10 mph, the actual infiltration rate equals the design infiltration rate.

Table 15 contains the baseline infiltration rates recommended by PNNL based on ASHRAE Standard 90.1 2004 for envelope elements. PNNL further recommends adjusting these numbers based on HVAC, environmental, and geometry-induced pressure gradients, however, this model does not consider those effects. Appendix F contains the infiltration rate calculations for each space via windows and/or doors. Each space, regardless of fenestration elements, has a

baseline infiltration rate of 0.04 cfm/ft^2 of the above-ground wall area. Finally, the infiltration schedule fraction is 0.25 when the HVAC system is in operation and 1.0 when off [41].

Table 15 – Component Infiltration Rate [41]

Component	Infiltration Rate (cfm/ft^2)	Area used for calculation
Roofs	0.04	Net area of roof
Above Grade Walls	0.04	Net area of above-grade walls
Floor	0.04	Net area of floor over unconditioned space
Opaque Doors	0.4	Area of doors
Swinging Glass Doors	1.0	Area of doors
Vestibule	1.0	Area of doors
Sliding Glass Doors	0.4	Area of doors
Windows	0.4	Area of windows

3.3.3 Equipment Assumptions

The boiler in the steam loop is modeled as a hot water boiler since OpenStudio does not support the steam calculations of EnergyPlus. The model calculates boiler load, Q_B, using the mass flow rate, a constant specific heat of water at the average temperature of the inlet and outlet nodes, and the temperature difference of the water using equation 2 [40]. This is different from the steam boiler model which also considers latent heating.

$$Q_B = m_w C_{p_w}(T_{out} - T_{in}) \quad (2)$$

The model then uses equations 3, 4, and 5 to calculate the performance characteristics of the boiler throughout the simulation [40].

$$OperatingPartLoadRatio = \frac{BoilerLoad}{BoilerNomCapacity} \quad (3)$$

$$TheoreticalFuelUse = \frac{BoilerLoad}{NominalThermalEfficiency} \quad (4)$$

$$FuelUsed = \frac{TheoreticalFuelUse}{BoilerEfficiencyCurveOutput} \quad (5)$$

This model assumes a nominal thermal efficiency of 80%. Since there is no efficiency modifier curve documented, the efficiency is taken as a constant of 80% during operation and the model ignores all inefficiencies due to part load operation. In equation 4, this means that $BoilerEfficiencyCurveOutput = 1$. This is per ASHRAE minimum efficiency standards for gas-fired steam boilers [42]. Furthermore, the EnergyPlus boiler model does not consider the combustion process meaning that the model is independent of fuel type [40]. The user specifies fuel type for energy accounting purposes only. This model, however, does provide fairly accurate results. The pumps within the steam and hot water loops have specified efficiency, however, this model assumes the efficiency modifier coefficients of a typical variable speed pump in the OpenStudio library. Throughout the simulation, the model calculates pumping power using equations 6 and 7 [40].

$$Power = FractionFullLoadPower * NomPowerUse \quad (6)$$

$$Shaft\ Power = Power * MotorEfficiency \quad (7)$$

The air-cooled chiller in the chilled water loop has a specified reference COP, however, the COP is modified via three curves. This model is based on the compression chiller model (COMREF) in the DOE-2.1 building energy simulation program and uses the default modifier curve values [40]. The three modifier curves are cooling capacity as a function of temperature (ChillerCapFTemp), energy input to cooling output ratio as a function of temperature (ChillerEIRFTemp), and energy input to cooling output ratio as a function of part load ratio (ChillerEIRFPLR). These curves modify the total cooling capacity as outdoor air temperature changes, COP as outdoor air temperature changes, and COP as part load ratio changes, respectively. The model calculates values for the cooling capacity of the chiller, power

consumption of the compressor, and power consumption of the condenser fans. The model uses equation 8 to calculate the available cooling capacity of the chiller which is based on the cooling capacity at reference conditions and the output of the chiller capacity as a function of temperature curve [40]. The model uses equations 9 and 10 to calculate the power of the compressor [40]. Equation 9 describes the chiller cycling ratio which is a function of part load operation and equation 10 describes the power consumption as a function of the available cooling capacity, reference coefficient of performance, chiller cycling ratio, and the remaining two modifier curve outputs. The model uses equation 11 to calculate the condenser fan power which is a function of reference cooling capacity, condenser fan power ratio, and chiller cycling ratio [40]. The pump within the chilled water loop has a specified efficiency and operates using equations 6 and 7.

$$\dot{Q}_{avail} = \dot{Q}_{ref}(ChillerCapFTemp) \tag{8}$$

$$ChillerCyclingRatio = \min\left(\frac{PLR}{PLR_{min}}, 1.0\right) \tag{9}$$

$$P_{chiller} = \left(\dot{Q}_{avail}\right)\left(\frac{1}{COP_{ref}}\right)(ChillerEIRFTemp) \tag{10}$$

$$(ChillerEIRFPLR)(ChillerCyclingRatio)$$

$$P_{cond} = \dot{Q}_{ref}(P_{condfanratio})(ChillerCyclingRatio) \tag{11}$$

The air handling unit contains two fans. Similar to the pumps in the water loops, the fans have a specified efficiency. The EnergyPlus model for a variable speed fan operates using equations 12, 13, and 14 [40]. Equation 12 describes the flow fraction and is a function of the actual and design flow rates. Equation 13 describes the part load factor and is a function of the flow fraction and modifier coefficients. This model assumes the efficiency modifier curve coefficients of a typical variable speed fan in the OpenStudio library. Equation 14 describes the

fan power as a function of the part load factor, design flow rate, pressure rise (ΔP), fan total efficiency (ε_{tot}), and density of air at standard conditions (ρ_{air}).

$$f_{flow} = \frac{\dot{m}}{\dot{m}_{design}} \tag{12}$$

$$f_{pl} = c_1 + c_2 * f_{flow} + c_3 * f_{flow}^2 + c_4 * f_{flow}^3 + c_5 f_{flow}^4 \tag{13}$$

$$P_{fan} = f_{pl} * \dot{m}_{design} * \Delta P / (\epsilon_{tot} * \rho_{air}) \tag{14}$$

This model further sizes both the steam and chilled water coil in the air handler based on specified capacity and rated inlet and outlet fluid temperatures. The model calculates the heating load required via equation 15 and adjusts the water flow rate to meet demands [40].

$$\dot{Q}_{load} = \dot{m}_{air} * C_{p,air} * (T_{air,out} - T_{air,in}) \tag{15}$$

The model for the cooling coil is slightly more complicated due to both sensible and latent characteristics. EnergyPlus approaches this by specifying operation modes for the coil. The operations modes are completely dry, completely wet, and partially wet. EnergyPlus has two analysis modes: simple and detailed. The detailed analysis considers all three modes whereas simple analysis only considers the completely dry and completely wet modes. According to the EnergyPlus engineering reference, the simple analysis provides accurate annual data but inconsistent time step data. Since this analysis is primarily focused on annual energy use, the model assumes simple analysis. If the air temperature dewpoint is less than the water inlet temperature, then the coil is considered completely dry. If the air temperature dewpoint is above the water inlet temperature, then the coil is considered completely wet. If completely dry, the cooling coils operate using equation 15. If completely wet, equation 16 calculates the total cooling load of the coil and adjusts the chilled water supply accordingly [40].

$$\dot{Q}_{load} = \dot{m}_{air} * \left(h_{air,in} - h_{air,out}\right) - \dot{m}_w h_w \tag{16}$$

The humidifier assumes a thermal efficiency of 80% and does not consider any part load operation inefficiencies.

The model assumes a zone supply air temperature of 55°F for cooling and 90°F for heating. Furthermore, each zone features a ceiling supply and return, therefore the model assumes a zone air distribution effectiveness of 1.0 and 0.8 for cooling and heating operations respectively [43]. These values are per ASHRAE Standard 62.1-2010. The model sizes the hot water coils within the VAV boxes and unit heaters based on specified capacity and rated inlet and outlet fluid temperatures. The model for these hot water coils is the same as the AHU preheat coil.

3.3.4 Setpoints

Creating accurate setpoints is difficult due to large variations in occupancy and personal comfort. This model takes a simplified approach and defines a constant temperature setpoint for the entire year. Thermostats within the spaces are set to 72°F except for patient rooms which have a setpoint of 75°F. Patient rooms have a higher setpoint due to the nature of their use.

There are two setpoints in the air handler; one for temperature and one for humidity. Since the cooling coil works as a dehumidifier during cooling operation, these two setpoints work hand in hand to create an appropriate indoor environment. This model assumes an outdoor air reset temperature setpoint. This setpoint requires specifying a minimum and maximum outdoor air temperature and the setpoints associated with them. At or above the maximum outdoor air temperature, the setpoint equals the minimum temperature setpoint. At or below the minimum outdoor air temperature, the setpoint equals the maximum temperature setpoint. If the outdoor air temperature is between these two outdoor air temperatures, the model interpolates and specifies a middle setpoint temperature. Table 16 contains the parameters for this setpoint.

The advantage of this control strategy over specifying a constant setpoint is that it limits cooling when the outdoor air temperature is between the air-handler setpoint and the space thermostat setpoint thus resulting in energy savings. The system still requires some level of cooling due to dehumidification requirements. The amount of cooling relies largely on geographic location.

Table 16 – Temperature Setpoint Parameters for Air-Handling Unit

Parameter	**Temperature (°F)**
Setpoint at Outdoor Low Temperature	62
Outdoor Low Temperature	55
Setpoint at Outdoor High Temperature	55
Outdoor High Temperature	62

ASHRAE Standard 62.1-2010 states that for facilities with dehumidification capabilities, relative humidity shall be limited to 65% or less [43]. Furthermore, for comfort standards, this model keeps relative humidity above 40%. The humidity setpoint that achieves this relative humidity range given the temperature setpoints is 0.008 lbs. of water vapor/lb. of dry air.

3.4 Schedules

Schedules provide the most variation and are often the most difficult pieces to achieve accuracy in a whole building energy model. A schedule provides the program with guidelines for occupancy, equipment operation, lighting use, etc. Some schedules act as dimensionless scalars with which to multiply nominal values such as lighting and equipment schedules, whereas some define the end value such as activity or temperature schedules. Since the facility provided no information regarding these schedules, this model employs the default schedules for a hospital contained within the OpenStudio library. The hospital schedule set provides occupancy, activity, electrical equipment, and lighting schedules for different space types. The five schedule sets are ER_Trauma, Lobby, Office, PatCorridor, and PatRoom. Figure 21 shows the ER_Trauma

schedule set, Figure 22 shows the Lobby schedule set, Figure 23 shows the Office schedule set, Figure 24 shows the PatCorridor schedule set, and Figure 25 shows the PatRoom schedule set.

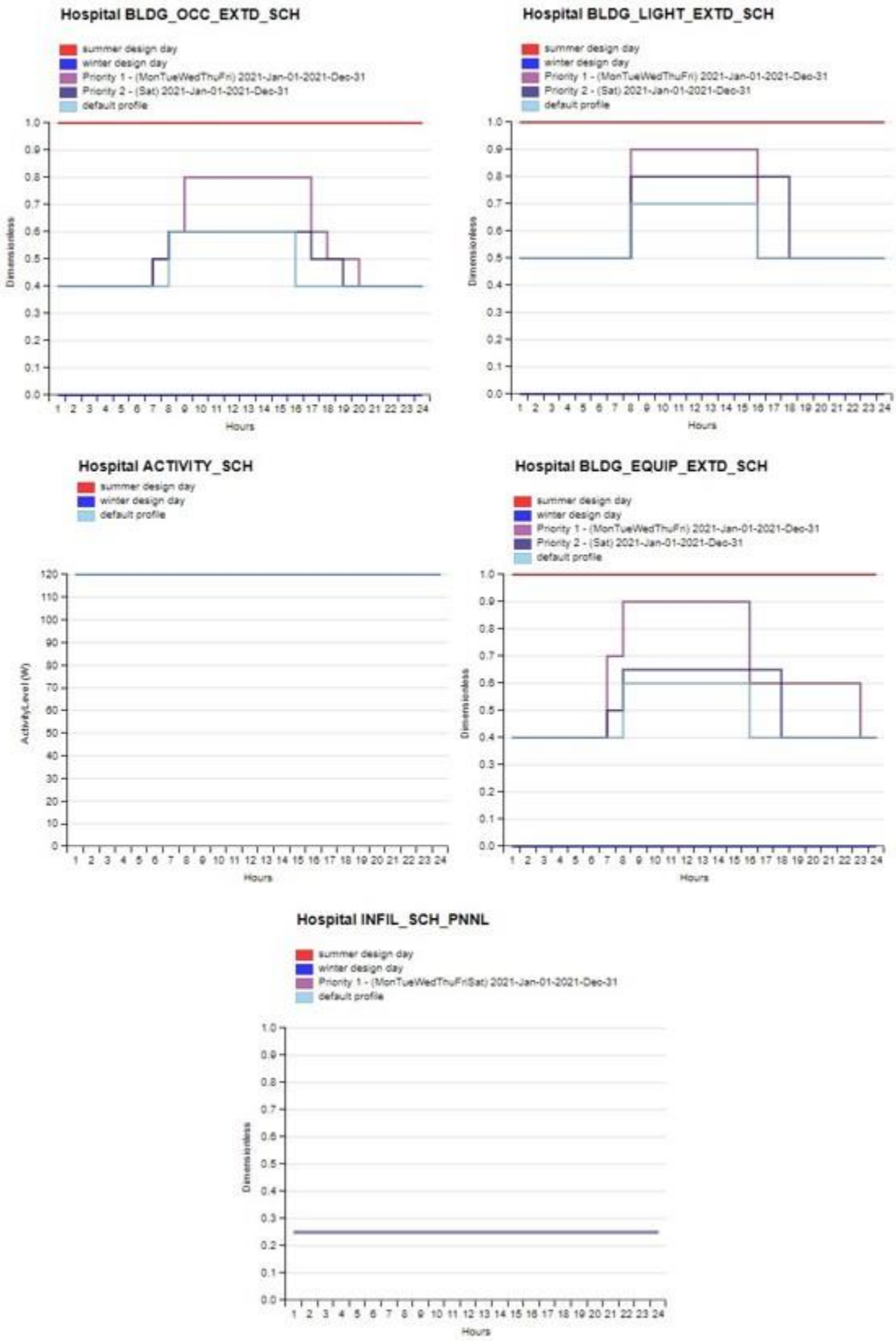

Figure 21 – ER_Trauma Schedule Set

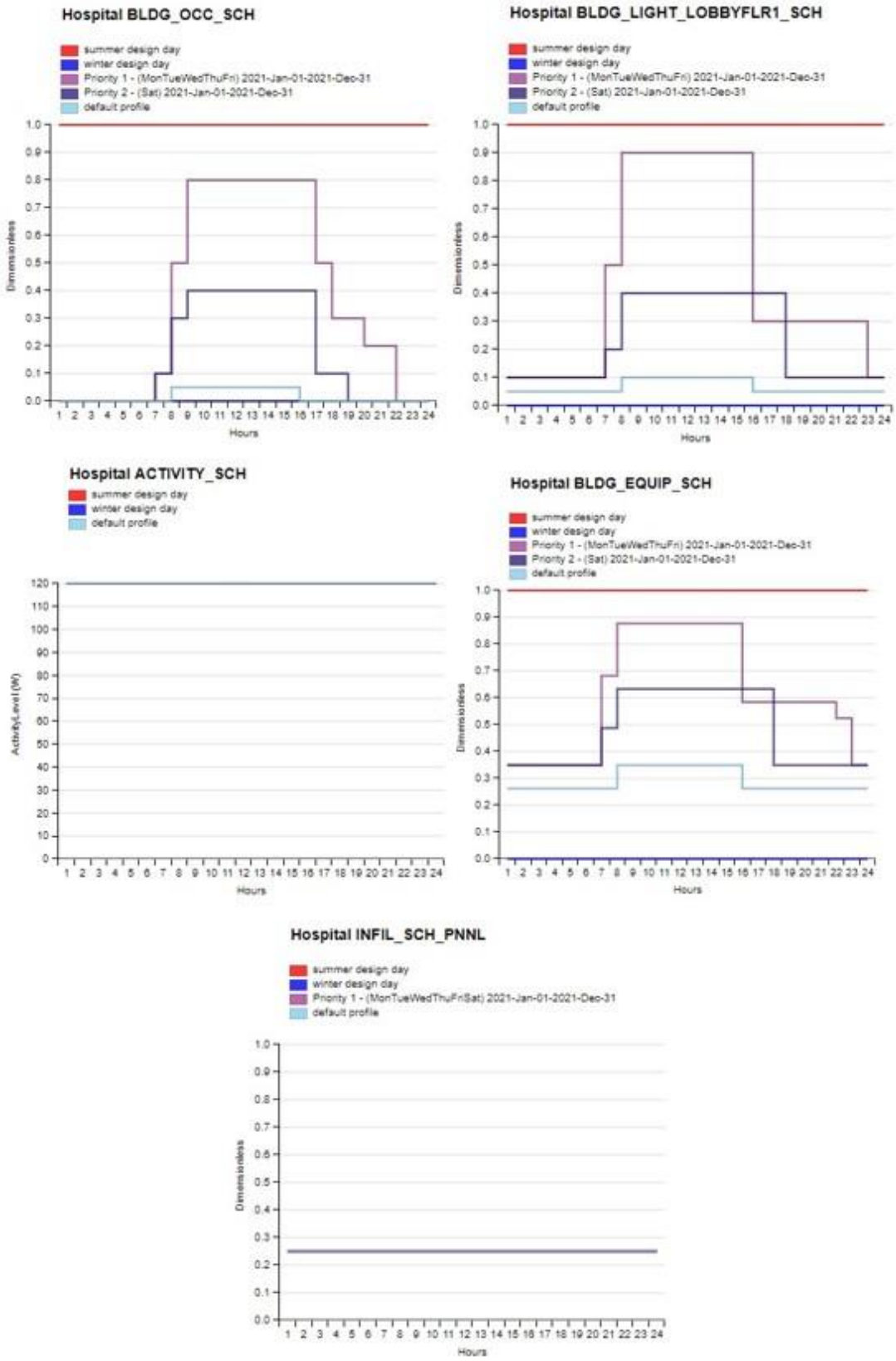

Figure 22 – Lobby Schedule Set

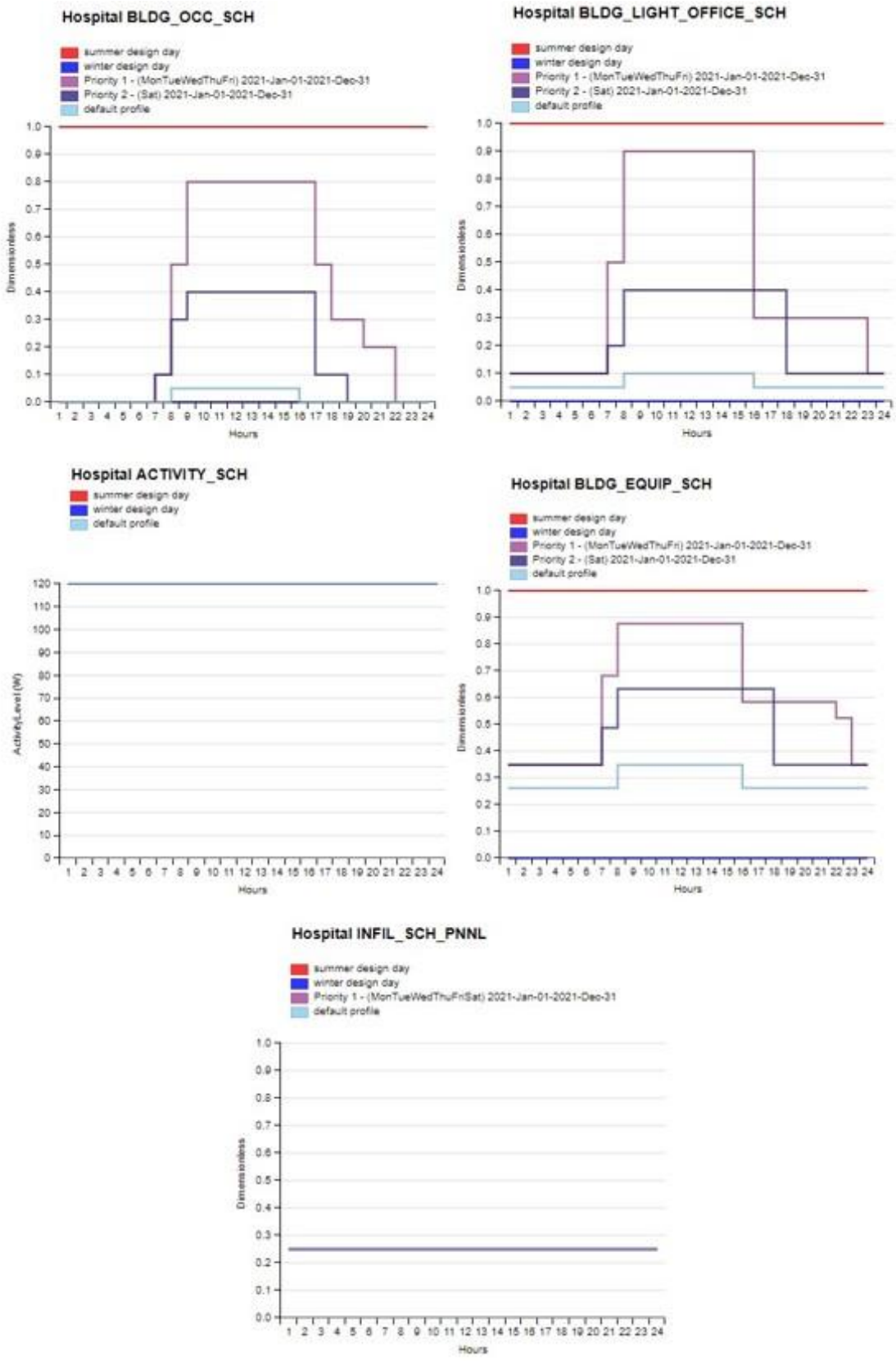

Figure 23 – Office Schedule Set

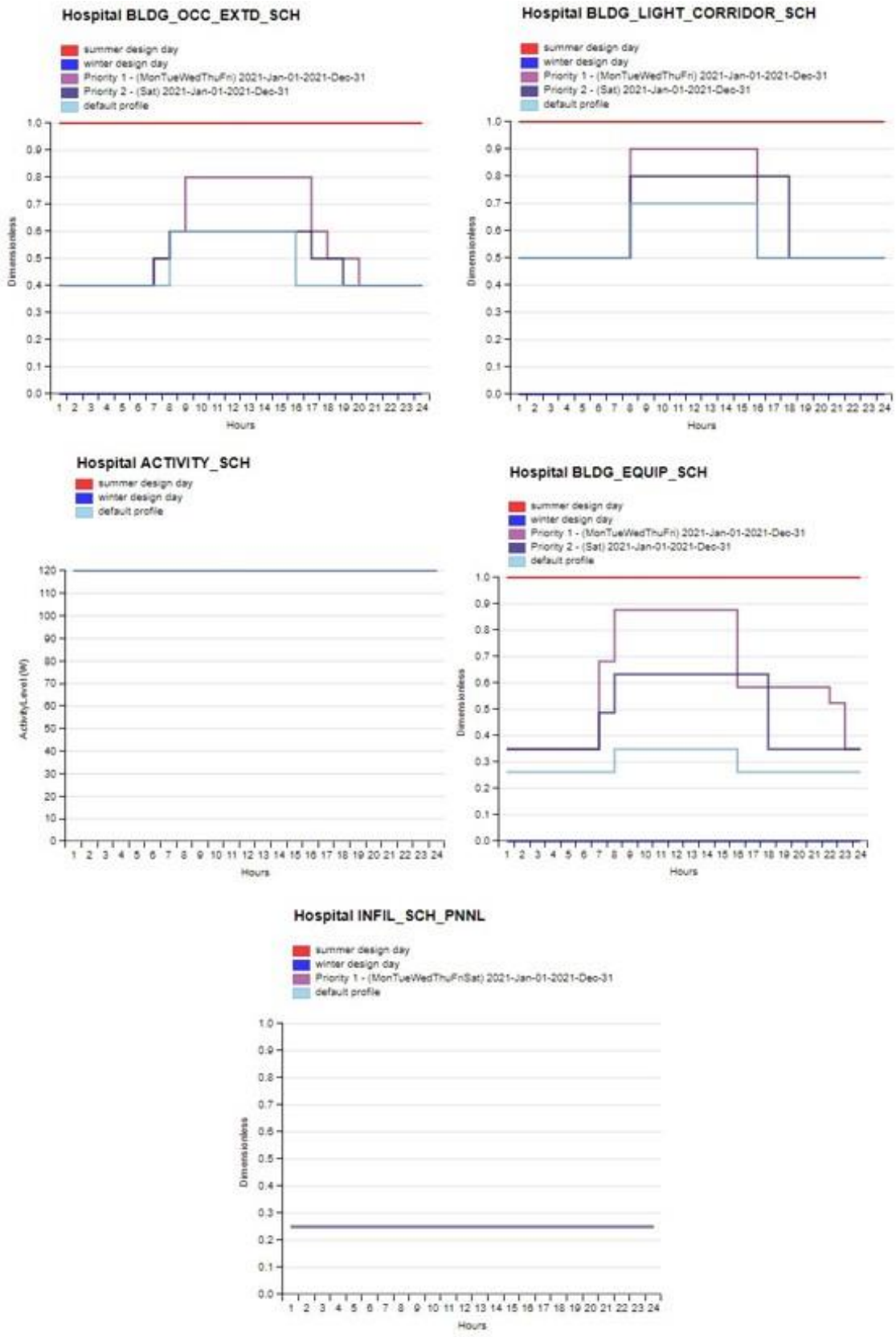

Figure 24 – PatCorridor Schedule Set

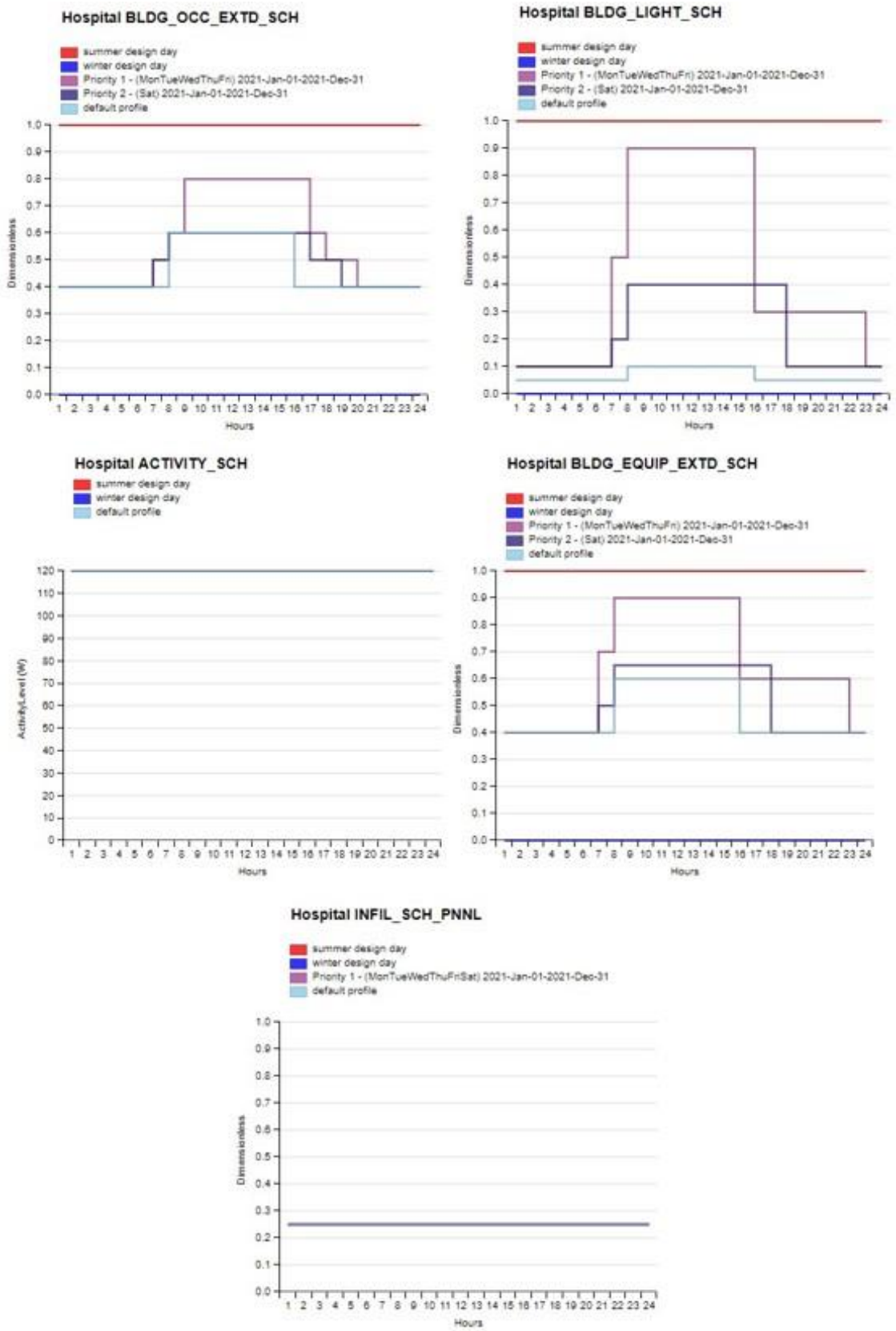

Figure 25 – PatRoom Schedule Set

This model assigns each space type a default schedule set with which to operate on. Table 17 contains each space type and its associated schedule set. Each space type contains the schedule set most closely resembling its use.

Table 17 – Schedule Sets by Space Type

Space Type	Schedule Set
Conference/Lounge/Break	Office
Corridor/Nursing	PatCorridor
Elevator	PatCorridor
Entryway	Lobby
ER Decontamination	ER_Trauma
Exam/Treatment	PatRoom
Isolation	PatRoom
Office	Office
Patient Room	PatRoom
Radiology	Office
Storage	Office
Toilet	PatCorridor
Trauma	ER_Trauma
Triage	ER_Trauma

In addition to the above schedule sets above, the model defines schedules for the temperature and humidity setpoints for all of the HVAC equipment. These schedules are assigned the setpoint value at all times throughout the year but could be varied for an investigation into different thermostat control strategies.

3.5 Weather Data

This model used the weather data from the EnergyPlus weather file for Brunswick, Maine [31]. Within the weather file, there is information regarding location (latitude, longitude, and time zone), elevation, annual design day conditions, and monthly average ground temperatures. Furthermore, the file contains the dry bulb and wet bulb temperatures for every hour of the year.

This data comes from a local weather station. EnergyPlus uses this data for ambient conditions while the model runs.

3.6 Model Validation

The facility provided energy use data for the date range of September 1, 2020, to September 31, 2021. The data, however, is for the entire facility and not just the section of the hospital in this model. For model validation, this analysis calculates total site energy use intensity (EUI) and compares those values to the actual data. EUI is calculated by dividing energy use by square footage. Table 18 contains the provided energy use metrics for Mid Coast Hospital. According to EnergyStar, the median site EUI for a hospital is the United States in 234.4 kBtu/ft^2 [44].

Table 18 – Actual Energy Use for Mid Coast Hospital

Measure	**Quantity**
Gross Floor Area	171,392 ft^2
Electricity Usage	20,118,074 kBtu
Electricity EUI	117.4 kBtu/ft^2
Natural Gas Usage	431,268.9 therms (43,162,890 kBtu)
Natural Gas EUI	2.323 therms/ft^2 (232.3 kBtu/ft^2)
Site EUI (Electricity and Natural Gas Only)	369.2 kBtu/ft^2

*Note: The 12-month energy use was simply taken as 12/13 of the 13-month energy use

The model ran for the date range specified above using weather data collected for Naval Air Station Brunswick, located two miles from Mid Coast Hospital. Furthermore, the model ran with four time steps per hour. Table 19 contains the results for simulated energy use.

Table 19 – Simulated Energy Use for Mid Coast Hospital

Measure	Quantity
Gross Floor Area	32,726 ft^2
Electricity Usage	3,607,456 kBtu
Electricity EUI	110.2 $kBtu/ft^2$
Natural Gas Usage	67,469 therms (6,746,900 kBtu)
Natural Gas EUI	2.062 $therms/ft^2$ (206.2 $kBtu/ft^2$)
Site EUI	316.3 $kBtu/ft^2$

There is a 6.13% error in the prediction of electricity usage and an 11.2% error in the prediction of natural gas usage. The total error in EUI is 14.3%. An article published in the ASHRAE journal speaks on the validity of energy models and concludes that no energy model can be deemed completely correct and that most energy models that try and precisely predict energy usage do so by chance [45]. This model does show, however, that it is at least fairly representative of actual operation and can serve as a comparison for the VRF model given all variables (except for those being investigated) remain equal. Furthermore, most assumptions are based upon published ASHRAE standards meaning they should be representative of the actual building.

3.7 Baseline Results

Both the EnergyPlus and OpenStudio results provide extensive data that engineers use to make decisions regarding building design. This analysis focuses on HVAC load profiles, zone comfort conditions, and overall energy use (with an emphasis on HVAC energy use).

Figure 26 shows the simulation HVAC load profile for the section of Mid Coast Hospital. As expected, the cooling and heating loads generally followed outdoor air temperature. The heating load increased slightly during the summer months due to the increased need for dehumidification. This intuitively makes sense because the higher moisture content in the air during the summer requires more cooling of the air to achieve the proper humidity setpoint. The

model predicted that there is a baseline minimum monthly heating load of 270.45 MBtu. Heating load peaks in the month of January at 591.38 MBtu. Table 20 contains the tabular data that comprise the graph.

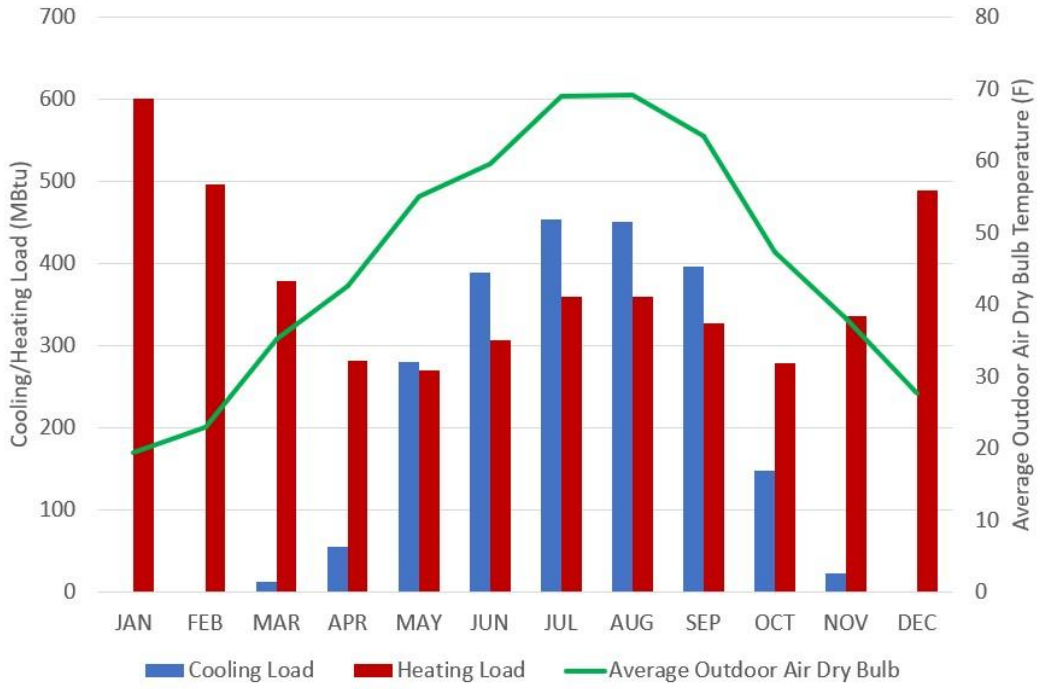

Figure 26 – HVAC Load Profiles

Table 20 – HVAC Load Profile Tabular Data

Month	Average Outdoor Air Dry Bulb Temperature (°F)	Cooling Load (MBtu)	Heating Load (MBtu)
January	19.5	0	600.16
February	22.9	0.33	496.67
March	35.3	13.05	378.82
April	42.6	55.91	281.83
May	55.0	280.99	270.51
June	59.6	389.06	306.37
July	69.0	453.36	360.13
August	69.1	451.23	360.08
September	63.4	397.03	327.28
October	47.3	147.42	279.34
November	38.0	23.70	336.65
December	27.7	0.21	488.69

In a facility that has regular occupancy, having an HVAC system that maintains zone comfort standards is of the utmost importance and is the driving force surrounding equipment sizing. Since this model is for an existing building, the expectation is that the existing HVAC equipment can maintain comfortable conditions. For temperature, the measure of an HVAC system's efficacy is unmet heating and cooling hours. This is the total number of hours in a year that the temperature setpoint is not achieved. For zones that have both heating and cooling equipment, there are no unmet heating or cooling hours in the simulation. As for humidity, no conditioned zone experiences a relative humidity outside of the range of 40-65%.

The two main energy sources for this building are electricity and natural gas. The facility did report a small amount of diesel and propane use; however, different sections of the building are responsible so this analysis ignores them. Figure 27 shows the simulated overall monthly electricity consumption, in MBtu, broken down by end-use. Unsurprisingly, cooling dominated electricity use during the summer months and becomes very small in the winter. Other users of electricity such as lighting, plug loads, pumps, and fans, remain relatively constant throughout the year.

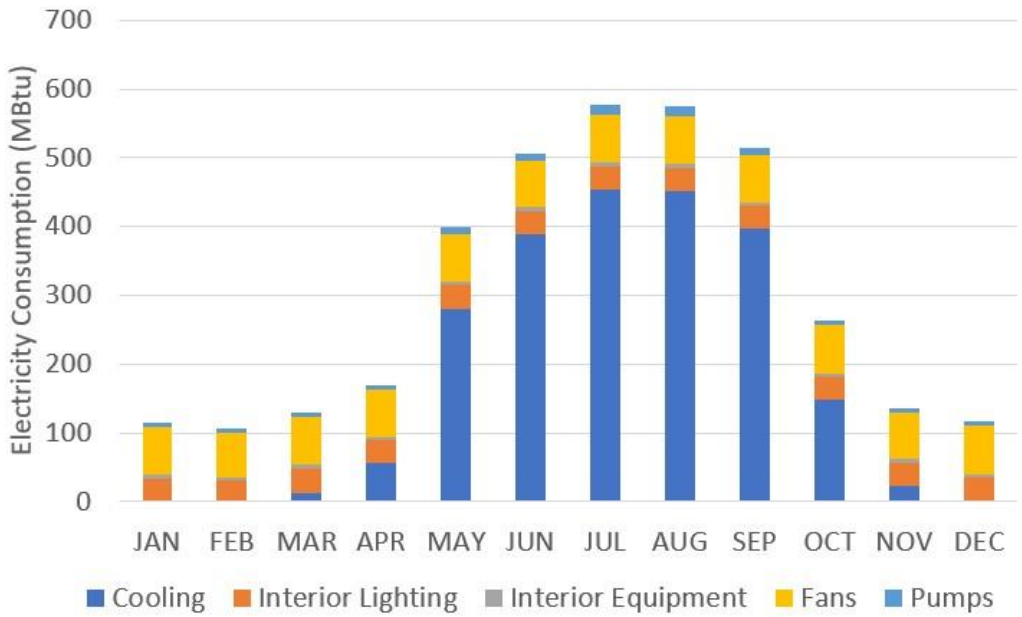

Figure 27 – Electricity Consumption

Figure 28 shows the simulated monthly electricity peak demand in MBH. Between April and October, it appears that peak demand stays steady. Even though peak demand is not representative of overall energy use, it is essential when considering grid capacity. Again, cooling dominates peak electricity loads in the summer months and other electricity uses stay relatively constant throughout the year.

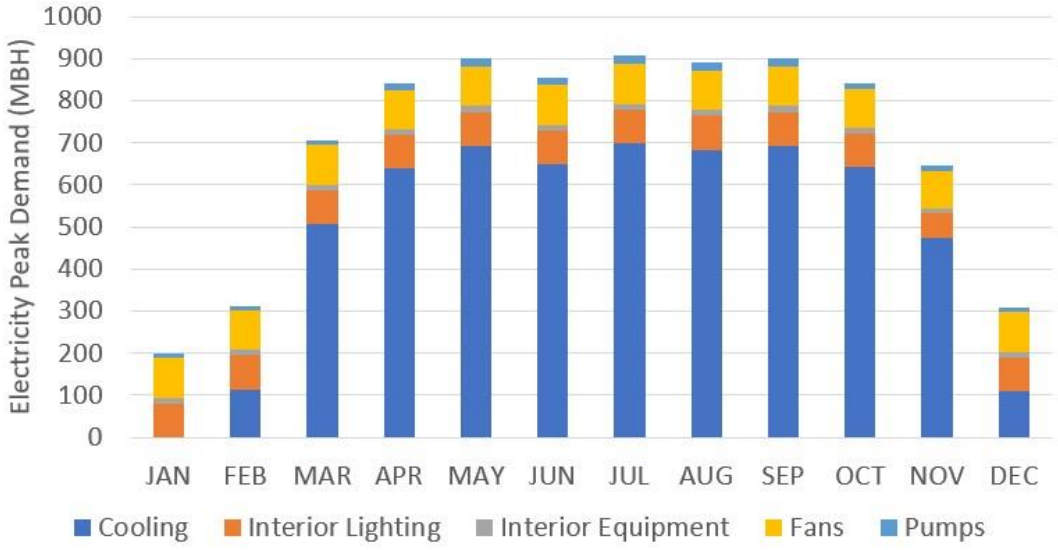

Figure 28 – Electricity Peak Demand

Table 21 contains the simulated total annual electricity use separated by end-use.

Table 21 – Electricity Consumption by End Use

End Use	Electricity (kBtu)	Percentage Share (%)
Cooling	2,212,197	61.3
Interior Lighting	400,776.9	11.1
Interior Equipment	69185.12	1.9
Fans	819,668.2	22.7
Pumps	105,628.7	2.9
Total	3,607,456	100

Figure 29 shows the simulated overall natural gas consumption, in MBtu, broken down by month. Of note, humidification is not present in the figure due to limitations in OpenStudio. The humidifier is specified as being a "gas" humidifier so its contributions are not tabulated in the OpenStudio results. As expected, natural gas use is higher in the winter months when the heating load is high. The slight increase in the summer months is likely due to reheating after dehumidification, however, the control strategy mentioned in section 3.3 may be the cause.

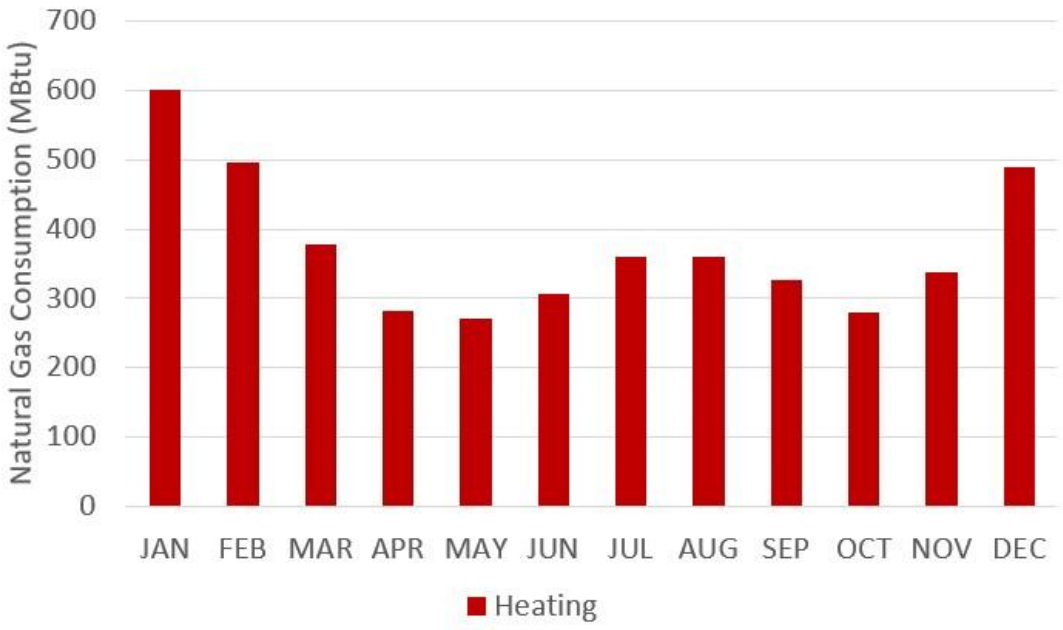

Figure 29 – Natural Gas Consumption

Figure 30 shows the simulated monthly natural gas peak demand in MBH. Again, this figure does not have the data for humidification. Peak demand is high from December to March and then drastically decreases as outdoor air temperature increases. Natural gas use in the summer months is largely due to low night temperatures as well as the use of VAV hot water reheat boxes after dehumidification.

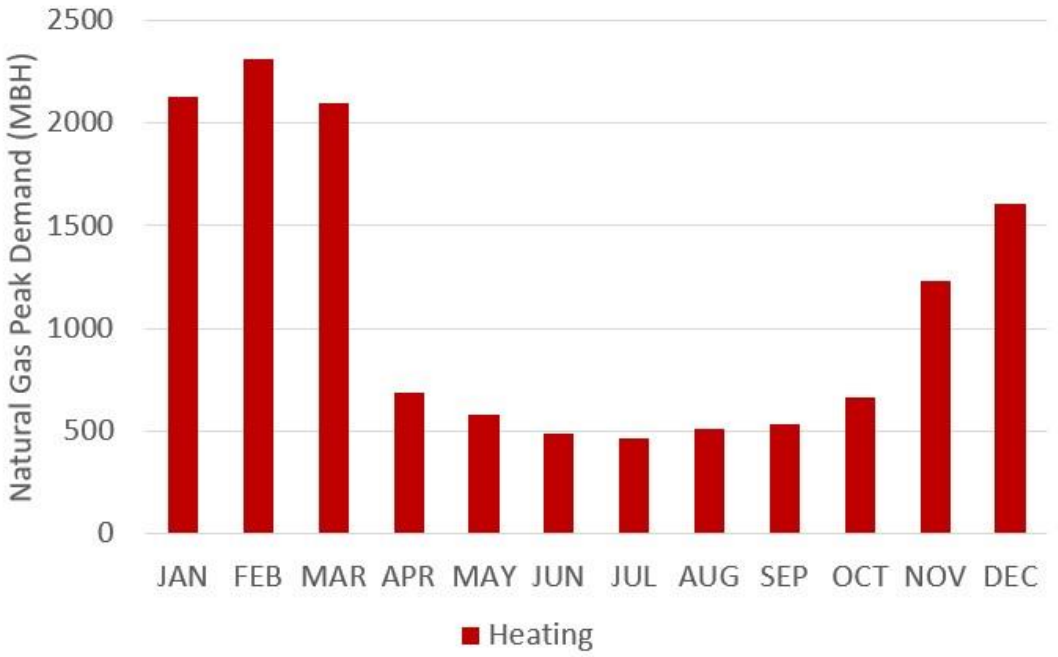

Figure 30 – Natural Gas Peak Demand

Table 22 contains the simulated total annual natural gas use separated by end-use. Table 23 contains the energy summary for the baseline model.

Table 22 – Natural Gas Consumption by End Use

End Use	Natural Gas (therms)	Percentage Share (%)
Heating	44,876 (4,487,600 kBtu)	66.5
Humidification	22,593 (2,259,300 kBtu)	33.5
Total	67,469 (6,746,900 kBtu)	100

Table 23 – Energy Summary

Energy Source	Value
Electricity	3,607,456 kBtu
Natural Gas	67,469 therms (6,746,900 kBtu)
Total	10,354,356 kBtu
Total (Site EUI)	316.3 kBtu/ft^2

The energy values used thus far have exclusively been site energy or the energy immediately used by the facility. Source energy is the total primary energy used to run the facility and considers inefficiencies with electricity and natural gas production and transmission. Energy Star, a program run by the U.S. Environmental protection agency aimed at ensuring buildings meet energy standards, provided general values for site-to-source conversion factors to estimate source energy from site energy. Table 24 contains the site-to-source conversion factors and the final source energy estimates for this facility.

Table 24 – Source Energy for Mid Coast Hospital

Energy Source	Site-to-Source Conversion Factor [46]	Primary Energy
Electricity	2.80	10,100,878 kBtu
Natural Gas	1.05	7,084,245 kBtu
Total (Source EUI)	-	524.8 kBtu/ft^2

The carbon emissions from burning natural gas based on the lower heating value are approximately 0.123 lbs/kBtu (source energy). The carbon emissions from electricity generation as calculated in Chapter 1 is approximately 0.1507 lbs/kBtu of electricity produced (i.e. site energy plus transmission losses). According to the U.S. Energy Information Administration, transmission losses on the U.S. grid are approximately 5% [47]. Table 25 contains the total estimated carbon dioxide emissions of the building.

Table 25 – Carbon Dioxide Emissions of Mid Coast Hospital

Energy Source	Energy	Emissions Rate	Emissions
Electricity	3,797,320 kBtu	0.1507 lbs/kBtu	572,200 lbs/year
Natural Gas	7,084,245 kBtu	0.123 lbs/kBtu	871,400 lbs/year
Total	-	-	654.8 MT/year

The facility provided current utility cost contract amounts. Table 26 provides an estimate of the energy operating costs of Mid Coast Hospital given current prices. This table converted the energy use into units of the electricity costs for ease of calculation.

Table 26 – Annual Operating Costs of Mid Coast Hospital

Source Energy	Energy	Cost (Per Unit Energy)	Cost
Electricity	1,057,285 kWh	$0.11256/kWh	$119,008
Natural Gas	67,469 therms	$1.871/therm	$126,235
Total	-	-	$245,243

Chapter 4: Energy-Saving Options

This analysis examines various heating system configurations with current, commercially available technologies with the intent of electrification. The discussion section compares each model against the baseline in terms of energy use (both site and source), cost, and resulting carbon emissions. For ease of reference, each model has a number. Table 27 contains the model reference numbers and their associated configurations.

Table 27 - Model Reference Numbers

Model Number	Configuration
1	Baseline
2	Natural Gas Boiler w/ VAV Electric Reheat
3	Electric Boiler w/ VAV Hot Water Reheat
4	Variable Refrigerant Flow Heat Pump
5	Ground Source Heat Pump

4.1 Natural Gas Boiler w/ VAV Electric Reheat

As discussed in the literature review, electric reheat is a suitable approach to reduce reliance on natural gas, however, it does have some drawbacks. Depending on use, it may result in more source energy due to the high site-to-source conversion factor for electricity. Furthermore, the relative price of electricity and natural gas may lead to higher operating costs. The relative carbon emissions depend on the breakdown of source energy for electricity production. This analysis addresses those factors.

4.1.1 EnergyPlus Modeling

In terms of modeling, OpenStudio has a VAV terminal unit with electric reheat as part of its library. This VAV unit has two components: the air terminal device and the electric heating coil. The model assumes the same minimum and maximum airflow rates as the VAV units with hot water reheat to maintain proper ventilation. The model replaces the hot water reheat coil with

an electric reheat coil. The coil runs on an always-on schedule with its efficiency set to one. The literature supports the fact that practically all electrical energy becomes heat in an electric heating coil so this assumption is reasonable. The model keeps all other variables equal to the baseline.

4.1.2 Model Results

Concerning zone conditions, there were no unmet heating or cooling hours in zones with both heating and cooling equipment. Furthermore, the relative humidity of conditioned zones fell within the range of 40-65% for all times throughout the year.

Figure 31 shows the estimated electricity consumption by month, in MBtu. Electricity consumption peaks at around 865 MBtu in the months of July and August and is expectedly much smaller in the winter months. Electricity used for heating remains relatively steady throughout the year with electricity used for cooling peaking (and dominating) in the summer months. Electricity consumption is as much as a 50% increase in the high-use months and as much as a 195% increase in the low-use months as compared to the baseline.

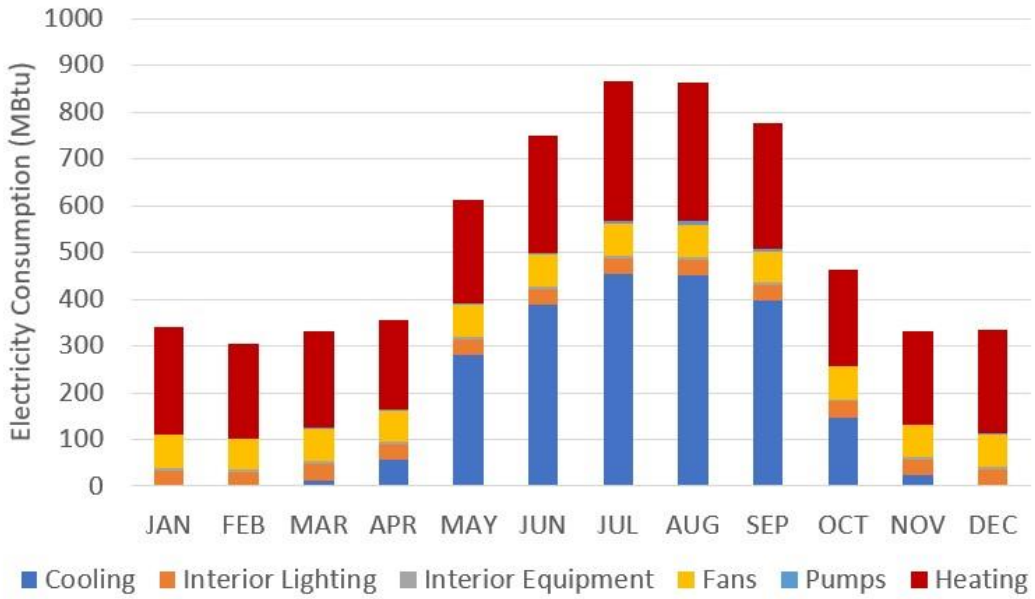

Figure 31 – Electricity Consumption (Model 2)

Figure 32 shows the simulated monthly electricity peak demand in MBH. Between March and November, cooling dominates peak electricity loads while heating dominates from December to February. Similar to consumption, the increase in peak demand is more drastic in the winter months. For example, January shows the largest increase in peak demand at 151% whereas July only had around a 36% increase.

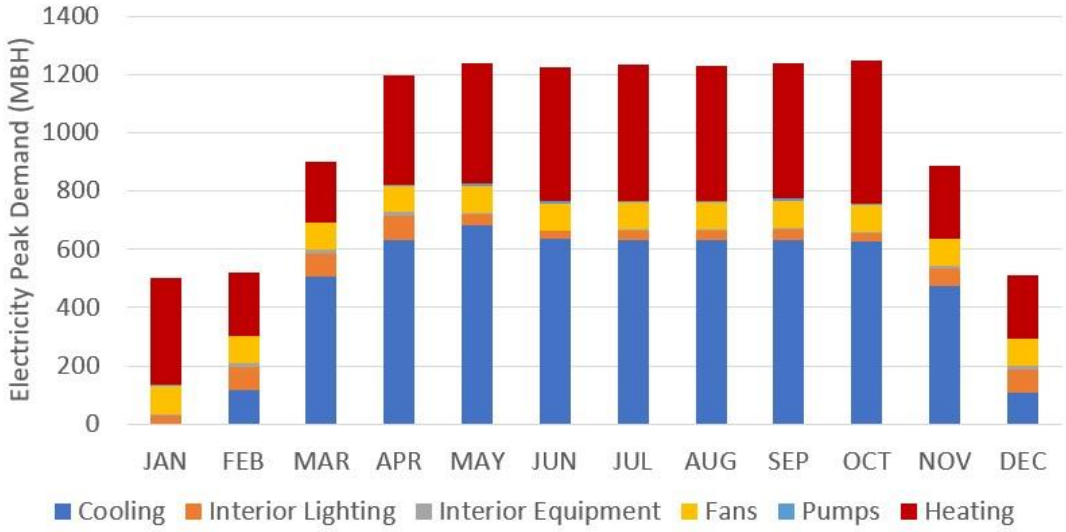

Figure 32 – Electricity Peak Demand (Model 2)

Table 28 contains the annual simulated electricity consumption broken down by end-use. Compared to the baseline, electricity usage increased by 75%.

Table 28 – Electricity Consumption by End Use (Model 2)

End Use	Electricity (kBtu)	Percentage Share (%)
Cooling	2,211,249	34.5
Heating	2,793,671	44.1
Interior Lighting	400,777	6.3
Interior Equipment	69,189	1.1
Fans	820,235	13.0
Pumps	33,106	0.5
Total	6,328,226	100

Figure 33 shows the estimated natural gas consumption by month, in MBtu. Note again that this figure does not include gas used for humidification purposes due to OpenStudio

limitations. Since the only use of natural gas is the preheat coil in the air handler natural gas consumption goes to zero in the summer months. In January when the building uses the most natural gas, it is still a 45% decrease over the baseline.

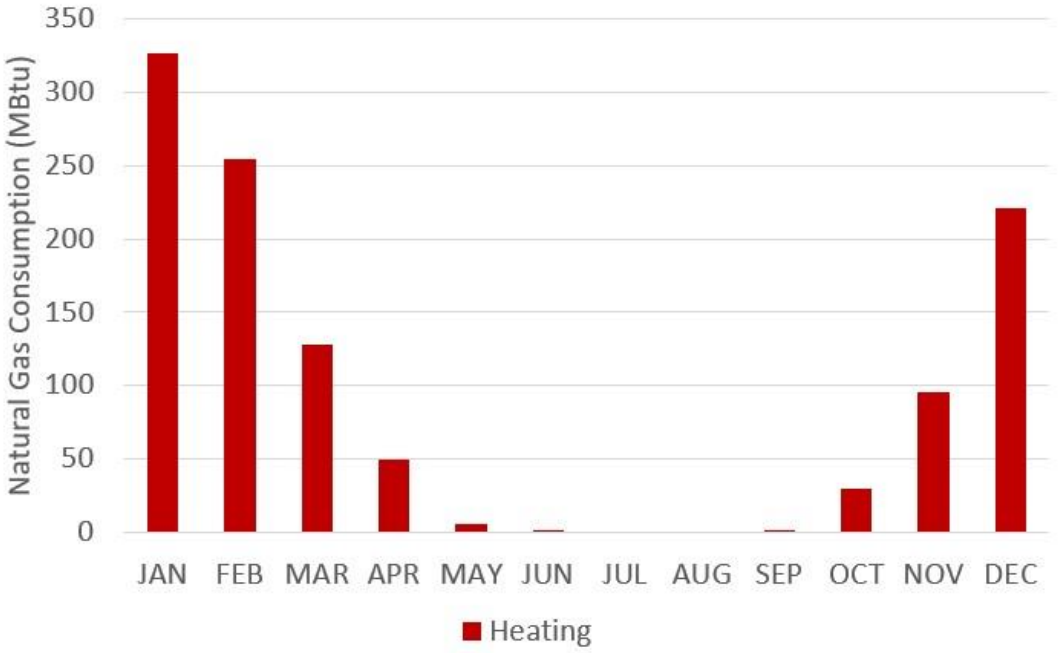

Figure 33 – Natural Gas Consumption (Model 2)

Figure 34 shows the simulated peak demand of natural gas per month, in MBH. Peak demand is zero in the summer months when there is no natural gas use. From December to March, natural gas use is between 48% and 62% lower than the baseline. This is due to the use of electricity for reheating over natural gas heated hot water. In the months of April, October, and November, peak use is only 8%, 9%, and 27% lower respectively. In these months, the outdoor air temperature and humidity are such that the VAV hot water reheat coils did not operate much meaning that most of the natural gas use was by the preheat coil. This led to the peak loads being similar to the baseline.

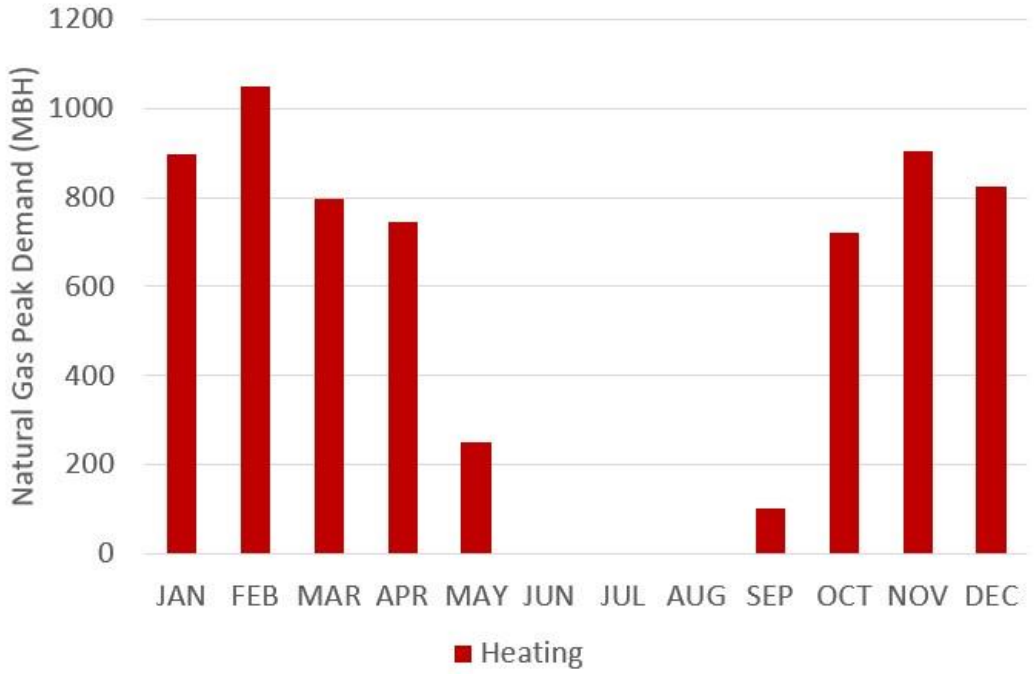

Figure 34 – Natural Gas Peak Demand (Model 2)

Table 29 contains the simulated total annual natural gas use broken down by end-use. Table 30 contains the energy summary for model 2. Compared to the baseline, natural gas usage decreased by 50% with a reduction in site EUI of around 6.3%.

Table 29 – Natural Gas Consumption by End Use (Model 2)

End Use	Natural Gas (therms)	Percentage Share (%)
Heating	11,113 (1,111,300 kBtu)	33.0
Humidification	22,593 (2,259,300 kBtu)	67.0
Total	33,706 (3,370,600 kBtu)	100

Table 30 – Energy Summary (Model 2)

Energy Source	Value
Electricity	6,328,226 kBtu
Natural Gas	33,706 therms (3,370,600 kBtu)
Total	9,698,826 kBtu
Total (Site EUI)	296.5 kBtu/ft^2

Using the same site-to-source conversion factors as the baseline, Table 31 contains the estimated source energy for this configuration. The total source EUI is approximately 24% higher than the baseline source EUI. This is consistent with the literature.

Table 31 – Source Energy for Mid Coast Hospital (Model 2)

Energy Source	Site-to-Source Conversion Factor [41]	Primary Energy
Electricity	2.80	17,719,033 kBtu
Natural Gas	1.05	3,529,130 kBtu
Total (Source EUI)	-	649.6 kBtu/ft^2

Table 32 contains the estimated carbon emissions for model 2 using the same data from the baseline model. This configuration resulted in a reduction in carbon emissions by 0.3% when compared to the baseline model.

Table 32 – Carbon Dioxide Emissions of Mid Coast Hospital (Model 2)

Energy Source	Energy	Emissions Rate	Emissions
Electricity	6,661,292 kBtu	0.1507 lbs/kBtu	1,004,000 lbs/year
Natural Gas	3,539,130 therms	0.123 lbs/kBtu	435,300 lbs/year
Total	-	-	652.8 MT/year

Table 33 contains the estimated operating costs of model 2. Compared to the baseline model, model 2 resulted in an 11% increase in operating costs. This is consistent with the literature.

Table 33 – Operating Costs of Mid Coast Hospital (Model 2)

Source Energy	Energy	Cost (Per Unit Energy)	Cost
Electricity	1,854,697 kWh	$0.11256/kWh	$208,765/year
Natural Gas	33,706 therms	$1.871/therm	$63,064/year
Total	-	-	$271,829/year

4.2 Electric Boiler w/ VAV Hot Water Reheat

As discussed in the literature review, electric water is another suitable approach to reducing reliance on natural gas. Similar to electric reheat, this change may result in increased

source energy use due to inefficiencies in electricity production and an increased operating cost due to the low price of natural gas. This analysis addresses these factors.

4.2.1 EnergyPlus Modeling

Within the EnergyPlus model, an electric steam boiler simply replaced the natural gas steam boiler. Since the simple hot water boiler model is independent of fuel type, the model used the same equations to govern performance and the fuel type became electricity. The model assigned a nominal thermal efficiency of 0.99 which is consistent with the literature. The model kept all other variables equal to the baseline.

4.2.2 Model Results

In zones with both heating and cooling equipment, there were no unmet cooling hours and no more than two unmet heating hours per zone. This is per ASHRAE Standard 90.1-2019 which states that unmet load hours shall not exceed 300 (of the 8760) [42]. In conditioned zones, relative humidity fell within the range 40-65%.

Figure 35 shows the simulated total electricity consumption, in MBtu, broken down by month. Cooling dominates electricity consumption in the summer months and heating/humidification dominates in the winter months. January had the largest increase in electricity consumption at 682% above the baseline. July had the smallest increase at 51% over the baseline which is similar to the increase in model 2. The drastic increase in the winter months is largely due to humidification which now requires electrically heated water. In terms of total energy use in the month of January, model 3 estimated 906.4 MBtu, and the baseline estimated 1,098 MBtu (17.4% decrease). This decrease gets smaller in the summer months due to the

domination of an already electrified cooling system. This is due to the increased on-site efficiency of electric heating over natural gas heating.

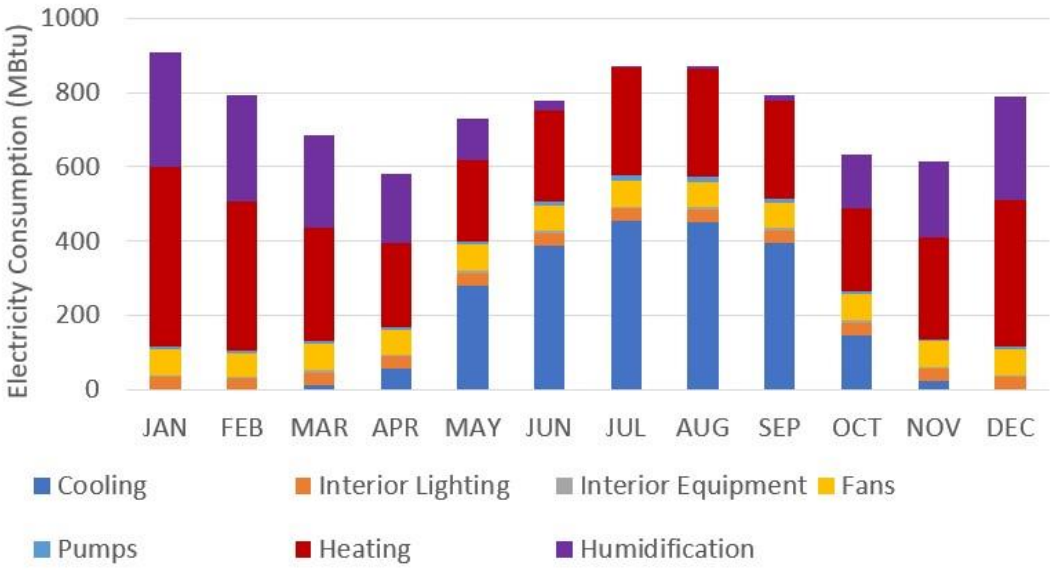

Figure 35 – Electricity Consumption (Model 3)

Figure 36 contains the simulated peak electricity loads, in MBH. In the winter months, the heating load dominates the peak load, and in the summer months cooling dominates. In the winter, peak electricity loads are much higher than the baseline. December, January, February, and March showed a 515%, 1060%, 703%, and 227% increase over the baseline, respectively. Demand peaked in February at 2511 MBH. In the summer months when there is not much heating demand, the peak electricity load had a much smaller increase. For example, July only experienced around a 48% increase.

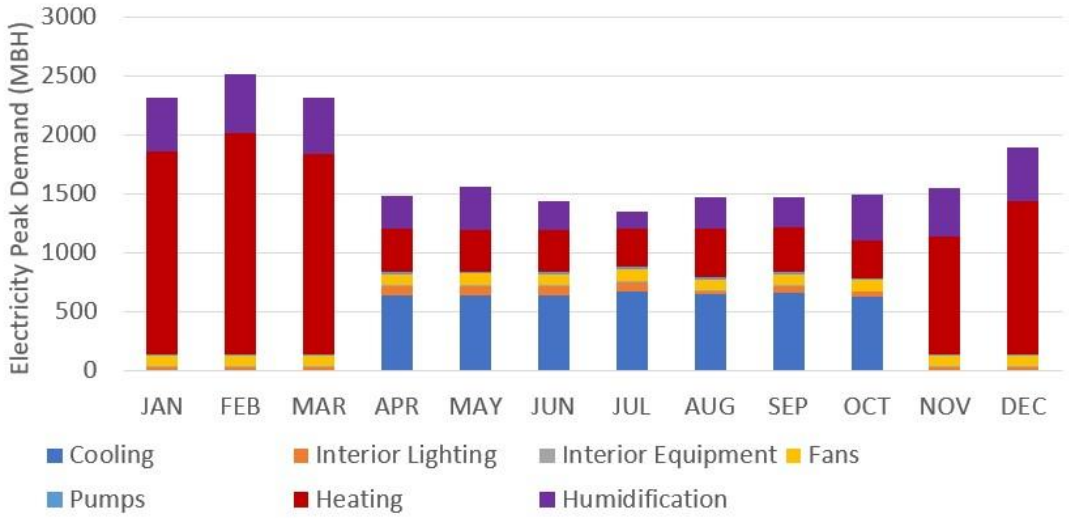

Figure 36 – Electricity Peak Demand (Model 3)

Table 34 contains the annual simulated electricity consumption broken down by end-use. Compared to the baseline, electricity usage increased by 151%.

Table 34 – Electricity Consumption by End Use (Model 3)

End Use	Electricity (kBtu)	Percentage Share (%)
Cooling	2,212,197	24.5
Heating	3,625,335	40.1
Interior Lighting	400,777	4.4
Interior Equipment	69,189	0.8
Fans	819,668	9.1
Pumps	105,629	1.2
Humidification	1,806,937	20.0
Total	9,039,732	100

At this point, the facility is completely electrified and has no natural gas (on-site) consumption. Table 35 contains the energy summary for model 3. Compared to the baseline, natural gas usage decreased by 100% with a reduction in site EUI of around 12.6%.

Table 35 – Energy Summary (Model 3)

Energy Source	Value
Electricity	9,039,732 kBtu
Natural Gas	0 therms (0 kBtu)
Total	9,039,732 kBtu
Total (Site EUI)	276.4 kBtu/ft^2

Using the same site-to-source conversion factors as the baseline, Table 36 contains the estimated source energy for this configuration. The total source EUI is approximately 47% higher than the baseline source EUI. This is consistent with the literature.

Table 36 – Source Energy for Mid Coast Hospital (Model 3)

Energy Source	Site-to-Source Conversion Factor [41]	Primary Energy
Electricity	2.80	25,311,250 kBtu
Natural Gas	1.05	0 kBtu
Total (Source EUI)	-	773.5 kBtu/ft^2

Table 37 contains the estimated carbon emissions for model 3 using the same data from the baseline model. This configuration resulted in a reduction in carbon emissions by 0.7% when compared to the baseline model.

Table 37 – Carbon Dioxide Emissions of Mid Coast Hospital (Model 3)

Energy Source	Energy	Emissions Rate	Emissions
Electricity	9,515,505 kBtu	0.1507 lbs/kBtu	1,434,000 lbs/year
Natural Gas	0 kBtu	0.123 lbs/kBtu	0 lbs/year
Total	-	-	650.5 MT/year

Table 38 contains the estimated operating costs of model 3. Compared to the baseline model, model 3 resulted in a 22% increase in operating costs. This is consistent with the literature.

Table 38 – Operating Costs of Mid Coast Hospital (Model 3)

Source Energy	Energy	Cost (Per Unit Energy)	Cost
Electricity	2,649,394 kWh	$0.11256/kWh	$298,220/year
Natural Gas	0 therms	$1.871/therm	$0/year
Total	-	-	$298,220/year

4.3 Variable Refrigerant Flow Heat Pump

A third suitable option is a variable refrigerant flow heat pump system. According to the literature, the expectation is a drop in both site and source energy, a decrease in operating costs,

and a decrease in carbon emissions. These effects should be limited by the extreme ambient conditions in the winter months resulting in a lesser decrease compared to other alternatives.

4.3.1 EnergyPlus Modeling

Since there is no existing VRF system for this facility, this model utilized the preloaded VRF model within OpenStudio and EnergyPlus. EnergyPlus contains two models for the variable refrigerant flow system; the system curve-based model and the physics-based model. OpenStudio utilizes the system curve-based model. This model uses modifier curves to describe part load operation. Since VRF systems are complex, the number of modifier curves is large. In simple terms, the model specifies a combination ratio which is defined as the total terminal unit rated capacity divided by the outdoor unit rated capacity. The model then uses modifier curves to describe the part load operation of the compressor, condenser heat exchanger, terminal unit electronic expansion valve, and terminal unit evaporator heat exchanger. All of these modifier curves are dependent on each other. The model assumed the default operation curves.

Since VRF systems are comprised of an outdoor unit and multiple indoor terminal units, the model broke up the conditioned zones into four groups with a similar total heating load. The model assumed the EnergyPlus default for COP of heating and cooling of 3.5 and 3.3 respectively. The model further assumed the default modifier curves. Airflow rates of the VRF system and terminal units remained constant from the baseline to ensure ventilation requirements, however, the model specified heating capacities of the VRF terminal units to match the existing VAV box capacities.

Due to humidity control requirements, the cooling coil and energy recovery ventilation in the AHU was necessary. Without the cooling coil, relative humidity in the summer months would greatly exceed the 65% limit. Dehumidification equipment would need to be present in

every individual zone which is not practical for such a large facility. Given this, the model kept the air-cooled chiller for dehumidification and thus cooling. This allowed the model to specify the VRF systems as heating only. Furthermore, comfort conditions specify a relative humidity of at least 40%. The humidity ratio for 40% and 50% relative humidity between 70°F and 75°F dry bulb temperature is ±0.008 lbs/lb of dry air. The minimum dry bulb temperature for air to hold this amount of moisture is around 51°F. If the air is not at least this temperature before the humidifier, the relative humidity will be too low for comfort. The model implemented energy recovery ventilation in the air handler to preheat incoming air using zone exhaust. This solved the problem of low humidity. The model removed the preheat coil in the AHU and replaced the boiler with a small electric water heater for the domestic hot water supply. The model further replaced the hot water coils in the unit heaters with electric heating coils and electrified the humidifier.

4.3.2 Model Results

Since the air-cooled chiller provided cooling, there were no unmet cooling hours in zones supplied by it. This is the same as the previous models. There were numerous unmet heating hours in the zones supplied by the VRF systems. The number of unmet heating hours ranged from zero to 99 with one large outlier of 327. While the majority still fell below the ASHRAE guideline of 300, the VRF systems were much less effective at maintaining zone conditions than the other configurations. This result is supported by the literature published by Wang [19]. As for humidity, the air handler ensured that the relative humidity fell between 40% and 65% at all times throughout the year.

Figure 37 shows the simulated total electricity consumption, in MBtu, broken down by month. Cooling dominates electricity consumption in the summer months and

heating/humidification power dominated in the winter months. February had the largest increase in electricity consumption at 320% above the baseline. July had the smallest increase at 22.3% over the baseline.

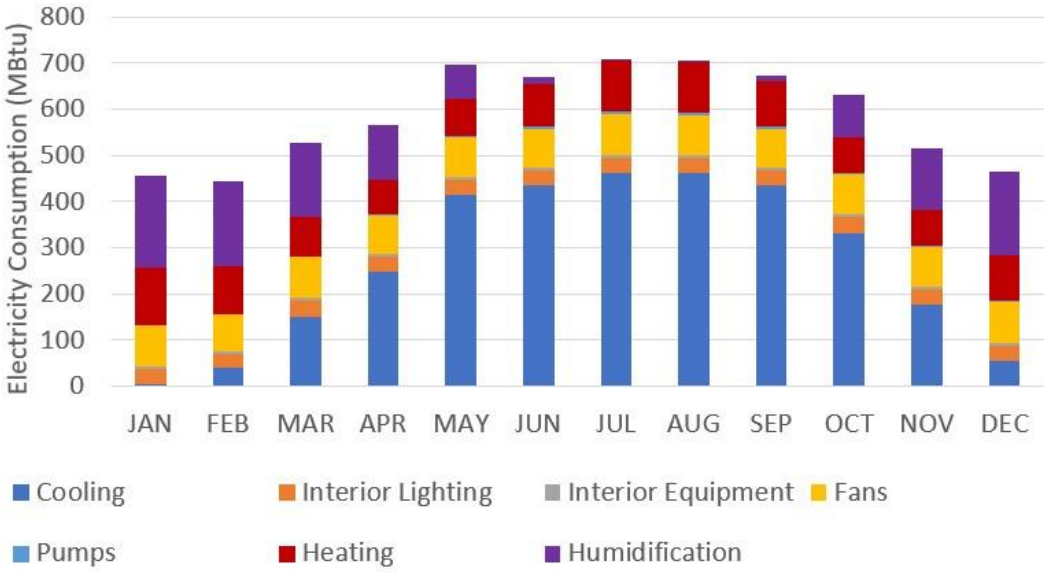

Figure 37 – Electricity Consumption (Model 4)

Figure 38 contains the simulated peak electricity loads, in MBH. This figure shows an interesting trend. It appears that electricity peak demand has a similar profile for every month except January which is heating and humidification dominated. All the other months seem to be cooling-dominated. This is likely due to the energy recovery ventilation in the AHU greatly lowering the need for heating. In January, the peak electricity load increased the most (298%). The summer months averaged only around a 22-35% increase. When compared to models 2 and 3, the demand was much lower.

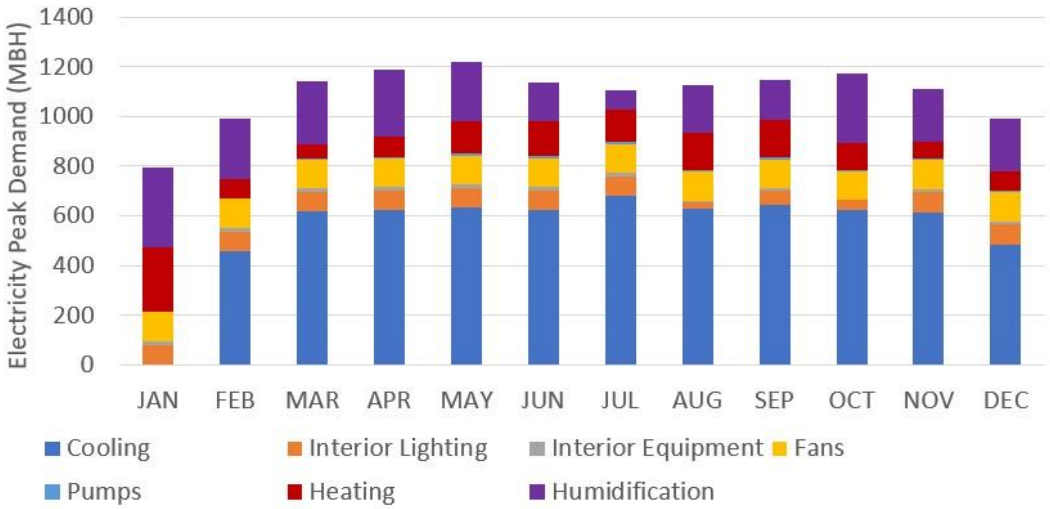

Figure 38 – Electricity Peak Demand (Model 4)

Table 39 contains the annual simulated electricity consumption broken down by end-use. Compared to the baseline, electricity usage increased by 95.6%.

Table 39 – Electricity Consumption by End Use (Model 4)

End Use	Electricity (kBtu)	Percentage Share (%)
Cooling	3,213,508	45.5
Heating	1,131,959	16.0
Interior Lighting	400,794	5.7
Interior Equipment	69,191	1.0
Fans	1,032,798	14.6
Pumps	30,975	0.4
Humidification	1,175,710	16.7
Total	7,054,935	100

Table 40 contains the energy summary for model 4. Model 4 had a reduction in site EUI of around 31.8% over the baseline.

Table 40 – Energy Summary (Model 4)

Energy Source	Value
Electricity	7,054,935 kBtu
Natural Gas	0 therms (0 kBtu)
Total	7,054,935 kBtu
Total (Site EUI)	215.6 kBtu/ft^2

Using the same site-to-source conversion factors as the baseline, Table 41 contains the estimated source energy for this configuration. The total source EUI is 15.0% higher than the baseline source EUI.

Table 41 – Source Energy for Mid Coast Hospital (Model 4)

Energy Source	Site-to-Source Conversion Factor [41]	Primary Energy
Electricity	2.80	19,753,818 kBtu
Natural Gas	1.05	0 kBtu
Total (Source EUI)	-	603.6 kBtu/ft^2

Table 42 contains the estimated carbon emissions for model 4 using the same data from the baseline model. This configuration resulted in a reduction in carbon emissions by 22.4% when compared to the baseline model.

Table 42 – Carbon Dioxide Emissions of Mid Coast Hospital (Model 4)

Energy Source	Energy	Emissions Rate	Emissions
Electricity	7,426,247	0.1507 lbs/kBtu	1,119,000 lbs/year
Natural Gas	0 kBtu	0.123 lbs/kBtu	0 lbs/year
Total	-	-	507.6 MT/year

Table 43 contains the estimated operating costs of model 5. Compared to the baseline model, model 4 resulted in a 5.1% decrease in operating cost. This is consistent with the literature.

Table 43 – Operating Costs of Mid Coast Hospital (Model 4)

Source Energy	Energy	Cost (Per Unit Energy)	Cost
Electricity	2,067,683 kWh	$0.11256/kWh	$232,738/year
Natural Gas	0 therms	$1.871/therm	$0/year
Total	-	-	$232,738/year

4.4 Ground-Source Heat Pump

Ground-sourced heat pumps are the final energy-saving option this analysis addresses. The expectation is a reduction in both site and source energy use, lower operating costs, and a

reduction in carbon emissions. Due to the increased efficiency, these effects should be greater than the VRF system.

4.4.1 EnergyPlus Modeling

Due to the need for central dehumidification, the chiller and the chilled water coil in the air handling unit remained part of the overall HVAC system. The result was that the GSHPs within the zones only supplied heating. EnergyPlus contains a water-to-air heat pump object which the model utilized as the template for the GSHPs. EnergyPlus models this water-to-air heat pump object via a single-speed equation fit model. According to the EnergyPlus engineering reference, the methodology utilizes five non-dimensional equations to predict heat pump performance. Since this particular model only utilizes the heat pumps in heating mode, only two equations are necessary. The model solves equations 17 and 18 to determine the performance of the heat pumps [40].

$$\frac{Q_h}{Q_{h,ref}} = E1 + E2\left[\frac{T_{db}}{T_{ref}}\right] + E3\left[\frac{T_{w,in}}{T_{ref}}\right] + E4\left[\frac{\dot{V}_{air}}{\dot{V}_{air,ref}}\right] + E5\left[\frac{\dot{V}_w}{\dot{V}_{w,ref}}\right] \quad (17)$$

$$\frac{P_h}{P_{h,ref}} = F1 + F2\left[\frac{T_{db}}{T_{ref}}\right] + F3\left[\frac{T_{w,in}}{T_{ref}}\right] + F4\left[\frac{\dot{V}_{air}}{\dot{V}_{air,ref}}\right] + F5\left[\frac{\dot{V}_w}{\dot{V}_{w,ref}}\right] \quad (18)$$

The coefficients come from a generalized least-squares method adapted from a 2005 M.S. dissertation by Tang [48]. The inputs are inlet air dry-bulb temperature, inlet air wet-bulb temperature, water inlet temperature, air volumetric flow rate, and water volumetric flow rate. The model specifies reference conditions based on loading and COP. The curve-fit model takes these parameters and develops a curve fit to catalog data. The model specified that the heating and cooling air supply rate had to match the ventilation requirements. The Federal Energy Management Program (FEMP) and EnergyStar provide minimum efficiencies to be designated

by their organizations. The minimum efficiency for a ground-sourced, closed-loop water-to-air heat pump is 3.6 for a single-phase system [49]. The model assigned 3.6 as the nominal COP to the GSHP units. The simulation auto-sized the remaining components based on loading.

The ground loop linked all of the terminal units to the vertical borehole ground heat exchanger that auto sized based on loading. The calculations for the ground heat exchanger object in EnergyPlus are long and complex. The engineering reference for EnergyPlus contains the full explanation. Essentially, the model uses a g-function to discretize the bore field and determine performance characteristics based on ground conditions. This model assumed the default g-function. The loop utilized a 30% propylene glycol solution to prevent freezing in the winter months. The nominal deep ground temperature was taken as 50°F. This value is the average annual topsoil temperature for Brunswick, Maine [50]. A performance curve governed the operation of the GSHP units. The performance curve is part of the EnergyPlus template and is from experimental water-to-air heat pump data.

A water-cooled chiller replaced the air-cooled chiller in this model. This was necessary to balance heating and cooling loads. The literature validates the claim that unbalanced loading leads to system degradation in the long term. The water-cooled chiller was linked to the ground loop to serve as its condensing loop. Theoretically, this should result in greater efficiency since the condenser operates at a constant temperature rather than varying outdoor air temperature. The model kept the cooling capacity and chilled water flow rate constant to the baseline. The FEMP and EnergyStar again specify minimum efficiency for a water-cooled chiller. The model assumed a minimum nominal COP of 5.75 [49].

Unlike the VRF system, the GSHP system's increased efficiency allowed it to maintain zone comfort conditions and setpoints without the use of a preheat coil. This allowed the model

to neglect the natural gas boiler altogether. As with the VRF system, however, without preheating, the incoming outdoor air could not hold enough moisture to maintain minimum relative humidity. Energy recovery ventilation (ERV) solved this problem. Due to the high ventilation requirements of a hospital, a large amount of heat is lost and gained through the outdoor air system. This left the door open for heat recovery in the air handler. The model applied an ERV heat exchanger within the air handler to preheat incoming air which resulted in proper humidity levels in the winter months.

The model added a small electric water heater to account for the small heating load of domestic hot water. Furthermore, an electric humidifier replaced the steam humidifier. Unit heaters with electric heating replaced the unit heaters with hot water reheat. At this point, the facility was completely free of natural gas use.

4.4.2 Model Results

There were no unmet heating or cooling hours in zones with both heating and cooling equipment. Furthermore, all relative humidity values fell between 40-65% at all times throughout the year.

The total cooling-to-heating ratio of the HVAC systems was 0.68:1. This value fell within the range specified by Zhou meaning that the system should be thermally stable [20].

Figure 39 shows the simulated total electricity consumption, in MBtu, broken down by month. Humidification was the largest electricity consumer throughout most of the year. As a result, the facility used more electricity in the winter when the humidification need was high. When compared to the previous models, the electricity used for cooling was much less due to the increased efficiency of the water-cooled chiller over the air-cooled chiller. The ERV system also significantly decreased the heating load in the winter making the heating electricity consumption

relatively constant throughout the year. When compared to the baseline, the winter months saw the greatest increase. December, January, and February saw a 240%, 273%, and 280% increase, respectively. The summer months, however, saw a significant decrease in electricity consumption with June, July, August, and September experiencing a 44%, 46%, 46%, and 43% decrease, respectively. Again, this was largely due to the increased efficiency of the chiller.

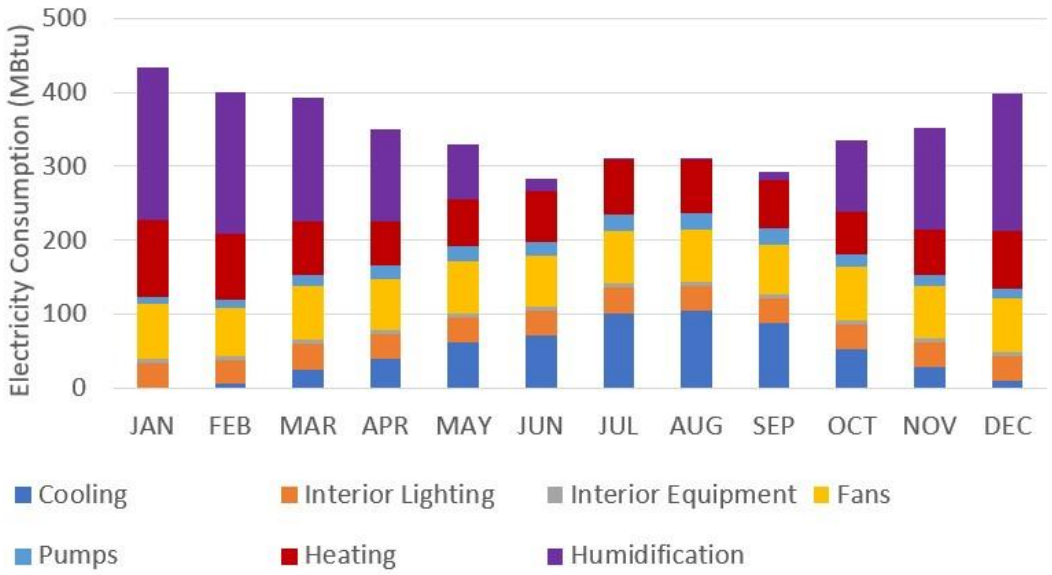

Figure 39 – Electricity Consumption (Model 5)

Figure 40 contains the simulated peak electricity loads, in MBH. In the winter months, humidification dominated. In the summer months, the peak load was more evenly spread across the sources. When compared to the baseline, January saw the greatest increase at 266%. The summer months saw a decrease in peak load over the baseline with July experiencing the most at 43%.

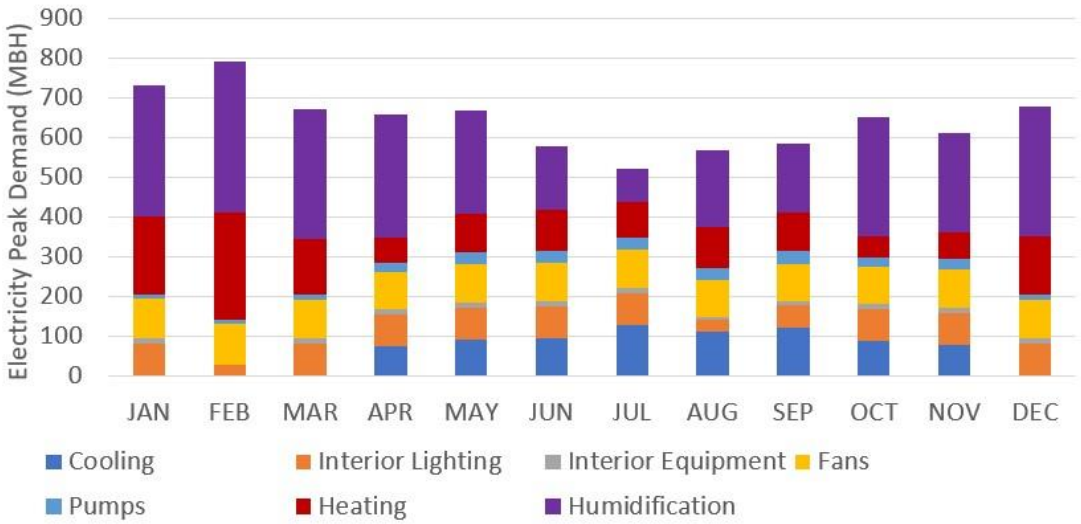

Figure 40 – Electricity Peak Demand (Model 5)

Table 44 contains the annual simulated electricity consumption broken down by end-use. Compared to the baseline, electricity usage increased by 16.1%.

Table 44 – Electricity Consumption by End Use (Model 5)

End Use	Electricity (kBtu)	Percentage Share (%)
Cooling	590,117	14.1
Heating	864,905	20.7
Humidification	1,213,536	29.0
Interior Lighting	400,776	9.6
Interior Equipment	69,189	1.7
Fans	844,517	20.2
Pumps	204,218	4.9
Total	4,187,258	100

Table 45 contains the energy summary for model 5. Compared to the baseline, natural gas usage decreased by 100% with a reduction in site EUI of around 59.5%.

Table 45 – Energy Summary (Model 5)

Energy Source	Value
Electricity	4,187,258 kBtu
Natural Gas	0 therms (0 kBtu)
Total	4,187,258 kBtu
Total (Site EUI)	128.0 kBtu/ft^2

Using the same site-to-source conversion factors as the baseline, Table 46 contains the estimated source energy for this configuration. The total source EUI is 31.7% lower than the baseline source EUI.

Table 46 – Source Energy for Mid Coast Hospital (Model 5)

Energy Source	Site-to-Source Conversion Factor [41]	Primary Energy
Electricity	2.80	11,724,322 kBtu
Natural Gas	1.05	0 kBtu
Total (Source EUI)	-	358.2 kBtu/ft^2

Table 47 contains the estimated carbon emissions for model 5 using the same data from the baseline model. This configuration resulted in a reduction in carbon emissions by 54.0% when compared to the baseline model.

Table 47 – Carbon Dioxide Emissions of Mid Coast Hospital (Model 5)

Energy Source	Energy	Emissions Rate	Emissions
Electricity	4,407,639 kBtu	0.1507 lbs/kBtu	664,200 lbs/year
Natural Gas	0 kBtu	0.123 lbs/kBtu	0 lbs/year
Total	-	-	301.3 MT/year

Table 48 contains the estimated operating costs of model 5. Compared to the baseline model, model 5 resulted in a 43.7% decrease in operating cost. This is consistent with the literature.

Table 48 – Operating Costs of Mid Coast Hospital (Model 5)

Source Energy	Energy	Cost (Per Unit Energy)	Cost
Electricity	1,227,215 kWh	$0.11256/kWh	$138,135/year
Natural Gas	0 therms	$1.871/therm	$0/year
Total	-	-	$138,135/year

4.5 Results Summary and Discussion

Table 49 contains the summary for all five models. Of note, models 3, 4, and 5 are completely fossil fuel free on-site as they only use electricity.

Table 49 – Complete Model Summary

Model	Site EUI (kBtu/ft^2)	Source EUI (kBtu/ft^2)	Operating Costs ($)	CO_2 Emissions (MT)
1	316.3	524.8	245,243	654.8
2	296.5	649.6	271,829	652.4
3	276.4	773.5	298,220	650.5
4	215.6	603.6	232,738	507.6
5	128.0	358.2	138,135	301.3

As is apparent, the GSHP system had the lowest values for all categories. The electric reheat and electric water heating models showed lower site EUI and lower carbon emissions, but higher source EUI and operating costs due to inefficiencies with electricity production and the relative price of electricity/natural gas, respectively. The VRF system was better than the baseline in site EUI, operating costs, and carbon emissions, however, was worse than the baseline in source EUI. The extreme ambient conditions in the winter months lowered the effectiveness of the VRF system. In the summer months, it performed similarly to the GSHP system.

A major consideration when discussing future electrification is the ability of the current power grid to meet demand specifically as it relates to peak loading. Table 50 contains the monthly peak loading for all five models in MBH. For the baseline system, the peak loading throughout the entire year was 907 MBH. As expected, electrifying heating resulted in higher peak loads. For models 2, 3, 4, and 5, the maximum peak loading was 1239 MBH, 2511 MBH, 1220 MBH, and 791 MBH, respectively. For the first three technologies, a large increase in peak demand (if the technology is widely adopted) is likely to put considerable strain on the power grid. In the long term, these solutions would require substantial investment in grid capacity improvements. Model 5, however, showed a decrease in peak demand. Furthermore, peak demand is greatest in the winter months whereas the baseline shows peak demand in the summer.

The increased demand in the winter is due to the heat pumps and the decrease in the summer is due to the increased efficiency of the water-cooled chiller. In the short term, this will likely result in further cost savings since the facility is using less electricity during times of high demand (and thus high prices) and more electricity when prices are cheaper. In the long term, the power grid is unlikely to need widespread infrastructure investment to meet demand.

Table 50 – Peak Electricity Demand by Month

	Month											
Model	**JAN**	**FEB**	**MAR**	**APR**	**MAY**	**JUN**	**JUL**	**AUG**	**SEP**	**OCT**	**NOV**	**DEC**
1	199	313	706	841	902	854	907	891	901	843	644	307
2	501	519	898	1195	1239	1225	1234	1227	1239	1248	886	512
3	2313	2511	2309	1484	1553	1438	1343	1473	1469	1488	1549	1886
4	794	992	1143	1187	1220	1134	1107	1125	1149	1174	1108	991
5	730	791	671	655	667	578	521	567	584	650	609	678

Another consideration is the economic implications in terms of the initial investment. Since the VRF and GSHP systems were the only configurations to result in decreased operating costs, this analysis only addresses those two. A more detailed economic analysis is necessary to obtain more accurate information; however, this analysis conducted a simple payback period calculation to assess the general time frame. A simple payback period does not consider the effects of inflation or the time value of money. Furthermore, given the high initial upfront investment cost, this analysis is for new construction only and does not consider a retrofit. Table 51 contains the estimated initial investment cost of the current system. These values are estimates based on RSMeans data and include labor costs. This analysis does not consider ductwork and piping costs. All prices were adjusted for inflation as of October 2022.

Table 51 – Initial Investment Cost of the Baseline System [51]

Component	Cost
Boiler	$253,942.48
Air-Cooled Chiller	$144,732.59
Air Handling Unit	$241,727.36
VAV Boxes	$80,848.26
Humidifier	$7,698.83
	$728,949.51

Table 52 contains the initial investment cost of the VRF system. All data except the VRF cost is from RSMeans data adjusted for inflation. VRF data is from research by Kim et al.

Table 52 – Initial Investment Cost of the VRF System [51, 52]

Component	Cost
Electric Water Heater	$7,329.07
Air-Cooled Chiller	$144,732.59
Air Handling Unit	$241,727.36
Energy Recovery Ventilator	$67,447.28
VAV Boxes	$47,032.84
Humidifier	$7,698.83
VRF	$767,751.96
	$1,283,719.93

Table 53 contains the initial investment cost of the GSHP system. All data except the GSHP costs are from RSMeans data adjusted for inflation. GSHP cost data comes from the U.S. EIA. Research by Liu et al. suggested that drilling costs for the ground heat exchangers are much higher in areas where the ground is comprised of mostly granite, such as Maine [54]. Given this information, this analysis assumed the upper level of cost for the GSHP.

Table 53 – Initial Investment Cost of the GSHP System [51, 53]

Component	Cost
Electric Water Heater	$7,329.07
Water-Cooled Chiller	$127,433.43
Air Handling Unit	$241,727.36
Energy Recovery Ventilator	$67,447.28
VAV Boxes	$47,032.84
Humidifier	$7,698.83
GSHP	$915,227.45
	$1,413,896.26

Equation 19 is the simple payback period for new construction. Table 54 contains the annual maintenance costs for the components that are different within the configurations. The cost multipliers are directly from the HVAC specifications provided by the facility. Note that the AHU cost is not considered since it is the same between the configurations. Table 55 contains the payback period for each of the configurations.

$$Payback\ Period = \frac{Investment\ Cost\ Difference}{Annual\ Savings} \tag{19}$$

Table 54: Annual Maintenance Costs [52, 53]

Component	Cost/unit	Total Cost
Air-Cooled Chiller	$24.18/ton	$3,170.00
VRF	$0.22/ft^2	$7,201.92
Water-Cooled Chiller	$30.22/ton	$3,961.84
GSHP	$45.33/ton	$5,942.76
Electric Water Heater	-	$60.44
Boiler	$2.72/kBtu/h	$22,756.20

Table 55: Payback Period Summary

System	Investment Cost Difference	Annual Savings	Payback Period
VRF	$554,770.41	$27,998.84	19.8 years
GSHP	$684,946.74	$123,069.16	5.6 years

The payback period for the VRF system is close to the service life of the equipment which makes it economically unattractive without any incentives. For new construction, the

GSHP system only has a payback period of around five and a half years meaning this could be economically feasible. Note that this payback period does not include demand charges by the utility company for electricity needs over the contracted amount. Furthermore, the RSMeans data is from 2011 adjusted for inflation and the relative prices of equipment and labor may have changed. Finally, these payback periods are estimates and only provide the order of magnitude of time.

Chapter 5: Conclusions

5.1 Research Summary

Hospitals are large energy consumers as compared to other commercial buildings due to their high ventilation requirements and continuous occupancy. This analysis took a section of a mid-size hospital in Brunswick, Maine, and evaluated various HVAC technologies and configurations to reduce energy use, operating costs, and, most importantly, carbon emissions. The four technologies were electric reheat, electric water heating, variable refrigerant flow, and ground-source heat pump. The facility provided all of the baseline parameters including building materials, HVAC diagrams, and building envelope plans. This analysis did not consider the true operation and instead made assumptions regarding temperature setpoints, occupancy, lighting, and plug loads which were informed by ASHRAE guidance.

The greatest site energy savings came from the GSHP system which showed a 59.5% decrease. All other technology options showed improvements as well with the VRF system, electric water heating, and electric reheat showing 31.8%, 12.6%, and 6.3% decrease, respectively. Furthermore, the energy savings of the VRF system was hampered by its decreased efficiency during times of extremely low ambient temperature. The decreased energy use of the electric water heating and electric reheat systems greatly was due to the greater efficiency of electric heating over combustion heating. They did, however, result in drastic increases in peak electricity demand which is not necessarily feasible in the short term.

The greatest source of energy savings again came from the GSHP system which showed a 31.7% decrease. The electric water heating, electric reheat, and VRF system showed an increase in source energy of 47%, 24%, and 15%, respectively. This was due to the inefficiencies

in electricity production and transmission. Again, this makes the first two technologies unappealing and not feasible in the short term and may cause hesitation with the VRF system.

The operating cost of the GSHP system was $138,135 which was a 43.7% decrease over the baseline. The VRF system also boasted a 5.1% decrease when compared to the baseline. The electric water heating and electric reheat showed a 22% and 11% increase over the baseline respectively providing no incentive to adopt these technologies. Furthermore, a simple payback period analysis showed that the GSHP system has the potential for lifetime cost savings as the payback period is only around five and a half years. Even though the VRF system has cheaper operating costs, the total payback period is almost its entire service life.

The GSHP systems decreased carbon emissions of the facility by 353.5 MT or 54.0%. The VRF system, electric water heating, and electric reheat decreased carbon emissions by 22.4%, 0.7%, and 0.3%, respectively. All technology options proved to reduce the carbon footprint of the facility in total. Since the GSHP and electric water heating resulted in a completely electrified facility, the local carbon emissions for these two technologies are zero.

In summary, the electric water heating and electric reheat systems proved to be unappealing based on operating cost and total source energy use. Furthermore, these two technologies (if widely adopted) would likely be infeasible given the current capacity of the power grid. The VRF system is a viable option as it reduces the carbon footprint of the facility, site EUI, and operating costs. The downside, however, is that VRF systems generally have high installation costs so further analysis may prove that it is not economically feasible in the long term and the source EUI proved to be worse than the baseline. The best technology option by far is the GSHP system as it showed the greatest improvement in all categories. Furthermore, the *Advanced Energy Design Guide for Large Hospitals* published by ASHRAE gives a target site

EUI for 50% energy savings in climate zone 6A as 125 kBtu/ft^2 [29]. The GSHP system resulted in a site EUI of 127.95 kBtu/ft^2. The actual number is likely to be slightly higher if all plug loads are considered. Installing a GSHP system is the best option to reduce carbon emissions in the future. These results are only for a mid-to-large size hospital in New England given their unique HVAC characteristics and further research into different building types should have a separate analysis.

5.2 Future Work

Now that this analysis has determined the best technology alternative to a conventional HVAC system and provided a general baseline for energy saving and CO_2 emissions reduction there are multiple avenues for future work. The first step for any of these avenues is applying this GSHP system to the entire facility. This analysis proved the concept and a more detailed analysis of the entire facility would provide a higher level of accuracy in the model. This includes attempting to capture the behavioral aspects of the model; occupancy, lighting schedule, plug load use, thermostat schedule, etc; more accurately instead of relying on assumptions. Furthermore, any future analysis should include a greater economic study which will help determine feasibility in the current market or help identify potential actions to spur future investment.

Future work in this field could include optimal control strategies. There is extensive literature on the control of HVAC systems to maximize energy savings, however, the strategy largely depends on location. Examples of this include optimizing energy recovery ventilation to reduce the need for supplemental heating and cooling and better controlling the air handler to minimize the introduction of unneeded outdoor air. These control strategies will vary throughout the year. In hospitals, this is increasingly important.

Another topic of future work includes the integration of the GSHP system for steam production for laundry and sanitation purposes. Aside from heating, healthcare facilities use large amounts of steam for cleaning. This analysis did not consider this need since section C of the building does not contain the corresponding equipment. There is research regarding a GSHP system for water heating and a dual configuration of both air and water heating should be considered in future analysis.

The third avenue for future work is the optimization of the configuration itself. OpenStudio is useful in that it allows for the general modeling of numerous systems in a shorter time frame, however, the configurations are limited to objects contained within the library. The full EnergyPlus library is much more extensive and allows for greater experimentation with this technology. There are also other energy modeling software packages that allow for greater flexibility.

The fourth topic of future work is the integration of on-site power generation into the configuration. Solar heating is commonly coupled with GSHP systems; however, capacity largely depends on factors such as location, shading, demand, etc. Optimization of a coupled GSHP with an on-site power generation system has the potential for further energy savings.

Future work that is external to the system itself is an analysis of the current power grid to identify areas for expansion. The quickest route to de-carbonization of the future is through electrification which will undoubtedly result in increasing demand. Generally, large facilities such as these have contracts with energy companies that specify max loading. Depending on demand, there would need substantial investment on the part of electricity companies to establish the ability to supply the right load. This would likely influence utility prices. As mentioned previously, on-site power generation is an option to relieve grid demand. Furthermore, an

investigation into the use of clean energy for mass electricity production would provide a path forward.

Appendix A

HVAC Chilled Water Piping Schematic [55]

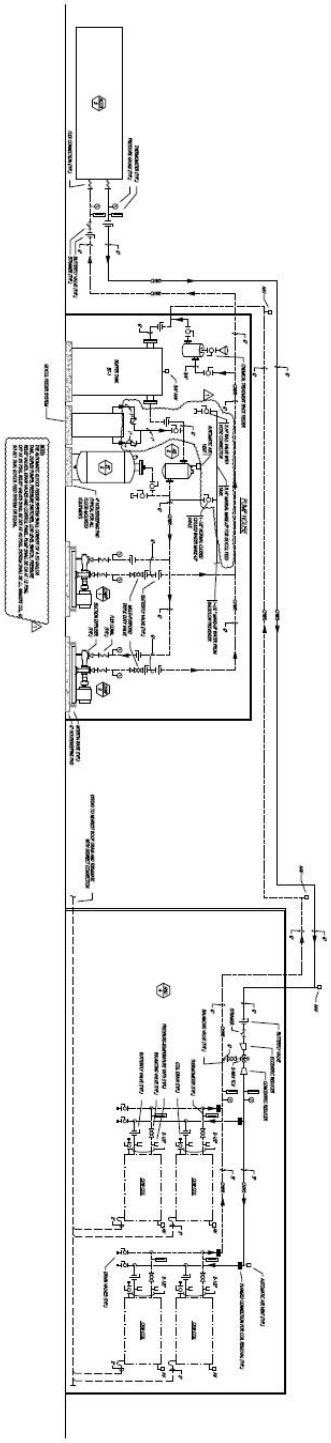

Appendix B

HVAC Steam Piping Schematic [56]

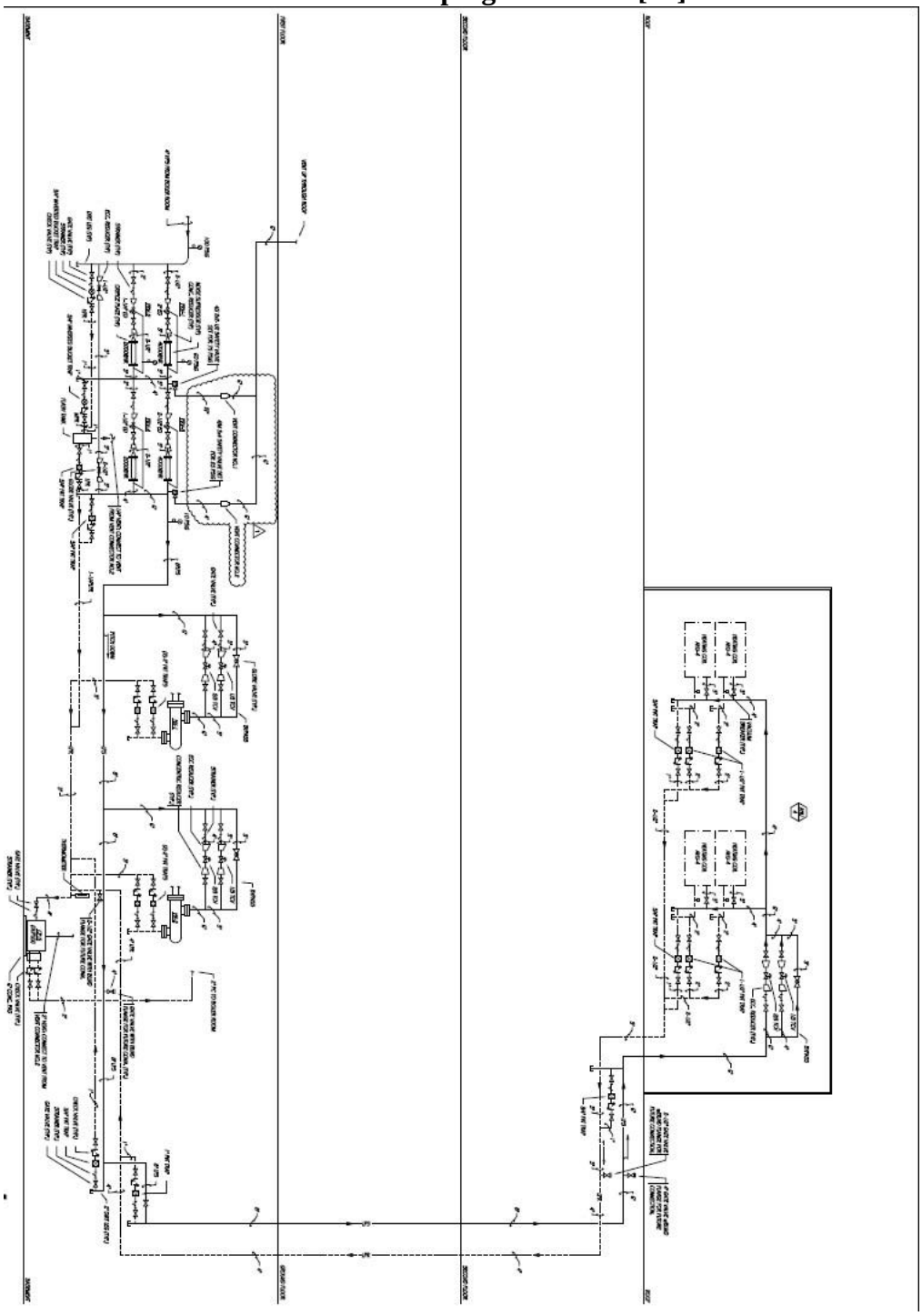

Appendix C

HVAC Hot Water Piping Schematic [57]

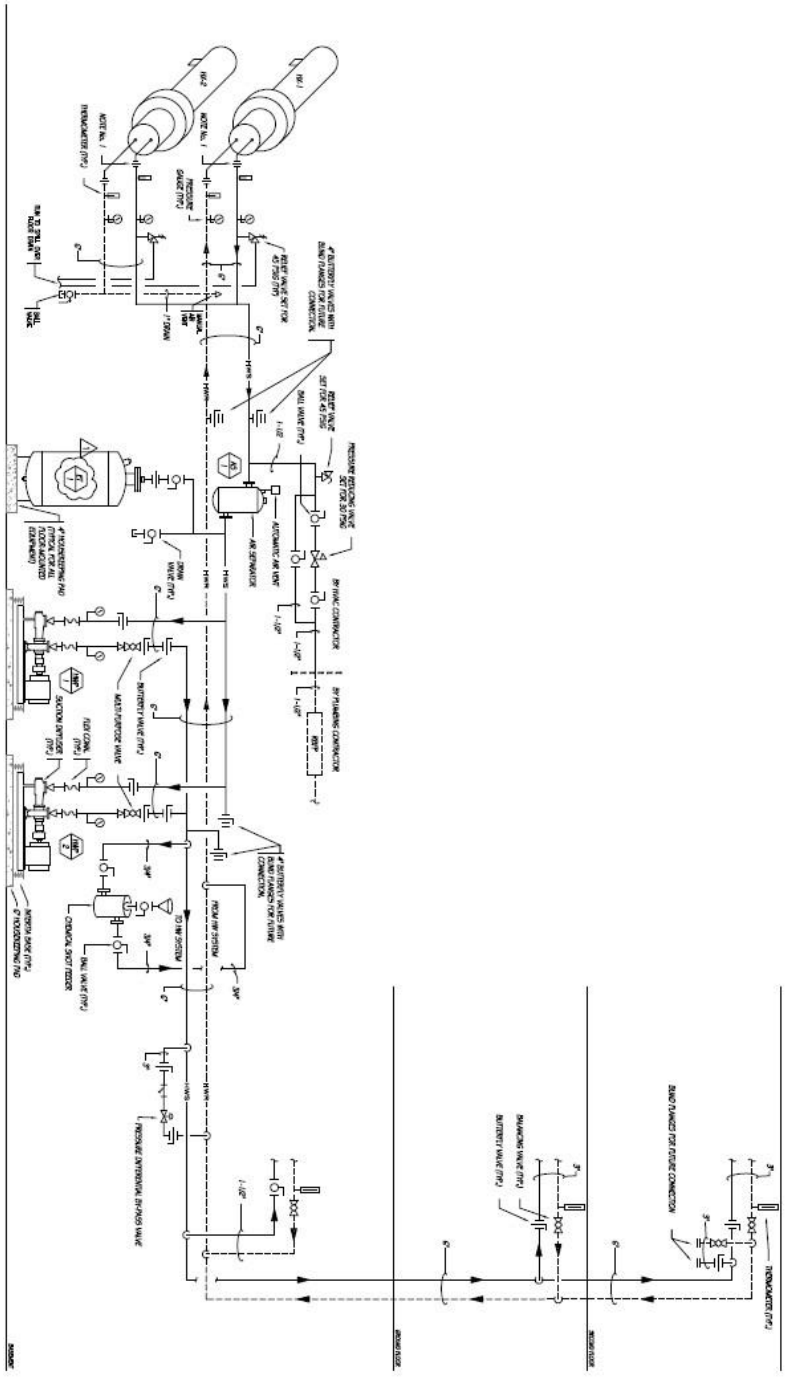

Appendix D

VCV Box Schedules [27]

VARIABLE & CONSTANT VOLUME BOX SCHEDULE (WITH INTEGRAL SOUND ATTENUATOR) SCHEDULE

DESIGNATION	LOCATION	SERVICE	TYPE	DESIGN RANGE (CFM)	ΔP_{in} PRESS IN. H_2O (MAX)	HOT WATER COIL								INLET STATIC PRESS (IN.)	MODE CRITERIA (AT LISTED INLET SP) MAX RPM SOUND POWER LEVEL (dB) (PREFERRED OR DESCHARGE)							DUCT CONNECTIONS			MAX. BOX DEPTH (IN)	LINING THICKNESS	LINING HOSP. GRADE	ACCESS DOOR BEFORE COIL	ACCESS DOOR AFTER COIL	MANUFACTURER/MODEL NUMBER	OPTIONS/REMARKS
						MBH	GPM	ΔP_{in}	AIR ΔP_{in}	FPI MAX	MIN. NO. OF ROWS	EAT_{in}	LAT_{out}		MAX. ΔP_{in}	125Hz	250Hz	500Hz	1KHz	2KHz	4KHz	INLET DUCT CONNECT SIZE (IN)	OUTLET DUCT CONNECT SIZE (IN)	OUTLET DUCT SIZE (IN)						
VCV-5	SEE PLANS	SEE PLANS	VARIABLE VOLUME	65~250	0.7	SEE PLANS	55	0.5	10	10	180	160	SEE PLANS	1.5	8	54	54	49	41	35	27	64	12X12	-	13	1"	YES	YES	AIR HAMC	ENVIRO-TEC SDR-SA-MC	OR APPROVED EQUAL
VCV-6	SEE PLANS	SEE PLANS	VARIABLE VOLUME	75~400	0.7	SEE PLANS	55	0.5	10	10	180	160	SEE PLANS	1.5	8	61	54	55	45	37	27	69	12X12	-	13	1"	YES	YES	AIR HAMC	ENVIRO-TEC SDR-SA-MC	OR APPROVED EQUAL
VCV-8	SEE PLANS	SEE PLANS	VARIABLE VOLUME	150~700	0.7	SEE PLANS	55	0.5	10	10	180	160	SEE PLANS	1.5	8	58	57	53	48	38	33	84	14X12	-	13	1"	YES	YES	AIR HAMC	ENVIRO-TEC SDR-SA-MC	OR APPROVED EQUAL
VCV-10	SEE PLANS	SEE PLANS	VARIABLE VOLUME	225~1000	0.7	SEE PLANS	55	0.5	10	10	180	160	SEE PLANS	1.5	8	58	58	58	49	39	38	104	16X12	-	13	1"	YES	YES	AIR HAMC	ENVIRO-TEC SDR-SA-MC	OR APPROVED EQUAL
VCV-12	SEE PLANS	SEE PLANS	VARIABLE VOLUME	350~1500	0.7	SEE PLANS	55	0.5	10	10	180	160	SEE PLANS	1.5	8	63	60	59	52	45	42	1468⟺1384	16X12	-	13	1"	YES	YES	AIR HAMC	ENVIRO-TEC SDL-SA-MC	OR APPROVED EQUAL
VCV-14	SEE PLANS	SEE PLANS	VARIABLE VOLUME	475~1950	0.7	SEE PLANS	55	0.5	10	10	180	160	SEE PLANS	1.5	8	63	63	58	51	46	44	1728⟺1644	24X12	-	13	1"	YES	YES	AIR HAMC	ENVIRO-TEC SDL-SA-MC	OR APPROVED EQUAL
VCV-16	SEE PLANS	SEE PLANS	VARIABLE VOLUME	650~2800	0.7	SEE PLANS	55	0.5	10	10	180	160	SEE PLANS	1.5	8	-	-	-	-	-	-	-	24X17	-	13	1"	YES	YES	AIR HAMC	ENVIRO-TEC SDL-SA-MC	OR APPROVED EQUAL
VCV-19	SEE PLANS	SEE PLANS	VARIABLE VOLUME	1100~3300	0.7	SEE PLANS	55	0.5	10	10	180	160	SEE PLANS	1.5	8	-	-	-	-	-	-	164	17X20	-	13	1"	YES	YES	AIR HAMC	ENVIRO-TEC SDL-SA-MC	OR APPROVED EQUAL

Appendix E

Unit Heater Schedules [27]

UNIT HEATER SCHEDULE

DESIGNATION	LOCATION	TYPE	FAN							HOT WATER COIL				ELECTRIC HEAT DATA				DIMENSIONS (IN.)			MANUFACTURER/MODEL NUMBER	OPTIONS/REMARKS
			CFM	RPM	# FANS	MOTOR (HP)	V	ø	HZ	MBH	EAT	GPM	EWT	MBH	EAT	KW	AMPS	LENGTH	WIDTH	HEIGHT		
CUH-1	SEE PLANS	FLOOR	345	875	1	1/10	120	1	60	25	60	4.0	180	–	–	–	–	47	9.5	27	STERLING / F-04	OR APPROVED EQUAL ①②③
CUH-2	SEE PLANS	CEILING	505	875	1	1/10	120	1	60	45	30	4.0	180	–	–	–	–	59	9.5	27	STERLING / RC-06	OR APPROVED EQUAL ①②③
CUH-3	SEE PLANS	CEILING	345	875	1	1/10	120	1	60	25	60	4.0	180	–	–	–	–	59	9.5	27	STERLING / RC-04	OR APPROVED EQUAL ①②③
UH-1	SEE PLANS	HORIZONTAL	480	1,350	1	16 W	120	1	60	30	60	3.5	180	–	–	–	–	17	11	20.5	STERLING / HC-48	OR APPROVED EQUAL ②③
EUH-1	CHILLED WTR. PUMP PENTHOUSE	ELECTRIC	750	1,550	1	1/10	460	3	60	–	–	–	–	34.1	0	10	18.8	18	18	8.0	O'MARK / EUH-1548	OR APPROVED EQUAL ②

Appendix F

Infiltration Rate Calculations for Windows/Doors

Rooms	Height (ft)	Width (ft)	No. of Windows/Doors	Window/Door Area (s.f)	Infiltration (cfm/sf window/door area)	Infiltration (cfm)
1_031	5.25	3.33	4	69.93	0.4	27.972
1_032	5.25	3.33	3	52.4475	0.4	20.979
1_033	5.25	3.33	1	17.4825	0.4	6.993
1_034	5.25	3.33	4	69.93	0.4	27.972
1_011	8.25	10.67	5	440.1375	0.4	176.055
1_011	8.25	4.5	1	37.125	0.4	14.85
1_011	7	12	1	84	1	84
1_036	8.9	17.6	2	313.28	0.4	125.312
1_036	8.9	2.5	2	44.5	0.4	17.8
1_036	7	12	1	84	0.4	33.6
1_004	8.25	10.67	1	88.0275	0.4	35.211
1_037	7.5	6	1	45	0.4	18
1_002	7.36	6.33	1	46.5888	0.4	18.63552
1_035	7.5	3.5	1	26.25	0.4	10.5
1_035	8.49	2.5	1	21.225	0.4	8.49
1_035	1	3.5	1	3.5	0.4	1.4
1_024	7	4.33	1	30.31	0.4	12.124
1_028	7	8	1	56	1	56
1_029	7	4.33	1	30.31	0.4	12.124
1_029	1.5	4.33	1	6.495	0.4	2.598
2_038	7.36	4.33	2	63.7376	0.4	25.49504
2_005	7.36	6.5	1	47.84	0.4	19.136
2_037	7.36	4.33	1	31.8688	0.4	12.74752
2_037	7.36	6.5	3	143.52	0.4	57.408
2_037	7.36	12	1	88.32	0.4	35.328
2_037	7.36	20	1	147.2	0.4	58.88
2_002	7.36	6.5	2	95.68	0.4	38.272
2_003	7.36	6.5	1	47.84	0.4	19.136
2_016	7.36	6.5	2	95.68	0.4	38.272
2_018	7.36	6.5	1	47.84	0.4	19.136
2_039	7.36	4.33	2	63.7376	0.4	25.49504
2_023	7.36	6.5	1	47.84	0.4	19.136
2_025	7.36	6.5	2	95.68	0.4	38.272
2_027	7.36	6.5	2	95.68	0.4	38.272
2_029	7.36	6.5	1	47.84	0.4	19.136
2_030	7.36	6.5	1	47.84	0.4	19.136
2_032	7.36	6.5	2	95.68	0.4	38.272
2_034	7.36	6.5	2	95.68	0.4	38.272
2_036	7.36	6.5	1	47.84	0.4	19.136
2_014	7.36	6.5	1	47.84	0.4	19.136
2_012	7.36	6.5	2	95.68	0.4	38.272
2_010	7.36	6.5	2	95.68	0.4	38.272
2_008	7.36	6.5	1	47.84	0.4	19.136

References

[1] *Annual Energy Outlook 2022*, U.S. Energy Information Administration, 2022.
[2] "Power Profiler," U.S. Environmental Protection Agency, https://www.epa.gov/egrid/power-profiler#/NEWE (accessed August 8, 2022).
[3] "Table 8.1 – Average Operating Heat Rate for Selected Energy Sources (2010-2020." U.S. Energy Information Administration. https://www.eia.gov/electricity/annual/html/epa_08_01.html (accessed August 8, 2022).
[4] "Fuels – Higher and Lower Calorific Values." Engineering Toolbox. https://www.engineeringtoolbox.com/fuels-higher-calorific-values-d_169.html (accessed August 8, 2022).
[5] "Carbon Dioxide Emissions Coefficients." U.S. Energy Information Administration. https://www.eia.gov/environment/emissions/co2_vol_mass.php (accessed August 8, 2022).
[6] S.A Klein, Engineering Equation Solver (EES), F-Chart Software, Madison, WI, USA. https://fchartsoftware.com/.
[7] P. Raftery, A. Geronazzo, H. Cheng, and G. Paliaga. "Quantifying energy losses in hot water reheat systems," *Energy and Buildings*, vol. 179, pp. 183-199, 2018, doi: 10.1016/j.enbuild.2018.09.020.
[8] O. Ibrahim, F. Fardoun, R. Younes, and H. Louahlia-Gualous, "Review of water-heating systems: General selection approach based on energy and environmental aspects," *Building and Environment*, vol. 72, pp. 259-286, 2014, doi: 10.1016/j.buildenv.2013.09.006.
[9] Y.P. Zhou, J.Y. Wu, R.Z. Wang, S. Shiochi, and Y.M. Li, "Simulation and experimental validation of the variable-refrigerant-volume (VRV) air-conditioning system in EnergyPlus," *Energy and Buildings*, vol. 40, pp. 1041-1047, 2008, doi: 10.1016/j.enbuild.2007.04.025.
[10] Y. Zhu, X. Jin, Z. Du, B. Fan, and S. Fu, "Generic simulation model of multi-evaporator variable refrigerant flow air conditioning system for control analysis," *International Journal of Refrigeration*, vol. 36, pp. 1602-1615, 2013, doi: 10.1016/j.ijrefrig.2013.04.019.
[11] Y. Zhu, X. Jin, Z. Du, B. Fan, and S. Fu, "Simulation of variable refrigerant flow air conditioning system in heating mode combined with outdoor air processing unit," *Energy and Buildings*, vol. 68, pp. 571-579, 2014, doi: 10.1016/j.enbuild.2013.09.042.
[12] Y. Zhu, X. Jin, Z. Du, X. Fang, and B. Fan, "Control and energy simulation of variable refrigerant flow air conditioning system combined with outdoor air processing unit," *Applied Thermal Engineering*, vol. 64, pp. 385-395, 2014, doi: 10.1016/j.applthermaleng.2013.12.076.
[13] Y. Zhu, X. Jin, Z. Du, and X. Fang, "Online optimal control of variable refrigerant flow and variable air volume combined air conditioning system for energy savings," *Applied Thermal Engineering*, vol. 80, pp. 87-96, 2015, doi: 10.1016/j.applthermaleng.2015.01.030.
[14] E. Ozahi, A. Abusoglu, A.I. Kutlar, and O. Dagci, "A comparative thermodynamic and economic analysis and assessment of a conventional HVAC and a VRF system in a social and cultural center building," *Energy and Buildings*, vol. 140, pp. 196-209, 2017, doi: 10.1016/j.enbuild.2017.02.008.
[15] D. Kim, S. Cox, H. Cho, and P. Im, "Evaluation of energy savings potential of variable refrigerant flow (VRF) from variable air volume (VAV) in the U.S. climate locations," *Energy Reports*, vol. 3, pp. 85-93, 2017, doi: 10.1016/j.egyr.2017.05.002.
[16] G. Zhang et al., "Review on recent developments of variable refrigerant flow systems since 2015," *Energy and Buildings*, vol. 198, pp. 444-466, 2019, doi: 10.1016/j.enbuild.2019.06.032.

[17] O. Ozgener and A. Hepbasli, "Modeling and performance evaluation of ground-source (geothermal) heat pump systems," *Energy and Buildings*, vol. 39, pp. 66-75, 2007, doi: 10.1016/j.enbuild.2006.04.019.
[18] X. Liu and T. Hong, "Comparison of energy efficiency between variable refrigerant flow systems and ground source heat pump systems," *Energy and Buildings*, vol. 42, pp. 584-589, 2010, doi: 10.1016/j.enbuild.2009.10.028.
[19] S. Wang, "Energy modeling of ground source heat pump vs. variable refrigerant flow systems in representative US climate zone," *Energy and Buildings*, vol. 72, pp. 222-228, 2014, doi: 10.1016/j.enbuild.2013.12.017.
[20] Z. Zhou et al., "Feasibility of ground coupled heat pumps in office buildings: A China study," *Applied Energy*, vol. 162, pp. 266-277, 2016, doi: 10.1016/j.apenergy.2015.10.055.
[21] Z. Liu, W. Xu, X. Zhai, C. Qian, and X. Chen, "Feasibility and performance study of the hybrid ground-source heat pump system for one office building in Chinese heating dominated areas," *Renewable Energy*, vol. 101, pp. 1131-1140, 2017, doi: 10.1016/j.renene.2016.10.006.
[22] S. Karytsas and I. Choropanitis, "Barriers against and actions towards renewable energy technologies diffusion: A Principal Component Analysis for residential ground source heat pump (GSHP) systems," *Renewable and Sustainable Energy Reviews*, vol. 78, pp. 252-271, 2017, doi: 10.1016/j.rser.2017.04.060.
[23] P. Yin, M. Pate, and F. Battaglia, "In-field performance evaluation and economic analysis of residential ground-source heat pumps in heating operation," *Journal of Building Engineering*, vol. 26, 2019, doi: 10.1016/j.jobe.2019.100932.
[24] A. Kapicioglu and H. Esen, "Economic and environmental assessment of ground source heat pump system: The case of Turkey," *Sustainable Energy Technologies and Assessments*, vol. 53, 2022, doi: 10.1016/j.seta.2022.102562.
[25] "Floor Plans." Mid Coast Hospital. https://www.midcoasthealth.com/findus/floorplans.aspx (accessed August 10, 2022).
[26] "Architectural Floor Plan – Ground Level Area C (AC101)." Mid Coast Hospital.
[27] "HVAC Schedules (H001)." Mid Coast Hospital.
[28] D.B. Lu and D.M. Warsinger, "Energy savings of retrofitting residential buildings with variable air volume systems across different climates," *Journal of Building Engineering*, vol. 30, 2020, doi: 10.1016/j.jobe.2020.101223.
[29] *Advanced Energy Design Guide for Large Hospitals*, ASHRAE, Atlanta, GA, United States, 2012.
[30] "Wall Section (A401)." Mid Coast Hospital.
[31] EnergyPlus, Version 9.6.0, U.S. Department of Energy, 2021. https://energyplus.net/.
[32] OpenStudio, Version 3.3.0, National Renewable Energy Laboratory, 2021. https://openstudio.net/.
[33] OpenStudio Application, Version 1.3.0, OpenStudio Coalition, 2021. https://openstudiocoalition.org/.
[34] M. Shin and J.S. Haberl, "Thermal zoning for building HVAC design and energy simulation: A literature review," *Energy and Buildings*, vol. 203, 2019, doi: 10.1016/j.enbuild.2019.109429.
[35] "Architectural Floor Plan – Second Level Area C (AC102)." Mid Coast Hospital.
[36] "Dell – Inspiron Compact Desktop – Intel Core i5-12400-12GB-Memory-256GB SSD-Mist Blue." Best Buy. https://www.bestbuy.com/site/dell-inspiron-compact-desktop-intel-core-i5-

12400-12gb-memory-256gb-ssd-mist-blue/6501295.p?skuId=6501295 (accessed August 15, 2022).
[37] "Acer – 27" IPS LED FHD FreeSync Monitor (HDMI, VGA) – Black." Best Buy. https://www.bestbuy.com/site/acer-27-ips-led-fhd-freesync-monitor-hdmi-dvi/6437411.p?skuId=6437411 (accessed August 15, 2022).
[38] "TV Wattage – 2022's Most Efficient TVs Revealed [With Data]." Eco Cost Savings. https://ecocostsavings.com/tv-wattage/ (accessed September 1, 2022).
[39] *Standard 170-2013: Ventilation of Health Care Facilities*, ANSI/ASHRAE/ASHE, Atlanta, GA, United States, 2013.
[40] *EnergyPlus Engineering Reference*, Version 9.6.0, U.S. Department of Energy, 2021.
[41] *Infiltration Modeling Guidelines for Commercial Building Energy Analysis*, Pacific Northwest National Laboratory, 2009.
[42] *Standard 90.1-2019: Energy Standard for Buildings Except Low-Rise Residential Buildings*, ANSI/ASHRAE/IES, Atlanta, GA, United States, 2019.
[43] *Standard 62.1-2010: Ventilation for Acceptable Indoor Air Quality*, ANSI/ASHRAE, Atlanta, GA, United States, 2010.
[44] *Technical Reference: U.S. Energy Use Intensity by Property Type*, EnergyStar, 2021.https://portfoliomanager.energystar.gov/pdf/reference/US%20National%20Median%20Table.pdf.
[45] J.V. Dirks, "Modeled Performance Isn't Actual Performance," *ASHRAE Journal*, vol. 58, no. 5, 2016.
[46] "What are the Site-to-Source Conversion Factors?" Energy Star, https://energystar-mesa.force.com/PortfolioManager/s/article/What-are-the-Site-to-Source-Conversion-Factors-1600088532330 (accessed September 10, 2022).
[47] "How much electricity is lost in electricity transmission and distribution in the United States?" U.S. Energy Information Administration, https://www.eia.gov/tools/faqs/faq.php?id=105&t=3 (accessed September 10, 2022).
[48] C.C. Tang, "Modeling Packaged Heat Pumps in Quasi-Steady State Energy Simulation Program," M.S. Thesis, Department of Mechanical and Aerospace Engineering, Oklahoma State University, Stillwater, OK, U.S., 2005.
[49] "Incorporate Minimum Efficiency Requirements for Heating and Cooling Products into Federal Acquisition Documents." U.S. Department of Energy. https://www.energy.gov/eere/femp/incorporate-minimum-efficiency-requirements-heating-and-cooling-products-federal (accessed September 20, 2022).
[50] "Soil Temperature Maps." GreenCast Online. https://www.greencastonline.com/tools/soil-temperature (accessed September 21, 2022).
[51] RSMeans Data, Gordian, 2022. https://www.rsmeans.com/?utm_source=google&utm_medium=cpc&utm_campaign=Brand_Exact&utm_content=rs_means&utm_term=rsmeans&gclid=Cj0KCQiAsdKbBhDHARIsANJ6-jdsT_UGzFrwPQ8EABZ_cIirvwxrhalZru2gX1TnecRs7yJwuzHLf3saAqgeEALw_wcB.
[52] D. Kim, J. Koh, and P. Im, "Net-zero energy building design and life-cycle cost analysis with air-source variable refrigerant flow and distributed photovoltaic systems," *Renewable and Sustainable Energy Reviews*, vol. 118, 2020, doi: 10.1016/j.rser.2019.109508.
[53] *Updated Buildings Sector Appliance and Equipment Costs and Efficiencies*, U.S. Energy Information Administration, 2018.

[54] X. Liu, Y. Polsky, D. Qian, and J. McDonald, “An Analysis on Cost Reduction Potential of Vertical Bore Ground Heat Exchangers Used for Ground Source Heat Pump Systems,” 44th Workshop on Geothermal Reservoir Engineering, 2019.
[55] “HVAC Chilled Water Piping Schematic (H303).” Mid Coast Hospital.
[56] “HVAC Steam Piping Schematic (H301).” Mid Coast Hospital.
[57] “HVAC Hot Water Piping Schematic (H302).” Mid Coast Hospital.